Multi-scale Studies of Microbial Mats and Biocrusts: Integrating Remote Sensing with Field Investigations in Antarctica's McMurdo Dry Valleys

Sarah Nicole Power

Dissertation submitted to the faculty of the Virginia Polytechnic Institute and State University in partial fulfillment of the requirements for the degree of

Doctor of Philosophy
In
Biological Sciences

John E. Barrett, Chair
Cayelan C. Carey
Erin R. Hotchkiss
Mark R. Salvatore
Valerie A. Thomas

August 16, 2024
Blacksburg, Virginia

Keywords: biocrust, carbon, desert, ecosystem, microbial mat, nitrogen, remote sensing, soil

Multi-scale Studies of Microbial Mats and Biocrusts: Integrating Remote Sensing with Field Investigations in Antarctica's McMurdo Dry Valleys

Sarah Nicole Power

ABSTRACT

Primary productivity is a fundamental ecosystem process driven by vascular plants in most terrestrial ecosystems and by microbes in more extreme ecosystems. In dense associations, microbial organisms can form visually conspicuous layers on sediment, soil, and rock surfaces, called microbial mats and biological soil crusts (*i.e.*, biocrusts). Both microbial mats and biocrusts consist of cyanobacteria, moss, diatoms, and green algae, and also support diverse heterotrophic taxa. These communities exist in harsh environments worldwide such as hypersaline environments, tundra ecosystems, and hot and cold deserts where they are foundational taxa, providing most of the primary production and nitrogen fixation, as well as promoting cohesion and stability to soil surfaces. In the McMurdo Dry Valleys of Antarctica, microbial mats are the main source of fixed carbon in lentic and lotic environments, but their contribution to soil carbon and nitrogen cycling has not been systematically examined. In my dissertation, I investigated the relationships between microbial mats and the soil environments in which they occur. Using a combination of field surveys, soil analyses, and remote sensing, my objectives were to examine the influence of microbial mats and biocrusts on underlying soils and model the main drivers of their distribution and abundance. In Chapter 2, I investigated the relationships between underlying soil chemistry and microbial mat distribution, composition, and function in the Taylor Valley, finding that microbial mats enrich underlying soils, contributing to soil organic carbon and nitrogen. In Chapter 3, I assessed the spectral detectability of patchy biocrusts using multispectral satellite imagery to examine the environments in which biocrusts occur, finding that spectral unmixing of satellite imagery can successfully detect the presence of

biocrust and its association with seasonal snow patches. As a direct continuation, in Chapter 4, I created a habitat suitability model using machine learning algorithms to determine the distribution and abundance of biocrusts in the Lake Fryxell basin. I found that biocrusts contribute a significant amount of carbon to the surface soil in the Lake Fryxell basin, with biocrust presence primarily driven by snow frequency, moisture content, and salinity. This dissertation contributes to ongoing questions about the sources of energy fueling soil food webs and regional carbon balance in the Taylor Valley, and how we can use remote sensing techniques for researching these critical soil communities in the dynamic Antarctic landscape.

Multi-scale Studies of Microbial Mats and Biocrusts: Integrating Remote Sensing with Field Investigations in Antarctica's McMurdo Dry Valleys

Sarah Nicole Power

GENERAL AUDIENCE ABSTRACT

Photosynthesis is the process where plants and other organisms use sunlight to transform carbon dioxide into chemical energy. This is crucial because it provides the energy and nutrients that support all other life forms. In this dissertation, I focused on colonial microorganisms, which are the main primary producers in extreme environments, like deserts. I used a combination of field surveys and satellite imaging to study these organisms in the McMurdo Dry Valleys, Antarctica, which is a harsh polar desert environment that lacks vascular plants. Microbes colonize the surface of soil and form mm-cm thick microbial mats and biological soil crusts (called biocrusts). These organisms are found within the glacial-melt streams that flow on and off for only a few weeks each year, and they also occur on the stream margins and other periodically wet areas like near snow patches. This dissertation investigates the ecological importance of microbial mats and biocrusts, the ability to measure where they are using satellite imagery, and how much organic material they contribute to the broader landscape. Field work in the McMurdo Dry Valleys and laboratory analyses were required for each of these chapters. In Chapter 2, I investigated the relationships between microbial mats and the soils below them, and I found that microbial mats increase the organic matter and nutrient content in the soils. In Chapter 3, I assessed whether satellite imagery could be used to study the presence of sparse biocrusts and examined the environments in which biocrusts occur. I discovered that satellite imagery can successfully detect the presence of biocrust and that biocrusts occurred near melting snow patches. Lastly, in Chapter 4, I created models to determine where biocrusts occur in the Lake Fryxell basin and why biocrusts occur in those areas. I found that biocrusts occur over a

significant area of the Lake Fryxell basin, containing a lot of organic material, and that biocrusts thrive in wet areas near snow patches where the soils are less salty. This dissertation contributes to ongoing questions about the sources of nutrients fueling soil food webs and contributing to the amount of organic material in the McMurdo Dry Valleys, and how we can use satellite imagery for monitoring these important soil communities in the changing Antarctic landscape.

DEDICATION

This dissertation is dedicated to my father, who spent evenings in my childhood helping me practice spelling words for school, unaware that one day I would become a published scientist.

ACKNOWLEDGMENTS

First and foremost, I thank my advisor, Jeb Barrett, for his continued support and encouragement throughout my graduate career. I have made significant strides as a scientist over the past several years, and his guidance has played a key role in that growth. I also thank my committee members: Cayelan Carey, Erin Hotchkiss, Mark Salvatore, and Valerie Thomas, who all made unique contributions to the work described herein and always encouraged me to think broadly. I am also grateful to the current and past members of the Barrett Lab for being a supportive academic family. The research communities I have been involved with have been invaluable to my graduate school experience, impacting me both professionally and personally. To the McMurdo Dry Valleys LTER team: you all have become the weirdest family members, and the memories we made in the field are truly unforgettable. To the Remote Sensing IGEP group: the camaraderie and support I found through you all has been incredibly impactful. I am deeply grateful for this community. To the Biological Sciences Department and VT Stream Team: thanks to you, I truly feel like an ecologist. This dissertation would not have been possible without the assistance of Bobbie Niederlehner, whose expertise and patience in the analytical lab was essential. I also want to acknowledge some of the friendships I have made here that I hope last a lifetime: Stephen Plont, Katherine Pérez Rivera, Meredith Snyder, Paige Williams, Simona Fried, Beth Prior – graduate school would have been way less fun without you. I thank my family and friends back home for their continued support and understanding, even as I remained in "school" into my thirties. To Jonathan: your support over the past two years greatly reduced my stress. Thank you for helping me stay grounded and balanced. And finally, for the better part of 16 years, my dog Indie has reminded me that no matter how busy I am, I should always make time for a walk outside. I think it is time for one now –

Table of Contents

ABSTRACT ……. ii
GENERAL AUDIENCE ABSTRACT ……. iv
DEDICATION ……..... vi
ACKNOWLEDGEMENTS ……..... vii
CHAPTER 1 – INTRODUCTION …… 1
Microbial Mats and Biocrusts as Critical Ecosystems ……..…….. 1
Environmental Context ……..…. 3
Remote Sensing as a Transformative Technology ……...….. 6
Dissertation Goals and Outline ……..…… 7
References ……..……. 8
CHAPTER 2 – Terrestrial microbial mat composition and activity across a geochemical gradient in Taylor Valley, Antarctica ……..……. 13
Abstract ……...…. 13
Introduction …….. 14
Materials and Methods …..……...… 16
Site description ……..… 16
Field sampling ……..…. 18
Soil geochemical analyses ……..…. 19
Microbial mat organic matter and pigment analyses ……... 20
DNA extraction and qPCR ……..…. 21
Metagenomic sequencing and taxonomic assignment ……. 22
Statistical analyses ……..…. 23
Results …..…… 24
Distribution of “black” and “orange” microbial mats ……..……... 24
Soil geochemical characterization below microbial mats ……..…….. 25
Community composition of microbial mats ……..…….. 25
Organic matter content and pigment characterization of microbial mats ...……. 26
Nif gene characterization of microbial mats and soils ……..… 28
Relationships among microbial mats and underlying soil geochemistry ……..… 29
Discussion …..…….……. 29

Till composition influences soil chemistry and microbial mats …….. 30
Microbial mats enrich underlying soil organic matter ……..… 31
Data Availability Statement …… 34
Ethics Statement ……...…… 35
Funding Statement …..…… 35
Acknowledgments ….……..……. 35
References …..……..…… 35
Figures ….……...…….. 42
Figure 2.1 …..……..…. 48
Figure 2.2 …..……...……. 49
Figure 2.3 …..……...……. 50
Figure 2.4 …..……...…. 51
Figure 2.5 …..……... 52
Figure 2.6 …..……... 53
Figure 2.7 …..……... 54
Figure 2.8 …..……... 56
Figure 2.9 …..……... 57
Tables ……... 58
Table 2.1 ……... 58
Table 2.2 ……... 59
Table 2.3 ……... 60
Table 2.4 ……... 61
Table 2.5 ……... 62
Table 2.6 ……... 63
CHAPTER 3 – Remotely characterizing photosynthetic biocrust in snowpack-fed microhabitats of Taylor Valley, Antarctica ……..…… 64
Abstract ….……..……. 64
Introduction …..……...……. 65
Materials and Methods ……..……...…… 68
Site description ……..… 68
Spectral detection limit experiment ……..… 69

Orbital spectral collection and processing 71
Field site identification and in-situ environmental sample collection 71
Analysis of environmental field samples 73
Vegetation index analysis using orbital data 75
Spectral linear unmixing of orbital data 76
Albedo analysis of orbital data 79
Results 80
Laboratory spectral validation study 80
Field surveys and spectral analyses 80
Soil characterization 82
Spectral linear unmixing of orbital data 83
Albedo analysis of orbital data 83
Discussion 84
Laboratory spectral detection of biocrust 84
Oxidized granite impedes use of vegetation indices 85
Biocrust distribution is associated with seasonal snowpacks 86
Comparisons between multispectral and hyperspectral data 88
Spectral linear unmixing models predict biocrust abundance 90
Snowpacks as microhabitats for biocrusts and diverse soil communities 91
Conclusion 93
Data Availability Statement 94
Funding Statement 94
Acknowledgments 95
References 95
Figures 105
Figure 3.1 105
Figure 3.2 106
Figure 3.3 107
Figure 3.4 108
Figure 3.5 109
Figure 3.6 111

Figure 3.7 ……..……. 113
Figure 3.8 ……..……. 114
Figure 3.9 ……..……. 115
Tables …..……...… 116
Table 3.1 ……. 116
Table 3.2 ……. 117
Table 3.3 ……. 118
Table 3.4 ……. 119
Supplemental Figures …..……..……..... 120
Figure S3.1 ……. 120
Figure S3.2 ……. 121
Figure S3.3 ……. 122
Supplemental Tables ……..…… 123
Table S3.1 ……...…...…… 123
Table S3.2 ……...……...… 124
CHAPTER 4 – Habitat suitability of biocrust communities in a cold desert ecosystem …..…. 125
Abstract ….……. 125
Introduction ….……..…. 126
Materials and Methods ….…….……. 129
Field site selection ……..…… 129
In-situ surveying and sampling ……..…… 130
Laboratory analyses ……...… 131
Habitat description and characterization ……..…….……. 132
Machine learning algorithm development ……. 133
Predicting biocrust presence/absence with random forest models ……...…. 134
Predicting biocrust AFDM with random forest models ……. 135
Mapping biocrust presence and AFDM ……..... 135
Results …..……...…… 136
Biocrust field surveys …… 136
Soil physical and biochemical properties …….. 137
Biocrust presence/absence and AFDM model performance …….. 138

Biocrust maps and carbon estimates 139
Discussion 140
Primary drivers of biocrust distribution and biomass 140
Contribution of biocrusts to carbon budget 143
The future of Antarctic biocrusts in a changing climate 145
Data Availability Statement 146
Ethics Statement 146
Funding Statement 147
Acknowledgments 147
References 147
Figures 159
Figure 4.1 159
Figure 4.2 161
Figure 4.3 162
Figure 4.4 163
Figure 4.5 164
Figure 4.6 165
Tables 166
Table 4.1 166
Table 4.2 167
Supplemental Text 168
Supplemental Figures 169
Figure S4.1 169
Figure S4.2 170
Figure S4.3 171
Figure S4.4 172
Figure S4.5 173
Supplemental Tables 174
Table S4.1 174
CHAPTER 5 – CONCLUSIONS 175
Dissertation Summary 175

Dissertation Synthesis …… 177
Future Directions ……...… 178
References ……..…… 181
Figures …… 184
Figure 5.1 ……...… 184

CHAPTER 1 – INTRODUCTION

Microbial Mats and Biocrusts as Critical Ecosystems

Primary productivity is a fundamental ecosystem process that serves as the foundation of energy flow through food webs and ecosystems (Pace et al. 2021). This occurs when autotrophs, primarily plants and algae, convert CO_2 into organic matter, primarily through chlorophyll-mediated oxygenic photosynthesis but also in other autotrophic pathways utilized by bacteria such as sulfur-based photosynthesis, and diverse forms of chemoautotrophic processes utilizing reduced inorganic compounds as electron sources (Shively et al. 1998). In turn, this organic matter not only fuels the growth of primary producers themselves, but also provides the essential energy and typically much of the macronutrients for all food webs and ecosystems globally (Pace et al. 2021). Primary productivity thus plays a critical role in nutrient cycling and supporting biodiversity, therefore understanding primary productivity is crucial for understanding the structure and function of ecosystems (Cardinale et al. 2004).

While vascular plants are the dominant primary producers of most terrestrial ecosystems, many extreme ecosystems (*e.g.*, hot deserts, polar deserts, and hydrothermal hot springs) lack vascular plants; in such environments the autotrophic community is composed of primarily microscopic organisms (*e.g.*, cyanobacteria, algae). Microbes have specific adaptations that allow them to thrive in extreme ecosystems where they are commonly exposed to extreme hot and cold temperatures, frequent desiccation, intense ultraviolet radiation, low nutrient availability, and osmotic stress like from high salinity. In dense concentrations, these microbial organisms form visibly conspicuous communities in layers on the surface of soil and rock, called microbial mats and biological soil crusts (*i.e.*, biocrusts).

Both microbial mats and biocrusts are made up of complex assemblages of organisms including cyanobacteria, algae, moss, lichen, among other autotrophic and heterotrophic taxa (Belnap 2003; Prieto-Barajas et al. 2018). While microbial mats and biocrusts overlap in similarity in terms of function, taxonomy, and physical structure, they do not commonly occur in the same environment, and therefore, they are operationally distinguished by their primary habitat and their physical connection, or lack thereof, with the underlying soil (Weber et al. 2022). Microbial mats often occur in saturated or inundated environments and are unattached to the underlying soil, while biocrusts are associated with drier soil environments and are connected to the underlying soil as bio-soil aggregates, forming an intimate association between soil particles and biocrust organisms and contributing to the stability of the desert surface (Belnap 2003; Belnap & Büdel 2016; Weber et al. 2022).

Both microbial mats and biocrusts are considered "ecosystem engineers", meaning they modify their environment by creating and maintaining microhabitats that would otherwise not exist for other organisms (Barrera et al. 2022; Prieto-Barajas et al. 2018). Microbial mats and biocrusts play foundational roles in the ecosystems in which they occur, including cycling and fixing nutrients like carbon and nitrogen, retaining water in soil, stabilizing soil (primarily biocrust), and supporting fully functioning and active food webs (Belnap et al. 2016; Prieto-Barajas et al. 2018). Moreover, non-vascular vegetation, like microbial mats and biocrusts, is often the primary source of fixed carbon in some drylands (Elbert et al. 2012). Biocrusts currently occur on 12% of Earth's terrestrial surface, though they are expected to decrease be 25 – 40% within the next 60 years due to climate change and land-use intensification (Rodríguez-Caballero et al. 2018). This coverage estimate does not even include microbial mats, which are more challenging to map systematically over large areas since they are usually inundated by

water. However, both microbial mats and biocrusts are widespread and they inhabit all continents, including Antarctica (Belnap et al. 2016; Prieto-Barajas et al. 2018).

Environmental Context

The McMurdo Dry Valleys of Antarctica are a harsh polar desert environment which lacks vascular vegetation and vertebrates but hosts microbial mats, biocrusts, and soil and sediment communities of archaea, bacteria, fungi, and multiple phyla of micro-invertebrates (Kohler et al. 2023; Simmons et al. 2009; Stone et al. 2024; Van Horn et al. 2016). In the Taylor Valley, microbial mats commonly occur within and on the margins of streams, lakes, ponds, and wetlands (Kohler et al. 2015; Power et al. 2020; Stone et al. 2024), while biocrusts are found in the drier terrestrial landscape near less frequent sources of moisture, for example, downhill of melting seasonal snow patches (Büdel & Colesie 2014; Power et al. 2024a, 2024b). Previous work has described a typology for the microbial mats found in this region based upon the dominant color and pigment chemistry, *i.e*., "black mats" are dominated by *Nostoc* and maintain high concentrations of the accessory sheath pigment scytonemin (Power et al. 2020; Vincent et al. 1993), *i.e*., microbial sunscreen (Garcia-Pichel et al. 1992), while "orange" and "red" mats, dominated by *Oscillatoria* spp. contain carotenoids and other pigments that give these mats their distinctive color. Biocrusts are often described as being cyanobacteria- or bryophyte-dominated based on their most dominant organism present (cyanobacteria or moss; Power et al. 2024b). In the McMurdo Dry Valleys, the distinction between microbial mat and biocrust is operational, and made mainly on the basis of density and habitat, *i.e*., biocrusts are sparser in coverage and occur outside of stream channels and lake margins. Both microbial mats and biocrusts consist of similar organisms, primarily cyanobacteria (Power et al. 2024b; Van Horn et al. 2016), and are

both functionally important to the lake, stream, and soil ecosystems in which they occur (Büdel & Colesie 2014; Kohler et al. 2023).

Microbial mats and biocrusts occur over distinct habitats influenced by the local geomorphology and hydrology, especially within or near aquatic landscapes where most of the work on microbial mats has been conducted (Kohler et al. 2015; Stanish et al. 2011). These communities are thought to be responsible for the majority of carbon (C) fixation via photosynthesis and are the primary source of organic matter into this ecosystem (Kohler et al. 2023; McKnight et al. 2004), facilitating diverse food webs in the nearby waters and soils below (Simmons et al. 2009). The cyanobacteria taxa which make up most of the biomass of these communities are adapted to tolerate extreme environmental conditions such as frequent desiccation, freeze/thaw, intense ultraviolet solar radiation, osmotic stress, and low nutrient availability (Hawes et al. 1992; Prieto-Barajas et al. 2018; Vincent et al. 1993). For example, many cyanobacteria synthesize scytonemin which screens out ultraviolet radiation (Garcia-Pichel et al. 1992), and they are capable of nitrogen (N) fixation to overcome low N availability in much of the soil and aquatic environments (Kohler et al. 2023).

Although microbial mats and biocrust exist globally and could be researched anywhere, I have chosen to study those occurring in Antarctica for several reasons. The McMurdo Dry Valleys are a relatively pristine environment, where the extreme physical conditions support simple biotic communities, and are an ideal model system for studying microbial communities. Understanding the controls of the distribution and activity of simple biotic communities in such an environment may provide fundamental insights into ecosystem structure and function that are generally relevant to other non-extreme environments.

The McMurdo Dry Valleys are a Long-Term Ecological Research (LTER) site which has created and curated three decades of meteorological, hydrological, and ecological data, providing deeper insight into this region that provides much of the context and background to my research. This region is increasingly experiencing dynamic climate (*e.g.*, Barrett et al. 2024; Nielsen et al. 2024,) and its sensitive landscapes are on the precipice of change (Colesie et al. 2023). However, fundamental ecological questions about the sources of energy fueling the simple soil food webs and the role of primary producers remain unanswered. This sparked my interest in researching the dominant primary producers of this extreme system, contributing my efforts to better understand the distribution and activity of terrestrial microbial mats and biocrusts and the soil environments in which they occur.

There have been many studies on the soils of Taylor Valley, especially focused on understanding sources of organic matter pool to support food webs, the contemporary C budget, and controls over C cycling– where the organic matter came from and how much is there currently (*e.g.*, Barrett et al. 2006b; Burkins et al. 2000; Lawson et al. 2004; Parsons et al. 2004). Early research showed that soils below ~ 300 m elevation have been modified by lacustrine sedimentation from the Glacial Lake Washburn ~ 11,000 – 24,000 years ago (Denton et al. 1989). This periodic rise and fall of the lacustrine environments has significantly affected the distribution of organic matter and biota in the terrestrial environments of the Taylor Valley (Burkins et al. 2000). Therefore, much of the organic matter in Taylor Valley has ancient origins – it was deposited as entrained detritus within glacial tills and as primary productivity in ancient glacial paleolakes, but it remains unclear, despite decades of research, how much of the current C balance is also influenced by contemporary *in-situ* autotrophic activity (*e.g.*, Barrett et al. 2006b), such as microbial mats and biocrusts, especially at higher elevations where the soils have

been exposed for a longer amount of time (Burkins et al. 2000). Understanding the landscape history of this environment is crucial to understanding contemporary variation in ecological communities and ecosystem processes (Barrett et al. 2006a). Previously, there were no systematic methods of measuring microbial mats and biocrusts and the processes they facilitate that were scalable to the broader region. Such systematic, *i.e.*, repeatable through time, and scalable measurements are necessary not only for conducting effective inventories of the C in microbial mats and biocrusts and understanding their influences on the underlying soils, but also for benchmarking current C inventories against anticipated responses to ongoing changes to the climate of this region.

Remote Sensing as a Transformative Technology

Advances in technology have promoted remote sensing as a systematic and scalable method for measuring vegetation and C content across ecosystems (Running et al. 2000). Remote sensing can be used to detect the spectral composition of landscape surfaces, and when integrated with *in-situ* field surveying and sampling, can be used to quantify surface properties such as microbial mat and biocrust presence/absence and organic matter content in coastal ecosystems (*e.g.*, Andréfouët et al. 2003), hot deserts (*e.g.,* Rodríguez-Caballero et al. 2017; Young & Reed 2017), and the Antarctic desert (*e.g.*, Colesie et al. 2022; Fretwell et al. 2011; Jawak et al. 2019; Salvatore et al. 2020). This capability is transformative for studies in the Antarctic, which is particularly climate-sensitive and difficult to access, and where we have lacked understanding of some fundamental ecosystem questions, *e.g.*, regarding primary production. *In-situ* field surveying and sampling offers insights into the ecological importance of microbial mats and biocrusts and how they influence the underlying soils, while the integration of field work with advanced remote sensing technologies offers insights into which

environmental factors influence microbial mat and biocrust distribution and abundance *and* the ability to systematically quantify landscape-scale organic matter and C content for the first time.

Dissertation Goals and Outline

This dissertation investigates the relationships between microbial mats or biocrusts and the soil environments in which they occur, the ability to model their distribution and abundance with remote sensing data, and how they contribute to the C budget of the McMurdo Dry Valleys, by addressing the following questions:

(1) How do microbial mats influence the ecological functioning of soil ecosystems and contribute to underlying soil organic matter? In Chapter 2 (Power et al. *In Prep*), I examine the ecological importance of microbial mats by analyzing taxonomic composition, underlying soil geochemistry, and pigment abundance of microbial mats, and the interactions between nutrient availability in the soils and the functional ecology of the microbial mats.

(2) What is the spectral detectability of patchy biocrusts using multispectral satellite imagery? In Chapter 3 (Power et al. 2024a), I investigate the lower detection limits of biocrusts using a combination of multi- and hyperspectral tools, field-based survey and sampling approaches, and spectral linear unmixing to model the abundances of biocrust and examine the environments in which they occur.

(3) How much carbon do biocrusts contribute to the surface organic C content of the Lake Fryxell basin? In Chapter 4 (Power et al. 2024b), I use a combination of field surveying and sampling, remote sensing, and machine learning algorithms to assess the environmental conditions that drive the presence and abundance of biocrust communities, to model biocrust distribution and biomass, and to estimate the surface organic C content of Lake Fryxell basin biocrusts.

References

Andréfouët, S., Payri, C., Hochberg, E.J., Che, L.M., Atkinson, M.J., 2003. Airborne hyperspectral detection of microbial mat pigmentation in Rangiroa atoll (French Polynesia). Limnol. Oceanogr. 48, 426–430. https://doi.org/10.4319/lo.2003.48.1_part_2.0426

Barrera, A., Acuña-Rodríguez, I.S., Ballesteros, G.I., Atala, C., Molina-Montenegro, M.A., 2022. Biological Soil Crusts as Ecosystem Engineers in Antarctic Ecosystem. Front. Microbiol. 13, 755014. https://doi.org/10.3389/fmicb.2022.755014

Barrett, J.E., Adams, B.J., Doran, P.T., Dugan, H.A., Myers, K.F., Salvatore, M.R., Power, S.N., Snyder, M.D., Wright, A.T., Gooseff, M.N., 2024. Response of a Terrestrial Polar Ecosystem to the March 2022 Antarctic Weather Anomaly. Earths Future 12, e2023EF004306. https://doi.org/10.1029/2023EF004306

Barrett, J.E., Virginia, R.A., Hopkins, D.W., Aislabie, J., Bargagli, R., Bockheim, J.G., Campbell, I.B., Lyons, W.B., Moorhead, D.L., Nkem, J.N., Sletten, R.S., Steltzer, H., Wall, D.H., Wallenstein, M.D., 2006a. Terrestrial ecosystem processes of Victoria Land, Antarctica. Soil Biol. Biochem. 38, 3019–3034. https://doi.org/10.1016/J.SOILBIO.2006.04.041

Barrett, J.E., Virginia, R.A., Parsons, A.N., Wall, D.H., 2006b. Soil carbon turnover in the McMurdo Dry Valleys, Antarctica. Soil Biol. Biochem. 38, 3065–3082. https://doi.org/10.1016/j.soilbio.2006.03.025

Belnap, J., 2003. The world at your feet: desert biological soil crusts. Front. Ecol. Environ. 1, 181–189. https://doi.org/10.1890/1540-9295(2003)001[0181:TWAYFD]2.0.CO;2

Belnap, J., Büdel, B., 2016. Biological Soil Crusts as Soil Stabilizers, in: Weber, B., Büdel, B., Belnap, J. (Eds.), Biological Soil Crusts: An Organizing Principle in Drylands. Springer International Publishing, Cham, pp. 305–320. https://doi.org/10.1007/978-3-319-30214-0_16

Belnap, J., Weber, B., Büdel, B., 2016. Biological Soil Crusts as an Organizing Principle in Drylands, in: Weber, B., Büdel, B., Belnap, J. (Eds.), Biological Soil Crusts: An Organizing Principle in Drylands. Springer International Publishing, Cham, pp. 3–13. https://doi.org/10.1007/978-3-319-30214-0_1

Büdel, B., Colesie, C., 2014. Biological Soil Crusts, in: Cowan, D.A. (Ed.), Antarctic Terrestrial Microbiology: Physical and Biological Properties of Antarctic Soils. Springer Berlin

Heidelberg, Berlin, Heidelberg, pp. 131–161. https://doi.org/10.1007/978-3-642-45213-0_8

Burkins, M.B., Virginia, R.A., Chamberlain, C.P., Wall, D.H., 2000. Origin and Distribution of Soil Organic Matter in Taylor Valley, Antarctica. Ecology 81, 2377–2391. https://doi.org/10.1890/0012-9658(2000)081[2377:OADOSO]2.0.CO;2

Cardinale, B.J., Ives, A.R., Inchausti, P., 2004. Effects of species diversity on the primary productivity of ecosystems: extending our spatial and temporal scales of inference. Oikos 104, 437–450. https://doi.org/10.1111/j.0030-1299.2004.13254.x

Colesie, C., Pan, Y., Cary, S.C., Gemal, E., Brabyn, L., Kim, J.-H., Green, T.G.A., Lee, C.K., 2022. The longest baseline record of vegetation dynamics in Antarctica reveals acute sensitivity to water availability. Earths Future 10. https://doi.org/10.1029/2022ef002823

Colesie, C., Walshaw, C.V., Sancho, L.G., Davey, M.P., Gray, A., 2023. Antarctica's vegetation in a changing climate. Wiley Interdiscip. Rev. Clim. Change 14. https://doi.org/10.1002/wcc.810

Denton, G.H., Bockheim, J.G., Wilson, S.C., Stuiver, M., 1989. Late Wisconsin and early Holocene glacial history, inner Ross Embayment, Antarctica. Quat. Res. 31, 151–182. https://doi.org/10.1016/0033-5894(89)90004-5

Elbert, W., Weber, B., Burrows, S., Steinkamp, J., Büdel, B., Andreae, M.O., Pöschl, U., 2012. Contribution of cryptogamic covers to the global cycles of carbon and nitrogen. Nat. Geosci. 5, 459–462. https://doi.org/10.1038/ngeo1486

Fretwell, P.T., Convey, P., Fleming, A.H., Peat, H.J., Hughes, K.A., 2011. Detecting and mapping vegetation distribution on the Antarctic Peninsula from remote sensing data. Polar Biol. 34, 273–281. https://doi.org/10.1007/s00300-010-0880-2

Garcia-Pichel, F., Sherry, N.D., Castenholz, R.W., 1992. Evidence for an ultraviolet sunscreen role of the extracellular pigment scytonemin in the terrestrial cyanobacterium Chlorogloeopsis sp. Photochem. Photobiol. 56, 17–23.

Hawes, I., Howard-Williams, C., Vincent, W., 1992. Desiccation and recovery of antarctic cyanobacterial mats. Polar Biol. 12, 587–594. https://doi.org/10.1007/BF00236981

Jawak, S.D., Luis, A.J., Fretwell, P.T., Convey, P., Durairajan, U.A., 2019. Semiautomated Detection and Mapping of Vegetation Distribution in the Antarctic Environment Using Spatial-Spectral Characteristics of WorldView-2 Imagery. Remote Sensing 11, 1909.

https://doi.org/10.3390/rs11161909

Kohler, T.J., Singley, J.G., Wlostowski, A.N., McKnight, D.M., 2023. Nitrogen fixation facilitates stream microbial mat biomass across the McMurdo Dry Valleys, Antarctica. Biogeochemistry 166, 247–268. https://doi.org/10.1007/s10533-023-01069-0

Kohler, T.J., Stanish, L.F., Crisp, S.W., Koch, J.C., Liptzin, D., Baeseman, J.L., McKnight, D.M., 2015. Life in the Main Channel: Long-Term Hydrologic Control of Microbial Mat Abundance in McMurdo Dry Valley Streams, Antarctica. Ecosystems 18, 310–327. https://doi.org/10.1007/s10021-014-9829-6

Lawson, J., Doran, P.T., Kenig, F., Des marais, D.J., Priscu, J.C., 2004. Stable Carbon and Nitrogen Isotopic Composition of Benthic and Pelagic Organic Matter in Lakes of the McMurdo Dry Valleys, Antarctica. Aquat. Geochem. 10, 269–301. https://doi.org/10.1007/s10498-004-2262-2

McKnight, D.M., Runkel, R.L., Tate, C.M., Duff, J.H., Moorhead, D.L., 2004. Inorganic N and P dynamics of Antarctic glacial meltwater streams as controlled by hyporheic exchange and benthic autotrophic communities. J. North Am. Benthol. Soc. 23, 171–188. https://doi.org/10.1899/0887-3593(2004)023<0171:INAPDO>2.0.CO;2

Nielsen, E.B., Katurji, M., Zawar-Reza, P., Cullen, N.J., 2024. Air temperature trends and extreme warming events across regions of Antarctica for the period 2003-2021. ESS Open Archive. https://doi.org/10.22541/essoar.171926315.55910608/v1

Pace, M.L., Lovett, G.M., Carey, C.C., Thomas, R.Q., 2021. Primary production: The foundation of ecosystems, in: Fundamentals of Ecosystem Science. Elsevier, pp. 29–53. https://doi.org/10.1016/b978-0-12-812762-9.00002-2

Parsons, A.N., Barrett, J.E., Wall, D.H., Virginia, R.A., 2004. Soil carbon dioxide flux in antarctic Dry Valley ecosystems. Ecosystems 7, 286–295. https://doi.org/10.1007/s10021-003-0132-1

Power, S.N., Salvatore, M.R., Sokol, E.R., Stanish, L.F., Barrett, J.E., 2020. Estimating microbial mat biomass in the McMurdo Dry Valleys, Antarctica using satellite imagery and ground surveys. Polar Biol. 43, 1753–1767. https://doi.org/10.1007/s00300-020-02742-y

Power, S.N., Salvatore, M.R., Sokol, E.R., Stanish, L.F., Borges, S.R., Adams, B.J., Barrett, J.E., 2024a. Remotely characterizing photosynthetic biocrust in snowpack-fed microhabitats of Taylor Valley, Antarctica. Science of Remote Sensing 9, 100120.

https://doi.org/10.1016/j.srs.2024.100120

Power, S.N., Thomas, V.A., Salvatore, M.R., Barrett, J.E., 2024b. Habitat suitability of biocrust communities in a cold desert ecosystem. Ecol. Evol. 14, e11649. https://doi.org/10.1002/ece3.11649

Power, S.N., Osburn, E.D., Barrett, J.E., *In Prep*, Terrestrial microbial mat composition and activity across a geochemical gradient in Taylor Valley, Antarctica.

Prieto-Barajas, C.M., Valencia-Cantero, E., Santoyo, G., 2018. Microbial mat ecosystems: Structure types, functional diversity, and biotechnological application. Electron. J. Biotechnol. 31, 48–56. https://doi.org/10.1016/J.EJBT.2017.11.001

Rodríguez-Caballero, E., Belnap, J., Büdel, B., Crutzen, P.J., Andreae, M.O., Pöschl, U., Weber, B., 2018. Dryland photoautotrophic soil surface communities endangered by global change. Nat. Geosci. 11, 185–189. https://doi.org/10.1038/s41561-018-0072-1

Rodríguez-Caballero, E., Paul, M., Tamm, A., Caesar, J., Büdel, B., Escribano, P., Hill, J., Weber, B., 2017. Biomass assessment of microbial surface communities by means of hyperspectral remote sensing data. Sci. Total Environ. 586, 1287–1297. https://doi.org/10.1016/J.SCITOTENV.2017.02.141

Running, S.W., Thornton, P.E., Nemani, R., Glassy, J.M., 2000. Global Terrestrial Gross and Net Primary Productivity from the Earth Observing System, in: Methods in Ecosystem Science. Springer New York, New York, NY, pp. 44–57. https://doi.org/10.1007/978-1-4612-1224-9_4

Salvatore, M.R., Borges, S.R., Barrett, J.E., Sokol, E.R., Stanish, L.F., Power, S.N., Morin, P., 2020. Remote characterization of photosynthetic communities in the Fryxell basin of Taylor Valley, Antarctica. Antarct. Sci. 1–16. https://doi.org/10.1017/S0954102020000176

Shively, J.M., van Keulen, G., Meijer, W.G., 1998. Something from almost nothing: carbon dioxide fixation in chemoautotrophs. Annu. Rev. Microbiol. 52, 191–230. https://doi.org/10.1146/annurev.micro.52.1.191

Simmons, B.L., Wall, D.H., Adams, B.J., Ayres, E., Barrett, J.E., Virginia, R.A., 2009. Terrestrial mesofauna in above-and below-ground habitats: Taylor Valley, Antarctica. Polar Biol. 32, 1549–1558. https://doi.org/10.1007/s00300-009-0639-9

Stanish, L.F., Nemergut, D.R., McKnight, D.M., 2011. Hydrologic processes influence diatom

community composition in Dry Valley streams. J. North Am. Benthol. Soc. 30, 1057–1073. https://doi.org/10.1899/11-008.1

Stone, M.S., Devlin, S.P., Hawes, I., Welch, K.A., Gooseff, M.N., Takacs-Vesbach, C., Morgan-Kiss, R., Adams, B.J., Barrett, J.E., Priscu, J.C., Doran, P.T., 2024. McMurdo Dry Valley lake edge "moats": the ecological intersection between terrestrial and aquatic polar desert habitats. Antarct. Sci. 1–17. https://doi.org/10.1017/S0954102024000087

Van Horn, D.J., Wolf, C.R., Colman, D.R., Jiang, X., Kohler, T.J., McKnight, D.M., Stanish, L.F., Yazzie, T., Takacs-Vesbach, C.D., 2016. Patterns of bacterial biodiversity in the glacial meltwater streams of the McMurdo Dry Valleys, Antarctica. FEMS Microbiol. Ecol. 92. https://doi.org/10.1093/femsec/fiw148

Vincent, W.F., Downes, M.T., Castenholz, R.W., Howard-Williams, A.C., 1993. Community structure and pigment organisation of cyanobacteria-dominated microbial mats in Antarctica. Eur. J. Phycol. 28, 213–221.

Weber, B., Belnap, J., Büdel, B., Antoninka, A.J., Barger, N.N., Chaudhary, V.B., Darrouzet-Nardi, A., Eldridge, D.J., Faist, A.M., Ferrenberg, S., Havrilla, C.A., Huber-Sannwald, E., Malam Issa, O., Maestre, F.T., Reed, S.C., Rodriguez-Caballero, E., Tucker, C., Young, K.E., Zhang, Y., Zhao, Y., Zhou, X., Bowker, M.A., 2022. What is a biocrust? A refined, contemporary definition for a broadening research community. Biol. Rev. Camb. Philos. Soc. 97, 1768–1785. https://doi.org/10.1111/brv.12862

Young, K.E., Reed, S.C., 2017. Spectrally monitoring the response of the biocrust moss Syntrichia caninervis to altered precipitation regimes. Sci. Rep. 7, 1–10. https://doi.org/10.1038/srep41793

CHAPTER 2 – Terrestrial microbial mat composition and activity across a geochemical gradient in Taylor Valley, Antarctica

Abstract

Primary production is fundamental to all ecosystems, and in many extreme environments, production is facilitated by microbial mats. These communities are complex assemblages of photo- and heterotrophic microorganisms, consisting generally of cyanobacteria, moss, diatoms, and green algae, which colonize the surface of sediments, soil and rock in extreme environments. These communities are well adapted to low nutrient availability, high solar radiation, freeze/thaw, salinity stress, and frequent desiccation, making them the dominant primary producers of the McMurdo Dry Valleys of Antarctica where they occupy lentic and lotic environments as well as intermittently wet soils. While the influence of microbial mats on stream nutrient dynamics and lake organic matter cycling is well documented, microbial mat influences on underlying soil, especially nitrogen (N) and carbon (C) fixation is less understood. Soils of the McMurdo Dry Valleys occur across distinct geochemical gradients that provide an opportunity to examine the influence of natural variation in nutrient availability on microbial mat communities and their functioning. In this study, I found that a geochemical gradient, primarily in inorganic phosphorus (P), is a driver of microbial mat composition and biomass. Additionally, P availability influences the functioning of microbial mats, specifically with regards to their N-fixation potential and pigment composition. Lastly, microbial mats influence the ecological functioning of underlying soils by enriching them in organic C and total N. This work contributes to ongoing questions about the sources of energy fueling soil food webs and regional carbon balance in the McMurdo Dry Valleys.

Introduction

Primary production is a fundamental ecosystem process that supports food webs and ecosystem energy flow. In water- or nutrient-limited ecosystems, and in environments where environmental stressors are common (*e.g.*, saline conditions, intense UV radiation), microbial mats are often foundational components of the autotrophic community. Microbial mats typically occur as laminated mm-cm thick colonial communities on the surface of soils, sediments, and rocks and are often the dominant primary producers in extreme environments like deserts, hypersaline ponds, and hydrothermal hot springs (Prieto-Barajas et al. 2018; Stal 1994). Microbial mats are self-sustaining communities that govern nutrient cycles and create a habitat supporting a diverse community of organisms in otherwise inhospitable sediment environments (Bolhuis et al. 2014; Davey & O'toole 2000; Guerrero et al. 2002; Prieto-Barajas et al. 2018). For these reasons, microbial mats are useful model systems for studying ecological relationships and biogeochemical cycling in extreme ecosystems (Stal 1994). In the polar desert of the Antarctic McMurdo Dry Valleys, microbial mats are present within and along the margins of glacial-melt streams, lakes, wetlands, snow-influenced soils, and even surface lake and glacial ice (McKnight et al. 1999; Paerl & Priscu 1998; Power et al. 2020; Stone et al. 2024). Microbial mats are dominated by cyanobacteria but also contain other autotrophic and heterotrophic prokaryotic taxa (Van Horn et al. 2016), as well as green algae, diatoms, moss, and invertebrates (*e.g.*, nematodes, rotifers, and tardigrades; Alger et al. 1997; Simmons et al. 2009).

The highly variable and physiologically stressful conditions of Antarctica require key adaptations of resident biota to these harsh environments. For eight to eleven months of the year, microbial mats are frozen and desiccated in a cryptobiotic state until the austral summer when snow melt and glacial thaw can rapidly reactivate microbial communities (Hawes et al. 1992;

Vincent & Howard-Williams 1986). Other stressors include: low nutrient availability, freeze/thaw cycles, and intense ultraviolet radiation (Hawes et al. 1992; Vincent et al. 1993). Previous studies have also demonstrated that the abundance and composition of microbial mat communities is influenced by the local geomorphology and hydrology (McKnight et al. 1999; Kohler et al. 2015; Stanish et al. 2011), but no work has systematically examined the influence of geochemical gradients in nutrient availability (*e.g.*, Barrett et al. 2007; Bate et al. 2008; Welch et al. 2010) on microbial mat distribution, composition, and activity.

In other ecosystems, microbial mats make important material (*e.g.*, carbon and nitrogen fixation) and functional (soil cohesion and UV protection) contributions to the environments they occupy (Prieto-Barajas et al. 2018). In the McMurdo Dry Valleys, cyanobacteria-dominated microbial mats are the dominant primary producers and strongly influence organic matter budgets (Burkins et al. 2000; Lawson et al. 2004; Parker et al. 1982) and nitrogen economy (Hawes et al. 1992; Kohler et al. 2018, 2023) of the lake, stream, and sediment environments they occupy. For example, while stream water chemistry is modulated by upstream glacial melt conditions and hyporheic interactions which alter the biogeochemistry (Gooseff et al. 2002, 2003; Maurice et al. 2002), microbial mat communities also influence water chemistry through biological uptake, recycling, and export downstream of nitrogen and phosphorus (Gooseff et al. 2004; Kohler et al. 2018; McKnight et al. 2004).

Most studies of microbial mats in the McMurdo Dry Valleys have been conducted in or adjacent to perennial aquatic landscape features, *i.e.*, streams, ponds, and lakes (Gooseff et al. 2004; McKnight et al. 2007; Moorhead et al. 2003; Stone et al. 2024). Intermittently wet soils and ephemeral, un-channelized streams have received comparatively much less attention, even though these landscapes occupy large proportions of the region and the functioning of microbial

mats and biocrusts is relevant to ongoing questions about the sources of energy fueling the simple soil food webs and regional carbon balance (*e.g.*, Burkins et al. 2000; Barrett et al. 2006b, Power et al. 2024b). Moreover, strong geochemical gradients in nitrogen and especially phosphorus (*e.g.*, Barrett et al. 2007; Welch et al. 2010) may influence the distribution and activity of microbial mats because of their unique contribution to nitrogen cycling through nitrogen fixation.

The objective of my study was to investigate the relationships between underlying soil chemistry and microbial mat distribution, composition, and function in Taylor Valley, Antarctica. Specifically, I characterized the taxonomic composition, underlying soil geochemistry, and pigment composition of microbial mats distributed across two glacial tills in the Taylor Valley, and examined the influence of microbial mats on nitrogen fixation potential and the soil carbon and nitrogen budgets of the underlying soils.

Materials and Methods

Site description

The McMurdo Dry Valleys (Figure 2.1) are the largest contiguous ice-free area on the Antarctic continent, with approximately 4500 km^2 of exposed soil, stream, and lake ecosystems (Levy 2013). They are one of Earth's coldest and driest deserts with mean annual temperatures between -15 and -30°C and less than 50 mm water equivalent of snowfall annually (Fountain et al. 2010; Obryk et al. 2020). Glacial meltwater during the austral summer (*i.e.*, 24 h of daylight) feeds streams that flow for an average of 4-9 weeks per year (Wlostowski et al. 2016). These streams drain into perennially ice-covered lakes along the floor of Taylor Valley, supporting microbial mats within and along the margins of the streams and lakes (McKnight et al. 1999). Additionally, other sources of moisture (*e.g.*, snow patches, wetlands, groundwater seeps) are

also activated during the austral summer, and many of these wetted environments also support microbial mats (Gooseff et al. 2013).

The parent material of Taylor Valley soils is composed of glacial till deposits (*i.e.*, unsorted rock/soil material deposited directly from glacial ice) from three types of glaciations: advances from the grounding of ice from the marine-based Ross Ice Shelf from the east, advances of glaciers from the East Antarctic Ice Sheet to the west, and the advances of alpine glaciers along the Taylor Valley walls (Bockheim et al. 2008). These glaciations are thought to have occurred over the past 10k-10M years (Bockheim et al. 2008), resulting in very different exposure ages and, given the regional variation in bedrock composition and mineralogy, distinct clast composition (Bate et al. 2008; Bockheim et al. 2008; Denton et al. 1989). The Ross till is on the eastern side of Taylor Valley (Figure 2.1) and has a younger surface exposure age in comparison to the Taylor tills on the western side of Taylor Valley. As a result of the atmospheric deposition of inorganic nitrogen (N) that has accumulated over time on tills of varying surface exposure age (Michalski et al. 2005), the older Taylor tills generally have higher nitrate concentrations (Barrett et al. 2007). In contrast, inorganic phosphorus (P) content is most abundant on the younger Ross tills due to greater weathering of local apatite (Bate et al. 2008; Barrett et al. 2007). The geochemistry of the tills in Taylor Valley have been previously described (*e.g.*, Bate et al. 2008; Barrett et al. 2007), however the impacts of the soil geochemical gradients on microbial mat composition and activity have not been studied. Additionally, while the influence of microbial mats on stream chemistry has been well-documented (*e.g.*, Kohler et al. 2018; McKnight et al. 2004), microbial mat influences on underlying soil (especially N- and C-fixation) alongside stream margins is less well understood.

Field sampling

In December of 2019 and January of 2020, I sampled microbial mats and underlying soils at 16 sites located on the Ross (n=8) and Taylor tills (n=8) of Taylor Valley, Antarctica (Figure 2.1; Table 2.1). These sites included landscapes that were intermittently wet environments but not within the thalweg of incised stream channels or in the littoral areas of lakes and ponds since my focus was on the contribution of the microbial mats to terrestrial soils. Stream-to-soil ecotones are not always clear in this region (*e.g.*, Gooseff et al. 2013; Harris et al. 2007; Wlostowski et al. 2019), but I sought landscape surfaces that were not subject to channelized stream flow where lotic processes dominate biogeochemistry and community composition of microbial mats (Gooseff et al. 2004; Kohler et al. 2015; Zoumplis et al. 2023). I selected sites situated alongside stream channels, pond margins, and snow melt patches. Dominant color typology composition (orange, typically described as dominated by *Oscillatoria*, or black mat, typically considered *Nostoc* dominated) was noted for each location (*e.g.*, Alger et al. 1997).

Studies of microbial mats in the McMurdo Dry Valleys, Antarctica have described microbial mats primarily by their visible color, along with the hydrologic conditions of their habitat (Alger et al. 1997; Kohler et al. 2015; Stanish et al. 2011; McKnight et al. 1999). From these studies a useful typology has emerged that is based on dominant pigments and visible color: black, orange, green, and red mats (Alger et al. 1997). The black mats primarily occupy intermittently saturated areas at the margins of lentic and lotic landscapes and beside melting snow patches, while orange, green, and red mats primarily occupy seasonally inundated areas generally within the thalweg of stream channels (Alger et al. 1997; Howard-Williams et al. 1986; Kohler et al. 2015). While this color typology should be understood as a description of community type rather than specific taxa, the generalization that black mats are dominated by

Nostoc, green mats by chlorophytes, and orange and red mats by *Oscillatoria*, is supported by early microscopy (*e.g.*, Alger et al. 1997; Parker et al. 1982; Vincent & Howard-Williams 1986), and later molecular sequencing approaches (*e.g.*, Van Horn et al. 2016).

I identified a 0.5 × 0.5 m area of microbial mat at each site (*e.g.*, Figure 2.2), and sampled five plugs of mat material (from the center and the four corners) using a sterilized #13 brass cork borer (2.27 cm^2) for organic matter content, pigment analysis, and molecular analysis, separately, for a total of 15 plugs. Directly beneath each sampled microbial mat, I also collected the underlying soil (0 - 5 cm depth) using a sterilized cork borer for later geochemical and molecular analysis. The five microbial mat and underlying soil samples were composited into one soil and one microbial mat sample per site, per analysis. All samples were kept frozen at -20°C in complete darkness until subsequent analyses were performed.

Soil geochemical analyses

Gravimetric water content (GWC) was measured for each of the soil samples, determined as the mass of water lost after oven drying the soils at 105°C for 24 hr. Soil pH and electrical conductivity (EC) were measured using a 1:2 and 1:5 soil to DI H_2O slurry, respectively, using a YSI pH meter (YSI, Yellow Springs, OH, United States) and Orion Star conductivity meter (Thermo Fisher Scientific, Waltham, MA, United States). I also extracted inorganic nitrogen (N; NH_4^+ and NO_3^-) in 2 M potassium chloride and inorganic phosphorus (P; PO_4^{3-}) in 0.5 M sodium bicarbonate. Major anions were measured on 1:5 dilutions of soil to DI H_2O. Inorganic N and P were measured on extracts using a Lachat QuikChem flow injection analyzer (Hach Company, Loveland, CO, United States; Knepel 2003; Prokopy 1995). Major anion concentrations were analyzed on a Dionex Ion Chromatograph (Thermo Fisher Scientific, Waltham, MA, United States; Pfaff 1993); only sulfate (SO_4^{2-}) and chloride (Cl^-) had consistent concentrations above

minimum detection levels. Additionally, I measured soil organic carbon (SOC) and total nitrogen (TN) using an Elementar Vario MAX Cube analyzer (Elementar Americas Inc., Mt. Laurel, NJ, United States) after fumigating samples with concentrated hydrochloric acid to remove the influence of carbonates on SOC values (Walthert et al. 2010).

Microbial mat organic matter and pigment analyses

Each microbial mat sample was measured for organic matter content as ash-free dry mass (AFDM) by oven drying at 100°C for 24 hr, weighing dry mass, combusting at 550°C for 15 hr using a muffle furnace, weighing ashed mass after cooling in a desiccator, and estimating AFDM as the mass lost during ashing per mass of dry material. Additionally, pigment composition and concentration (Table 2.2) was estimated at the Paerl Lab, University of North Carolina using high performance liquid chromatography (HPLC; Jeffrey et al. 1997; Mantoura & Llewellyn 1983; Van Heukelem 1992, 1994). Pigments were extracted from the microbial mat samples in 100% acetone for 24 hr before analysis on the Shimadzu HPLC system (Shimadzu Scientific Instruments, Columbia, MD, United States). The HPLC separated the pigments and measured absorbance of the extracts by scanning 340 - 700 nm every 1.28 sec. These data were analyzed using Shimadzu's LabSolutions Lite software and a combination of peak retention time, absorbance spectrum shape/signature, maximum wavelength, and the similarity match of the unknown pigment to a standard to identify the various pigments (Jeffrey et al. 1997). Pigments were then quantified from their peak areas, calculated at 388 nm for scytonemin and reduced scytonemin and 440 nm for all other pigments. A multipoint calibration curve was generated by injecting volumes of known quantities of pure pigment standards (DHI, Denmark), and then calculating the peak areas of those pigments. The standards' peak areas were then used to calculate the slope (response factor) for each pigment, which were multiplied by the samples'

peak areas of the chromatogram at 388 or 440 nm to quantify the pigments extracted in μg g^{-1} dry mat.

DNA extraction and qPCR

I determined the relative abundance of all nitrogenase (*nif)* genes, which are indicators of N-fixation potential, using shotgun metagenome sequencing and the absolute abundance of *nifH* specifically using qPCR for both the microbial mats and underlying soils. DNA was extracted from ~1.5 g soil and ~ 0.5 – 1.0 g microbial mat material using the DNeasy PowerSoil kit (QIAGEN), and the extracts were quantified using a Qubit 2.0 Fluorometer (Thermo Fisher Inc.). For qPCR, I used the IGK3/DVV primer set (Ando et al. 2005) because it exhibits less bias than other *nifH* primer sets (Gaby & Buckley 2017). Samples were amplified in triplicate and PCR reactions contained 10 μL Quantitect SYBR Green qPCR Mastermix (QIAGEN), 3 μL of 10 μM working stocks of each of the forward and reverse primers (for final primer concentrations of 1.5 μM), and 4 μL of DNA template for a total reaction volume of 20 μL. The high primer concentration I used was intended to maximize the efficiency of the qPCR reactions (Gaby & Buckley 2017). Thermal cycling conditions were as follows: 15 min at 95°C followed by 40 cycles of 15 sec at 95°C, 30 sec at 56°C, and 30 sec at 72°C. Standard curves were generated by amplifying serial dilutions of the target regions, with amplification efficiencies of 84.5% for the microbial mat samples and 74.2% for the soil samples, and both R^2 values > 0.99. For the qPCR gene standard, I used the *nifH* gene sequence from *Nostoc punctiforme* strain PCC 73102, which has a high similarity (99%) to Antarctic *Nostoc* sequences (Jungblut & Neilan 2010). Amplification specificity was assessed using melt curve analysis. The *nifH* gene copy numbers were corrected for dry soil mass and wet mat mass.

Metagenomic sequencing and taxonomic assignment

DNA libraries were prepared for shotgun metagenome sequencing using a KAPA HyperPrep Kit (Roche Molecular Systems, Inc.). Libraries were sequenced on an Illumina NextSeq500 in a 150 bp paired-end sequencing run at the Duke University School of Medicine Sequencing and Genomic Technologies Shared Resource. Raw sequence reads were uploaded to MG-RAST (accession# mgp95386) for merging of paired ends, quality control, and annotation using the recommended MG-RAST default parameters (Meyer et al. 2008). Functional annotations were performed by aligning the metagenomic sequences to the SEED Subsystems database (Overbeek et al. 2014) while taxonomic annotations were performed using the RefSeq and SILVA databases. For all functional and taxonomic annotations, I used an e-value cutoff of 1e-5, a sequence similarity threshold of 80% and a minimum alignment length of 20 bp. After processing with MG-RAST, I retained an average of ~7.2 million sequences per sample, ranging from ~4.3 million to ~ 8.9 million. Of these sequences, an average of 3.91% failed QC, 1.10% were rRNA genes, 41.25% were annotated proteins, and 57.65% were unknown proteins. To quantify N-fixation gene relative abundances, I summed all sequences annotated as *nif* genes for each sample and expressed *nif* gene relative abundance as the percentage of all annotated reads.

Taxonomy was assigned to the processed reads using the NCBI RefSeq and SILVA (version 138.1) databases. I determined community composition by analyzing the relative abundance of prokaryotic taxa that classified to at least a phylum (bacterial or archaeal). All eukaryotic taxa and any taxa unclassified to a phylum were removed from the analysis. To account for differences in sequence depth among samples, I used rarefied sequence counts. The rarefaction curves for the RefSeq data saturated, while the ones for the SILVA data did not, thus I based my interpretations and conclusions primarily on the RefSeq results.

Statistical analyses

All statistical analyses were performed in R Statistical Software (R Core Team 2021). Figures were created in R using the *ggplot2* package (Wickham, 2016). One-way analysis of variance (ANOVA; *aov* function, *stats* package; R Core Team 2021) was used to determine differences in soil geochemistry across till types. Relative abundance of prokaryotic genera was determined using the following packages: *vegan* for the rarefaction curve analysis (Oksanen et al. 2022), *funrar* for relative abundance calculation (Grenié et al. 2017), and *reshape*, *tidyr*, *plyr*, and *stringr* for data manipulation before visualizing the relative abundance (Wickham 2007; Wickham 2011; Wickham 2023; Wickham et al. 2023). Diversity was assessed using alpha (Shannon) and beta (Bray-Curtis dissimilarity) diversity metrics with the *diversity* function in the *vegan* package. One-way ANOVAs were used to determine differences in Shannon diversity by mat type. Bray-Curtis dissimilarity was calculated using the *vegdist* function in the *vegan* package after standardizing the data. A non-metric multidimensional scaling (NMDS) ordination was created with permutational analysis of variance (PERMANOVA) to assess differences in prokaryotic community composition between mat type (*metaMDS* and *adonis2* functions, *vegan* package). One-way ANOVAs were also performed for AFDM and pigment concentrations by mat type. I used principal components analysis (PCA) to visualize the relative abundance of pigments across sites (*princomp* function, *stats* package; *envfit* function, *vegan* package), and I used PERMANOVA on the standardized data to assess mat type differences with euclidean distance matrices. The relationships between metagenomic-derived *nifH* relative abundance and the qPCR-derived number of *nifH* genes for soils and microbial mats were assessed using Pearson correlation coefficients (r). Differences in *nif* and *nifH* gene abundance for the soils and microbial mats were assessed by mat type using one-way ANOVAs. I applied polynomial

regressions between AFDM and SOC, TN, and the relative abundance of *nif* in soils. Assumptions of polynomial regression were assessed and met, including normality (Q-Q plot assessment, Shaprio-Wilk Normality Test; *shapiro.test* function, *stats* package), homoscedasticity (Breusch-Pagan Test; *bptest* function, *lmtest* package; Zeileis & Hothorn, 2002), and no autocorrelation (Durbin-Watson Test; *dwtest* function, *lmtest* package). Spearman correlation coefficients (ρ) were calculated to assess relationships between inorganic P of the underlying soils and microbial mat parameters including AFDM, relative abundance of *nif*, and pigment concentrations of chlorophyll-a, scytonemin, β-carotene, and canthaxanthin since the distribution of these data did not meet the assumptions required for parametric analyses. I also used PCA to visualize variation in N and P availability, AFDM, *nif* gene relative abundance, and scytonemin concentration among sites, and I assessed differences by mat type using PERMANOVA on the standardized data with euclidean distance matrices. For all statistical analyses, $P < 0.05$ was considered statistically significant.

Results

Distribution of "black" and "orange" microbial mats

Dense black microbial mats were the most conspicuous mat type in the intermittently wet environments I sampled on the Ross till where I encountered dense black mats at the margins of streams and downhill of seasonal snowpacks (Table 2.1, Figure 2.2). Orange mats are also abundant in the thalweg of the streams in this part of Taylor Valley, as has been previously described (Alger et al. 1997; Howard-Williams et al. 1986; Kohler et al. 2015), but they were not apparent in the drier "terrestrial" environments I examined in this study. The Taylor tills had a lower abundance of microbial mats overall in comparison to the Ross till. Unlike the Ross till, I was able to identify and sample orange mat communities on the Taylor tills outside of the

thalweg of streams, typically on hillslopes downhill from large snowpacks that feed ephemeral "wetland" landscapes, *e.g.*, landscapes that do not support flowing surface water in most years, like the Wormherder Creek wetland (Harris et al. 2007; Wlostowski et al. 2019). Black mats were less common on the Taylor tills but found along ephemeral stream margins. I sought to collect an equal distribution of black and orange mats across the till types, however, the natural distribution of mat types resulted in an asymmetrical distribution of mat types across the till sequences.

Soil geochemical characterization below microbial mats

Soil geochemical characteristics below microbial mats varied among the plots, mainly associated with differences between Ross and Taylor tills. Soil pH, inorganic P, SOC, and TN were significantly higher in samples collected from the Ross compared to the Taylor tills (ANOVA, $P < 0.05$; Table 2.3). For example, Ross till soil contained 4× more inorganic P compared to the Taylor tills, with an average of 2.36 μg P g^{-1} dry soil compared to 0.60 μg P g^{-1} dry soil , and 4× lower N:P than the Taylor till samples. The average N:P (by mass) of the Ross and Taylor till samples were 0.87 and 3.78, respectively. SOC was 2× higher in the Ross till samples compared to the Taylor tills, with an average of 1.79 mg C g^{-1} dry soil compared to 0.85 mg C g^{-1} dry soil. TN was also 2× higher in the Ross till samples compared to the Taylor tills, with an average of 0.19 mg N g^{-1} dry soil compared to 0.11 mg N g^{-1} dry soil. Soil GWC, EC, NH_4^+, NO_3^-, SO_4^{2-}, and Cl^- were not significantly different between the Ross and Taylor till samples (Table 2.3).

Community composition of microbial mats

Community composition varied among the microbial mat samples, mainly associated with differences between black and orange mats. I based my interpretation and conclusions

primarily on RefSeq because while the SILVA database is more widely used for taxonomic assignments from metagenomic data, only RefSeq sequences achieved rarefaction. Both methods generated similar results with only small differences in relative abundance at the phylum level (primarily for Cyanobacteria, Proteobacteria, and Bacteroidetes; Figure 2.3a, 2.4a) and no meaningful differences at the genus level, which were dominated by cyanobacteria taxa (Figure 2.3b, 2.4b).

At the phylum level, all microbial mat types sampled consisted primarily of a mix of Cyanobacteria, Proteobacteria, and Bacteroidetes (Figure 2.3). In black mats of both the Ross and Taylor tills, Proteobacteria were the most abundant phyla, followed by Cyanobacteria and Bacteroidetes (Figure 2.3a). In contrast, orange mats were dominated by Cyanobacteria at the phylum level. At the genus level, every microbial mat sample contained a large proportion of rare genera (*i.e.*, genera constituting less than 1.4% of sequences), contributing to more than 50% of the relative abundance in the majority of the samples (Figure 2.3b). Black mats had a greater proportion of rare genera compared to orange mats. The cyanobacteria in black mats were predominately *Nostoc*, while in orange mats, *Oscillatoria* were typically the most abundant taxa followed by *Nostoc* and *Cyanothece*. Shannon Diversity was significantly greater in black mats with an average of 5.19, compared to an average Shannon Diversity of 4.17 in orange mat communities (ANOVA, $P < 0.05$). Black and orange mat community composition was significantly different (PERMANOVA, $P = 0.001$) and NMDS visualization using Bray-Curtis distances showed clear separation of communities based on mat type (Figure 2.5).

Organic matter content and pigment characterization of microbial mats

Organic matter content as AFDM and pigment concentration varied among the samples, mainly associated with differences in black and orange microbial mats. AFDM ranged over an

order of magnitude from 12.7 to 185.8 mg g^{-1} dry mat and was significantly different in black vs. orange mats (ANOVA, $P < 0.05$; Table 2.4). Black microbial mats contained 3× the mass of organic matter than orange mats, with an average of 78.5 mg AFDM g^{-1} dry mat.

The microbial mats sampled contained photosynthetic and accessory pigments common to many cyanobacteria: chlorophylls, multiple carotenoids, and extracellular sheath pigments. Out of 23 pigments analyzed using HPLC (Table 2.2), nine pigments had detectable concentrations present within the sampled microbial mats (Table 2.4). Pigment concentration and composition was significantly different between black and orange mats. Black mats had an overall greater pigment amount (Table 2.4), while orange mats had greater variation in pigment type (Figure 2.6).

Black microbial mats had 68× the total pigment concentration (267.5 μg g^{-1} dry mat on average) of orange mats (3.9 μg g^{-1} dry mat on average; ANOVA, $P < 0.001$; Table 2.4). Scytonemin, reduced scytonemin, myxoxanthophyll, and β-carotene concentration were significantly different between black and orange mats (ANOVA, $P < 0.05$; Table 2.4). Black mat pigment composition was dominated by scytonemin, which totaled to > 83% of the total pigment relative abundance, on average. Black mats contained 165× the concentration of scytonemin compared to orange mats, with an average of 225.3 μg g^{-1} dry mat. Similarly, black mats also contained a greater reduced scytonemin concentration: 35× the amount measured in orange mats. Black mats contained 6× the concentration of β-carotene than orange mats; however, β-carotene accounted for a greater relative abundance of the total pigment abundance of orange mats. Similarly, black mats contained, on average, a greater concentration of chlorophyll-a, while the relative abundance of chlorophyll-a was greater in orange mats. Multivariate visualization (PCA) of pigment relative abundance illustrates statistically significant differences among black and

orange microbial mat communities based on microbial mat type (PERMANOVA, $P = 0.001$), with orange mats containing a greater variation in pigment type (Figure 2.6). For example, three of the orange mat samples contained myxoxanthophyll (T12, T13, T14) while none of the black mat samples did.

Many of these pigments are photoprotective pigments that are important for microbial communities in the UV-intense McMurdo Dry Valleys, especially for "terrestrial" communities that are not inundated by water to aid in light absorption (Vincent et al. 1993). Scytonemin is a photoprotective, extracellular sheath pigment (Garcia-Pichel et al. 1992) which dominates black and orange mats. Differences in pigment composition were associated with differences in taxonomic composition even within black and orange mats. For example, samples R08 and T13 are notable outliers in the ordination of pigment content (Figure 2.6). T13 contained the lowest relative abundance of scytonemin (10.7%) and the highest relative abundance of myxoxanthophyll (8.5%). Field observations indicated that R08 was a dense colony of *Nostoc* with a reddish color in contrast to the other black mat samples and had the highest concentration of canthaxanthin (2.9 μg g^{-1} dry mat; 1% relative abundance), an orange-red ketocarotenoid. The taxonomic composition of R08 was also different from most of the other sampled black mats, with less rare taxa present and the highest relative abundance of *Nostoc*.

Nif gene characterization of microbial mats and soils

There was a significant linear correlation between the metagenomic-derived *nifH* relative abundance and the qPCR-derived number of *nifH* genes for soils ($r = 0.73$; $P < 0.01$) and microbial mats ($r = 0.72$; $P < 0.01$). The gene copy number and relative abundance of *nif* and *nifH* for mats and underlying soils (from both qPCR and metagenomics methods) were significantly different between black and orange mats (ANOVA, $P < 0.05$; Table 2.5). Overall,

black microbial mats had a greater gene copy number and relative abundance of *nif* and *nifH* genes compared to orange mats.

Relationships among microbial mats and underlying soil geochemistry

Significant correlations between the microbial mats and the soils underlying them were apparent, particularly in the mat characteristics (*i.e.*, AFDM and pigment content) and the soil geochemistry. Soil inorganic P was significantly correlated with mat AFDM, *nif*, chlorophyll-a and β-carotene concentration ($\rho = 0.53$, 0.58, 0.57, and 0.63, respectively, $P < 0.05$; Table 2.6). Additionally, the AFDM of the microbial mats was positively correlated with SOC, TN, and the relative abundance of *nif* in the soils ($R^2 = 0.66$, $P < 0.001$; $R^2 = 0.57$, $P < 0.01$; $R^2 = 0.44$, $P < 0.05$, respectively; Figure 2.7). A PCA ordination of N and P availability, AFDM, *nif* relative abundance, and scytonemin concentration exhibits statistically significant separation of microbial mat types (PERMANOVA, $P = 0.001$), with black mats containing a greater variation in biogeochemical parameters (Figure 2.8). This ordination illustrates a strong association between the black mat samples and inorganic P and TN, while orange mat samples were unrelated to variation in inorganic P and TN.

Discussion

Microbial mats are found globally in a range of ecosystems, including extreme environments (*e.g.*, polar deserts, hydrothermal hot springs, hypersaline lakes) where these communities are often the dominant primary producers (Prieto-Barajas et al. 2018). In the McMurdo Dry Valleys, microbial mats inhabit a range of environments where hydrology and salinity influence their abundance and activity (Power et al. 2024b). In this study, I focused on microbial mats that occurred on the margins of streams, wetlands, and downhill from melting seasonal snow patches in seasonally moist environments. I assessed the relationships between the

mats and underlying soil and developed a conceptual model to illustrate these interacting components for a synoptic understanding of the recursive relationship between microbial mats and underlying soil ecosystems (Figure 2.9). Here, I discuss how landscape history and till composition of Taylor Valley influence soil chemistry, which in part influences microbial mat distribution and composition, and how the presence of microbial mats influences the underlying soil chemistry.

Till composition influences soil chemistry and microbial mats

The landscape history of the Taylor Valley has created a geochemical gradient in inorganic N and P along the longitudinal axis of the valley, *i.e.*, east to west. The terrestrial surfaces of the younger Ross tills in the east and more coastal region have greater P availability due to higher apatite in the till clast composition and possibly greater weathering (Bate et al. 2008), and have typically less abundant inorganic N in comparison to the terrestrial surfaces of the older Taylor tills which accumulated more nitrate from long-term N deposition (Barrett et al. 2007; Michalski et al. 2005). My data show that soils underlying microbial mats on the Ross till contained significantly more inorganic P in comparison to the soils underlying microbial mats on the Taylor tills (Table 2.3), but inorganic N content was not significantly different between the Ross and Taylor tills, likely due to the flushing of N in these intermittently wet environments where microbial mats are most commonly encountered. Interpreting these observations through the lens of landscape history provides better understanding of the contemporary variation in microbial mat composition and functioning.

In the intermittently wet environments that I sampled, black microbial mats were more common on the Ross tills, while orange mats were more common on the Taylor tills. The utility of this color typology is validated by my data showing the prokaryotic community composition

was distinct between the two mat types (Figure 2.3). Specifically, *Nostoc*-dominated "black" mats, regardless of underlying till composition, hosted a complex and diverse community of autotrophic and heterotrophic microbes across many bacterial phyla with a high proportion of rare taxa, while the orange mats consisted primarily of cyanobacteria (*Oscillatoria*) and had lower Shannon diversity (Figure 2.3). This clear distinction in microbial diversity (Figure 2.5) and the associated variation in pigment content and composition (Figure 2.6) supports a binary analysis of the different characteristics of these two mat types and their potential influences on underlying soil properties and processes. For example, black microbial mats contained significantly more organic matter in the form of AFDM, higher absolute and proportional scytonemin content, as well as higher N-fixation potential and appeared to be preferentially located on P-rich soils (Table 2.4, 2.5). Moreover, P concentration was significantly correlated to microbial mat biomass (AFDM), N-fixation potential, and pigment concentration (Table 2.6). While the asymmetrical distribution of black and orange mats across the two tills prevents conclusive inferences about the influence of geochemistry on microbial mat distribution and activity, I hypothesize that the greater abundance of P on the Ross till may select for a greater abundance of strong N-fixers, such as *Nostoc*.

Microbial mats enrich underlying soil organic matter

While my data show that the geochemical gradient in inorganic P along the Taylor Valley is a factor influencing microbial mat distribution, microbial mats also make significant contributions to the chemical composition of the underlying soils, including greater SOC and TN (Figure 2.7). Although in this study I did not sample soils from uncolonized areas, previous studies conducted in the same general area and on the same tills have reported 4× less SOC on uncolonized areas (0.43 mg C g^{-1} dry soil on the Ross tills and 0.19 mg C g^{-1} dry soil on the

Taylor tills; Barrett et al. 2006a) compared to the SOC values I estimated beneath microbial mats (1.79 mg C g^{-1} dry soil on the Ross tills and 0.85 mg C g^{-1} dry soil on the Taylor tills; Table 2.3). Similarly, soils without microbial mats were shown to contain 3 - 9× less TN (0.02 mg N g^{-1} dry soil on the Ross tills and 0.03 mg N g^{-1} dry soil on the Taylor tills; Barrett et al. 2006a) compared to the TN values I estimated here for soils underlying microbial mats (0.19 mg N g^{-1} dry soil on the Ross tills and 0.11 mg N g^{-1} dry soil on the Taylor tills; Table 2.3).

All samples contained a high abundance of *nif* and *nifH* genes, suggesting a strong N-fixation potential in both black and orange microbial mats, as has been previously shown primarily for black microbial mats in the McMurdo Dry Valleys (*e.g.*, Coyne et al. 2020; Kohler et al. 2018, 2023). And while all nine of the most abundant genera of the black and orange mats are listed as common N-fixers, both metagenomic approaches and qPCR indicated that the *Nostoc*-dominated black mats had significantly greater N-fixation potential than the *Oscillatoria*-dominated orange mats, as has been previously reported (Coyne et al. 2020; Howard-Williams et al. 1989; Kohler et al. 2018). The high N-fixation potential of these mat types helps explain the higher TN content in the underlying soils due to N-fixation of the overlaying microbial mats.

Aquatic microbial mats influence stream chemistry in the Taylor Valley (*e.g.*, Kohler et al. 2018; McKnight et al. 2004) through biological uptake, recycling, and export downstream. For example, using stable isotope approaches, Kohler et al. (2018) showed that black mats were the dominant N-fixer in Von Guerard Stream and the Relict Channel and that N was repeatedly recycled and assimilated downstream as other sources of N were exhausted. My data show that terrestrial microbial mats at the margins of streams also influence underlying soil geochemistry. While the differences in P are of entirely geochemical origin from the weathering of greater

apatite content on the Ross Sea Till (Bate et al. 2008), the greater TN found in the soils underlying microbial mats is likely of biotic origin from N-fixation of the mats.

Differences in N-fixation potential may also illuminate microbial responses to physical stressors in the Antarctic environment, such as UV radiation. For example, Fleming & Castenholz (2008) reported a connection between scytonemin concentration and synthesis to N source and availability. In a laboratory experiment they showed that *Nostoc* synthesized significantly more scytonemin while fixing N than when utilizing available nitrate or ammonium (Fleming & Castenholz 2008). Fleming & Castenholz (2008) hypothesized that greater production in scytonemin following a greater restriction in N availability was due to sensitivity to UV radiation resulting from N limitation which acts as a signal to determine the amount of scytonemin to synthesize (Fleming & Castenholz 2008). In my field-based studies, I found a significant, positive correlation between scytonemin concentration and *nif* relative abundance as N-fixation potential ($r = 0.56$, $P < 0.05$; Figure 2.8). Although a mechanism remains unexamined, I hypothesize that this relationship may also be associated with greater UV stress under conditions of N limitation. The McMurdo Dry Valleys experience exceptionally high UV radiation, and it is possible that the increase in scytonemin with mats that have a higher N-fixation potential is due to a greater photosensitivity. Alternatively, scytonemin may be produced in larger quantities to protect the nitrogenase enzyme complex, which has been shown to be sensitive to UV radiation (Kumar et al. 2003; Singh et al. 2023).

Microbial mats are composed of diverse organisms which fix both C and N and contribute leached organic matter and nutrients into stream water and also underlying soils and thereby support diverse soil and sediment communities (Kohler et al. 2018, Moorhead et al. 2003, Simmons et al. 2009; Stanish et al., 2011). Moreover, previous work has also shown that

microbial mats have a homogenizing effect on the underlying soil bacteria communities in this region (Risteca 2023). These results and previous studies support the notion that microbial mats impart an "island of fertility" effect (Schlesinger et al. 1990) on local soils and sediments through their influence on organic matter availability, nitrogen (Hawes et al. 1992), and in promoting diverse soil fauna communities (*e.g.*, nematodes, tardigrades, rotifers, and ciliates; Simmons et al. 2009). In addition to influencing soil nutrient cycles and community composition, microbial mats can also influence soil hydrology due to their low permeability which promotes higher moisture content in the soils below (Perillo et al. 2019) and provide shelter from wind and UV radiation. These are essential functions, especially in the harsh and nutrient poor terrestrial environment of the McMurdo Dry Valleys. Current changes (Barrett et al. 2024; Nielsen et al. 2023, 2024) and anticipated changes in climate and hydrology (Vignon et al. 2021) will have an unknown influence on the distribution and activity of microbial mats in the McMurdo Dry Valleys. For example, greater snowfall or even rain in a potentially warmer region would likely expand microbial mat habitat to currently arid and inactive soils, while increased foehn winds and associated drier conditions could decrease low-density microbial mats in currently marginal habitats. Any future changes in microbial mat distribution and activity will likely have marked effects on underlying soil biota and chemistry.

Data Availability Statement

All data presented in this study are archived in the Environmental Data Initiative (EDI) repository (Power, Osburn, & Barrett, 2024). Metagenomic sequences are available on the MG-RAST database under project ID mgp95386: https://www.mg-rast.org/linkin.cgi?project=mgp95386.

Ethics Statement

Permission to enter the Canada Glacier Antarctic Specially Protected Area (ASPA 131) and sample soil and microbial mat was given by the National Science Foundation Division of Polar Programs through Antarctic Conservation Act Permit.

Funding Statement

This work was supported by the National Science Foundation (NSF) through grants #1637708 and #2224760 to the McMurdo Dry Valleys Long Term Ecological Research Project.

Acknowledgments

I acknowledge Antarctic Support Contractors and Air Center Helicopters for providing essential operational support in the field. I would also like to thank Bobbie Niederlehner (Virginia Tech) for her assistance with analytical chemistry techniques and Karen Rossignol (Paerl Lab, University of North Carolina - Chapel Hill Institute of Marine Sciences) for leading the HPLC analysis on the pigment samples. Additionally, Cayelan Carey, Erin Hotchkiss, and Ernie Osburn provided valuable comments during revision.

References

Alger, A.S., McKnight, D.M., Spalding, S.A., Tate, C.M., Shupe, G.H., Welch, K.A., Edwards, R., Andrews, E.D., House, H.R., 1997. Ecological Processes in a Cold Desert Ecosystem: The Abundance and Species Distribution of Algal Mats in Glacial Meltwater Streams in Taylor Valley, Antarctica. Institute of Arctic and Alpine Research Occasional Paper 51.

Ando, S., Goto, M., Meunchang, S., Thongra-ar, P., Fujiwara, T., Hayashi, H., Yoneyama, T., 2005. Detection of nifH Sequences in sugarcane (Saccharum officinarum L.) and pineapple (Ananas comosus [L.] Merr.). Soil Sci. Plant Nutr. 51, 303–308. https://doi.org/10.1111/j.1747-0765.2005.tb00034.x

Barrett, J.E., Adams, B.J., Doran, P.T., Dugan, H.A., Myers, K.F., Salvatore, M.R., Power, S.N., Snyder, M.D., Wright, A.T., Gooseff, M.N., 2024. Response of a Terrestrial Polar Ecosystem to the March 2022 Antarctic Weather Anomaly. Earths Future 12, e2023EF004306. https://doi.org/10.1029/2023EF004306

Barrett, J.E., Virginia, R.A., Hopkins, D.W., Aislabie, J., Bargagli, R., Bockheim, J.G., Campbell, I.B., Lyons, W.B., Moorhead, D.L., Nkem, J.N., Sletten, R.S., Steltzer, H., Wall, D.H., Wallenstein, M.D., 2006a. Terrestrial ecosystem processes of Victoria Land, Antarctica. Soil Biol. Biochem. 38, 3019–3034. https://doi.org/10.1016/J.SOILBIO.2006.04.041

Barrett, J.E., Virginia, R.A., Lyons, W.B., Mcknight, D.M., Priscu, J.C., Doran, P.T., Fountain, A.G., Wall, D.H., Moorhead, D.L., 2007. Biogeochemical stoichiometry of Antarctic Dry Valley ecosystems. J. Geophys. Res. 112. https://doi.org/10.1029/2005JG000141

Barrett, J.E., Virginia, R.A., Parsons, A.N., Wall, D.H., 2006b. Soil carbon turnover in the McMurdo Dry Valleys, Antarctica. Soil Biol. Biochem. 38, 3065–3082. https://doi.org/10.1016/j.soilbio.2006.03.025

Bate, D.B., Barrett, J.E., Poage, M.A., Virginia, R.A., 2008. Soil phosphorus cycling in an Antarctic polar desert. Geoderma 144, 21–31. https://doi.org/10.1016/J.GEODERMA.2007.10.007

Bockheim, J.G., Prentice, M.L., McLeod, M., 2008. Distribution of glacial deposits, soils, and permafrost in Taylor Valley, Antarctica. Arct. Antarct. Alp. Res. 40, 279–286. https://doi.org/10.1657/1523-0430(06-057)[BOCKHEIM]2.0.CO;2

Bolhuis, H., Cretoiu, M.S., Stal, L.J., 2014. Molecular ecology of microbial mats. FEMS Microbiol. Ecol. 90, 335–350. https://doi.org/10.1111/1574-6941.12408

Burkins, M.B., Virginia, R.A., Chamberlain, C.P., Wall, D.H., 2000. Origin and Distribution of

Soil Organic Matter in Taylor Valley, Antarctica. Ecology 81, 2377–2391. https://doi.org/10.1890/0012-9658(2000)081[2377:OADOSO]2.0.CO;2

Coyne, K.J., Parker, A.E., Lee, C.K., Sohm, J.A., Kalmbach, A., Gunderson, T., León-Zayas, R., Capone, D.G., Carpenter, E.J., Cary, S.C., 2020. The distribution and relative ecological roles of autotrophic and heterotrophic diazotrophs in the McMurdo Dry Valleys, Antarctica. FEMS Microbiol. Ecol. 96, fiaa010. https://doi.org/10.1093/femsec/fiaa010

Davey, M.E., O'toole, G.A., 2000. Microbial biofilms: From ecology to molecular genetics. Microbiol. Mol. Biol. Rev. 64, 847–867. https://doi.org/10.1128/mmbr.64.4.847-867.2000

Denton, G.H., Bockheim, J.G., Wilson, S.C., Stuiver, M., 1989. Late Wisconsin and early Holocene glacial history, inner Ross Embayment, Antarctica. Quat. Res. 31, 151–182. https://doi.org/10.1016/0033-5894(89)90004-5

Fleming, E.D., Castenholz, R.W., 2008. Effects of nitrogen source on the synthesis of the UV-screening compound, scytonemin, in the cyanobacterium Nostoc punctiforme PCC 73102. FEMS Microbiol. Ecol. 63, 301–308. https://doi.org/10.1111/j.1574-6941.2007.00432.x

Fountain, A.G., Nylen, T.H., Monaghan, A., Basagic, H.J., Bromwich, D., 2010. Snow in the McMurdo Dry Valleys, Antarctica. Int. J. Climatol. 30, 633–642. https://doi.org/10.1002/joc.1933

Gaby, J.C., Buckley, D.H., 2017. The use of degenerate primers in qPCR analysis of functional genes can cause dramatic quantification bias as revealed by investigation of nifH primer performance. Microb. Ecol. 74, 701–708. https://doi.org/10.1007/s00248-017-0968-0

Garcia-Pichel, F., Sherry, N.D., Castenholz, R.W., 1992. Evidence for an ultraviolet sunscreen role of the extracellular pigment scytonemin in the terrestrial cyanobacterium

Chlorogloeopsis sp. Photochem. Photobiol. 56, 17–23.

Gooseff, M.N., Barrett, J.E., Levy, J.S., 2013. Shallow groundwater systems in a polar desert, McMurdo Dry Valleys, Antarctica. Hydrogeol. J. 21, 171–183. https://doi.org/10.1007/s10040-012-0926-3

Gooseff, M.N., McKnight, D.M., Lyons, W.B., Blum, A.E., 2002. Weathering reactions and hyporheic exchange controls on stream water chemistry in a glacial meltwater stream in the McMurdo Dry Valleys. Water Resour. Res. 38, 15–1–15–17. https://doi.org/10.1029/2001wr000834

Gooseff, M.N., McKnight, D.M., Runkel, R.L., Duff, J.H., 2004. Denitrification and hydrologic transient storage in a glacial meltwater stream, McMurdo Dry Valleys, Antarctica. Limnol. Oceanogr. 49, 1884–1895. https://doi.org/10.4319/lo.2004.49.5.1884

Gooseff, M.N., McKnight, D.M., Runkel, R.L., Vaughn, B.H., 2003. Determining long time-scale hyporheic zone flow paths in Antarctic streams. Hydrol. Process. 17, 1691–1710. https://doi.org/10.1002/hyp.1210

Grenié, M., Denelle, P., Tucker, C.M., Munoz, F., Violle, C., 2017. funrar: An R package to characterize functional rarity. Diversity and Distributions, 10.1111/ddi.12629.

Guerrero, R., Piqueras, M., Berlanga, M., 2002. Microbial mats and the search for minimal ecosystems. Int. Microbiol. 5, 177–188. https://doi.org/10.1007/s10123-002-0094-8

Harris, K.J., Carey, A.E., Berry Lyons, W., Welch, K.A., Fountain, A.G., 2007. Solute and isotope geochemistry of subsurface ice melt seeps in Taylor Valley, Antarctica. GSA Bulletin 119, 548–555. https://doi.org/10.1130/B25913.1

Hawes, I., Howard-Williams, C., Vincent, W., 1992. Desiccation and recovery of antarctic cyanobacterial mats. Polar Biol. 12, 587–594. https://doi.org/10.1007/BF00236981

Howard-Williams, C., Priscu, J.C., Vincent, W.F., 1989. Nitrogen dynamics in two antarctic streams. Hydrobiologia 172, 51–61. https://doi.org/10.1007/bf00031612

Howard-Williams, C., Vincent, C.L., Broady, P.A., Vincent, W.F., 1986. Antarctic Stream Ecosystems: Variability in Environmental Properties and Algal Community Structure. Internationale Revue der gesamten Hydrobiologie und Hydrographie 71, 511–544. https://doi.org/10.1002/iroh.19860710405

Jeffrey, S.W., Mantoura, R.F.C., Wright, S.W., 1997. Phytoplankton pigments in oceanography: Guidelines to modern methods. UNESCO Publishing, Paris, France.

Jungblut, A.D., Neilan, B.A., 2010. NifHgene diversity and expression in a microbial mat community on the McMurdo Ice Shelf, Antarctica. Antarct. Sci. 22, 117–122. https://doi.org/10.1017/s0954102009990514

Kohler, T.J., Singley, J.G., Wlostowski, A.N., McKnight, D.M., 2023. Nitrogen fixation facilitates stream microbial mat biomass across the McMurdo Dry Valleys, Antarctica. Biogeochemistry 166, 247–268. https://doi.org/10.1007/s10533-023-01069-0

Kohler, T.J., Stanish, L.F., Crisp, S.W., Koch, J.C., Liptzin, D., Baeseman, J.L., McKnight, D.M., 2015. Life in the Main Channel: Long-Term Hydrologic Control of Microbial Mat Abundance in McMurdo Dry Valley Streams, Antarctica. Ecosystems 18, 310–327. https://doi.org/10.1007/s10021-014-9829-6

Kohler, T.J., Stanish, L.F., Liptzin, D., Barrett, J.E., McKnight, D.M., 2018. Catch and release: Hyporheic retention and mineralization of N-fixing Nostoc sustains downstream microbial mat biomass in two polar desert streams. Limnology and Oceanography Letters 3, 357–364. https://doi.org/10.1002/lol2.10087

Kumar, A., Tyagi, M.B., Jha, P.N., Srinivas, G., Singh, A., 2003. Inactivation of cyanobacterial

nitrogenase after exposure to ultraviolet-B radiation. Curr. Microbiol. 46, 380–384. https://doi.org/10.1007/s00284-001-3894-8

Knepel, K., 2003. Determination of nitrate in 2 M KCl soil extracts by flow injection analysis. QuikChem method 12-107-04-1-B. Lachat Instruments.

Lawson, J., Doran, P.T., Kenig, F., Des marais, D.J., Priscu, J.C., 2004. Stable Carbon and Nitrogen Isotopic Composition of Benthic and Pelagic Organic Matter in Lakes of the McMurdo Dry Valleys, Antarctica. Aquat. Geochem. 10, 269–301. https://doi.org/10.1007/s10498-004-2262-2

Levy, J.S., 2013. How big are the McMurdo Dry Valleys? Estimating ice-free area using Landsat image data. Antarct. Sci. 25, 119–120. https://doi.org/10.1017/S0954102012000727

Mantoura, R.F.C., Llewellyn, C.A., 1983. The rapid determination of algal chlorophyll and carotenoid pigments and their breakdown products in natural waters by reverse-phase high-performance liquid chromatography. Anal. Chim. Acta 151, 297–314. https://doi.org/10.1016/s0003-2670(00)80092-6

Maurice, P.A., McKnight, D.M., Leff, L., Fulghum, J.E., Gooseff, M., 2002. Direct observations of aluminosilicate weathering in the hyporheic zone of an Antarctic Dry Valley stream. Geochim. Cosmochim. Acta 66, 1335–1347. https://doi.org/10.1016/s0016-7037(01)00890-0

McKnight, D.M., Niyogi, D.K., Alger, A.S., Bomblies, A., Conovitz, P.A., Tate, C.M., 1999. Dry Valley Streams in Antarctica: Ecosystems Waiting for Water. Bioscience 49, 985–995. https://doi.org/10.1525/bisi.1999.49.12.985

McKnight, D.M., Runkel, R.L., Tate, C.M., Duff, J.H., Moorhead, D.L., 2004. Inorganic N and P dynamics of Antarctic glacial meltwater streams as controlled by hyporheic exchange and

benthic autotrophic communities. J. North Am. Benthol. Soc. 23, 171–188. https://doi.org/10.1899/0887-3593(2004)023<0171:INAPDO>2.0.CO;2

Mcknight, D.M., Tate, C.M., Andrews, E.D., Niyogi, D.K., Cozzetto, K., Welch, K., Lyons, W.B., Capone, D.G., 2007. Reactivation of a cryptobiotic stream ecosystem in the McMurdo Dry Valleys, Antarctica: A long-term geomorphological experiment. Geomorphology 89, 186–204. https://doi.org/10.1016/j.geomorph.2006.07.025

Meyer, F., Paarmann, D., D'Souza, M., Olson, R., Glass, E.M., Kubal, M., Paczian, T., Rodriguez, A., Stevens, R., Wilke, A., Wilkening, J., Edwards, R.A., 2008. The metagenomics RAST server - a public resource for the automatic phylogenetic and functional analysis of metagenomes. BMC Bioinformatics 9, 386. https://doi.org/10.1186/1471-2105-9-386

Michalski, G., Bockheim, J.G., Kendall, C., Thiemens, M., 2005. Isotopic composition of Antarctic Dry Valley nitrate: Implications for NOy sources and cycling in Antarctica. Geophys. Res. Lett. 32. https://doi.org/10.1029/2004GL022121

Moorhead, D.L., Barrett, J.E., Virginia, R.A., Wall, D.H., Porazinska, D., 2003. Organic matter and soil biota of upland wetlands in Taylor Valley, Antarctica. Polar Biol. 26, 567–576. https://doi.org/10.1007/s00300-003-0524-x

Nielsen, E.B., Katurji, M., Zawar-Reza, P., Cullen, N.J., 2024. Air temperature trends and extreme warming events across regions of Antarctica for the period 2003-2021. ESS Open Archive. https://doi.org/10.22541/essoar.171926315.55910608/v1

Nielsen, E.B., Katurji, M., Zawar-Reza, P., Meyer, H., 2023. Antarctic daily mesoscale air temperature dataset derived from MODIS land and ice surface temperature. Sci Data 10, 833. https://doi.org/10.1038/s41597-023-02720-z

Obryk, M.K., Doran, P.T., Fountain, A.G., Myers, M., McKay, C.P., 2020. Climate From the McMurdo Dry Valleys, Antarctica, 1986–2017: Surface Air Temperature Trends and Redefined Summer Season. J. Geophys. Res. D: Atmos. 125, e2019JD032180. https://doi.org/10.1029/2019JD032180

Oksanen J., Simpson, G.L., Blanchet, F.G., Kindt, R., Legendre, P., Minchin, P.R., O'Hara, R.B., Solymos, P., Stevens, M.H.H., Szoecs, E., Wagner, H., Barbour, M., Bedward, M., Bolker, B., Borcard, D., Carvalho, G., Chirico, M., Caceres, M.D., Durand, S., Evangelista, H.B.A., FitzJohn, R., Friendly, M., Furneaux, B., Hannigan, G., Hill, M.O., Lahti, L., McGlinn, D., Ouellette, M., Cunha, E.R., Smith, T., Stier, A., Ter Braak, C.J.F., Weedon, J. 2022. vegan: Community Ecology Package. R package version 2.6-4. https://CRAN.R-project.org/package=vegan

Overbeek, R., Olson, R., Pusch, G.D., Olsen, G.J., Davis, J.J., Disz, T., Edwards, R.A., Gerdes, S., Parrello, B., Shukla, M., Vonstein, V., Wattam, A.R., Xia, F., Stevens, R., 2014. The SEED and the Rapid Annotation of microbial genomes using Subsystems Technology (RAST). Nucleic Acids Res. 42, D206–14. https://doi.org/10.1093/nar/gkt1226

Paerl, H.W., Priscu, J.C., 1998. Microbial phototrophic, heterotrophic, and diazotrophic activities associated with aggregates in the permanent ice cover of lake Bonney, Antarctica. Microb. Ecol. 36, 221–230. https://doi.org/10.1007/s002489900109

Parker, B.C., Simmons, G.M., Jr, Wharton, R.A., Jr, Seaburg, K.G., Love, F.G., 1982. REMOVAL OF ORGANIC AND INORGANIC MATTER FROM ANTARCTIC LAKES BY AERIAL ESCAPE OF BLUEGREEN ALGAL MATS1. J. Phycol. 18, 72–78. https://doi.org/10.1111/j.1529-8817.1982.tb03158.x

Perillo, V.L., Maisano, L., Martinez, A.M., Quijada, I.E., Cuadrado, D.G., 2019. Microbial mat

contribution to the formation of an evaporitic environment in a temperate-latitude ecosystem. J. Hydrol. (Amst.) 575, 105–114. https://doi.org/10.1016/j.jhydrol.2019.05.027

Pfaff J.D., 1993. The Determination of Inorganic Anions by Ion Chromatography, Method 300.0, Rev 2.1. U.S. Environmental Protection Agency: Cincinnati, OH. https://www.epa.gov/sites/production/files/2015-08/documents/method_300-0_rev_2-1_1993.pdf

Power, S.N., Salvatore, M.R., Sokol, E.R., Stanish, L.F., Barrett, J.E., 2020. Estimating microbial mat biomass in the McMurdo Dry Valleys, Antarctica using satellite imagery and ground surveys. Polar Biol. 43, 1753–1767. https://doi.org/10.1007/s00300-020-02742-y

Power, S.N., Salvatore, M.R., Sokol, E.R., Stanish, L.F., Borges, S.R., Adams, B.J., Barrett, J.E., 2024a. Remotely characterizing photosynthetic biocrust in snowpack-fed microhabitats of Taylor Valley, Antarctica. Science of Remote Sensing. 9, 100120. https://doi.org/10.1016/j.srs.2024.100120

Power, S.N., Thomas, V.A., Salvatore, M.R., Barrett, J.E., 2024b. Habitat suitability of biocrust communities in a cold desert ecosystem. Ecol. Evol. 14, e11649. https://doi.org/10.1002/ece3.11649

Power, S.N., Osburn, E.D., Barrett, J.E., 2024. Biophysicochemical properties, pigment concentrations, and nif gene counts of microbial mats and soils from Taylor and Beacon Valleys, McMurdo Dry Valleys, Antarctica (2019-2020). [Dataset] Environmental Data Initiative, 10.6073/pasta/229fad394554735fea6ad2fac4b66761.

Prieto-Barajas, C.M., Valencia-Cantero, E., Santoyo, G., 2018. Microbial mat ecosystems: Structure types, functional diversity, and biotechnological application. Electron. J.

Biotechnol. 31, 48–56. https://doi.org/10.1016/J.EJBT.2017.11.001

Prokopy, W.R., 1995. Phosphorus in 0.5 M sodium bicarbonate soil extracts. QuikChem method 12-115-01-1-B. Lachat Instruments.

R Core Team, 2021. R: A language and environment for statistical computing. R Foundation for Statistical Computing. https://www.R-project.org.

Risteca, P.J., 2023. Influence of landscape-variation in geochemistry on taxonomic and functional composition of microbial mat communities in the McMurdo Dry Valleys, Antarctica. [Masters thesis, Virginia Tech]. Available at: http://hdl.handle.net/10919/115384

Schlesinger, W.H., Reynolds, J.F., Cunningham, G.L., Huenneke, L.F., Jarrell, W.M., Virginia, R.A., Whitford, W.G., 1990. Biological feedbacks in global desertification. Science 247, 1043–1048. https://doi.org/10.1126/science.247.4946.1043

Simmons, B.L., Wall, D.H., Adams, B.J., Ayres, E., Barrett, J.E., Virginia, R.A., 2009. Terrestrial mesofauna in above-and below-ground habitats: Taylor Valley, Antarctica. Polar Biol. 32, 1549–1558. https://doi.org/10.1007/s00300-009-0639-9

Singh, V.K., Jha, S., Rana, P., Mishra, S., Kumari, N., Singh, S.C., Anand, S., Upadhye, V., Sinha, R.P., 2023. Resilience and mitigation strategies of Cyanobacteria under ultraviolet radiation stress. Int. J. Mol. Sci. 24. https://doi.org/10.3390/ijms241512381

Stal, L.J., Caumette, P. (Eds.), 2011. Microbial mats: Structure, development and environmental significance, Nato ASI Subseries G: Springer, Berlin, Germany. https://doi.org/10.1007/978-3-642-78991-5

Stanish, L.F., Nemergut, D.R., McKnight, D.M., 2011. Hydrologic processes influence diatom community composition in Dry Valley streams. J. North Am. Benthol. Soc. 30, 1057–

1073. https://doi.org/10.1899/11-008.1

Stone, M.S., Devlin, S.P., Hawes, I., Welch, K.A., Gooseff, M.N., Takacs-Vesbach, C., Morgan-Kiss, R., Adams, B.J., Barrett, J.E., Priscu, J.C., Doran, P.T., 2024. McMurdo Dry Valley lake edge “moats”: the ecological intersection between terrestrial and aquatic polar desert habitats. Antarct. Sci. 1–17. https://doi.org/10.1017/S0954102024000087

Van Heukelem, L., Lewitus, A.J., Kana, T.M., Craft, N.E., 1992. High-performance liquid chromatography of phytoplankton pigments using a polymeric reversed-phase c18 column1. J. Phycol. 28, 867–872. https://doi.org/10.1111/j.0022-3646.1992.00867.x

Van Heukelem, L., Lewitus, A., Kana, T., Craft, N., 1994. Improved separations of phytoplankton pigments using temperature-controlled high performance liquid chromatography. Marine Ecology Progress Series 114, 303–313. https://doi.org/10.3354/MEPS114303

Vignon, É., Roussel, M.-L., Gorodetskaya, I.V., Genthon, C., Berne, A., 2021. Present and future of rainfall in Antarctica. Geophys. Res. Lett. 48. https://doi.org/10.1029/2020gl092281

Vincent, W.F., Downes, M.T., Castenholz, R.W., Howard-Williams, A.C., 1993. Community structure and pigment organisation of cyanobacteria-dominated microbial mats in Antarctica. Eur. J. Phycol. 28, 213–221.

Vincent, W.F., Howard-Williams, C., 1986. Antarctic stream ecosystems: physiological ecology of a blue-green algal epilithon. Freshw. Biol. 16, 219–233. https://doi.org/10.1111/j.1365-2427.1986.tb00966.x

Walthert, L., Graf, U., Kammer, A., Luster, J., Pezzotta, D., Zimmermann, S., Hagedorn, F., 2010. Determination of organic and inorganic carbon, δ 13 C, and nitrogen in soils containing carbonates after acid fumigation with HCl. J. Plant Nutr. Soil Sci. 173, 207–

216. https://doi.org/10.1002/jpln.200900158

Welch, K.A., Lyons, W.B., Whisner, C., Gardner, C.B., Gooseff, M.N., Mcknight, D.M., Priscu, J.C., 2010. Spatial variations in the geochemistry of glacial meltwater streams in the Taylor Valley, Antarctica. Antarct. Sci. 22, 662–672. https://doi.org/10.1017/S0954102010000702

Wickham, H., 2007. Reshaping data with the reshape package. Journal of Statistical Software, 21(12).

Wickham, H., 2011. The Split-Apply-Combine Strategy for Data Analysis. Journal of Statistical Software, 40(1), 1-29. https://www.jstatsoft.org/v40/i01/.

Wickham, H., 2016. ggplot2: Elegant Graphics for Data Analysis. Springer-Verlag, New York.

Wickham, H., 2023. stringr: Simple, Consistent Wrappers for Common String Operations. R package version 1.5.1. https://CRAN.R-project.org/package=stringr

Wickham, H., Vaughan D., & Girlich, M., 2023. tidyr: Tidy Messy Data. R package version 1.3.0. https://CRAN.R-project.org/package=tidyr

Wlostowski, A.N., Gooseff, M.N., McKnight, D.M., Jaros, C., Lyons, W.B., 2016. Patterns of hydrologic connectivity in the McMurdo Dry Valleys, Antarctica: a synthesis of 20 years of hydrologic data. Hydrol. Process. 30, 2958–2975. https://doi.org/10.1002/hyp.10818

Wlostowski, A.N., Schulte, N.O., Adams, B.J., Ball, B.A., Esposito, R.M.M., Gooseff, M.N., Lyons, W.B., Nielsen, U.N., Virginia, R.A., Wall, D.H., Welch, K.A., McKnight, D.M., 2019. The hydroecology of an ephemeral wetland in the McMurdo dry valleys, Antarctica. J. Geophys. Res. Biogeosci. 124, 3814–3830. https://doi.org/10.1029/2019jg005153

Zeileis, A. & Hothorn, T., 2002. Diagnostic Checking in Regression Relationships. R News 2(3),

7-10. https://CRAN.R-project.org/doc/Rnews/

Zoumplis, A., Kolody, B., Kaul, D., Zheng, H., Venepally, P., McKnight, D.M., Takacs-Vesbach, C., DeVries, A., Allen, A.E., 2023. Impact of meltwater flow intensity on the spatiotemporal heterogeneity of microbial mats in the McMurdo Dry Valleys, Antarctica. ISME Commun. 3, 3. https://doi.org/10.1038/s43705-022-00202-8

Figures

Figure 2.1

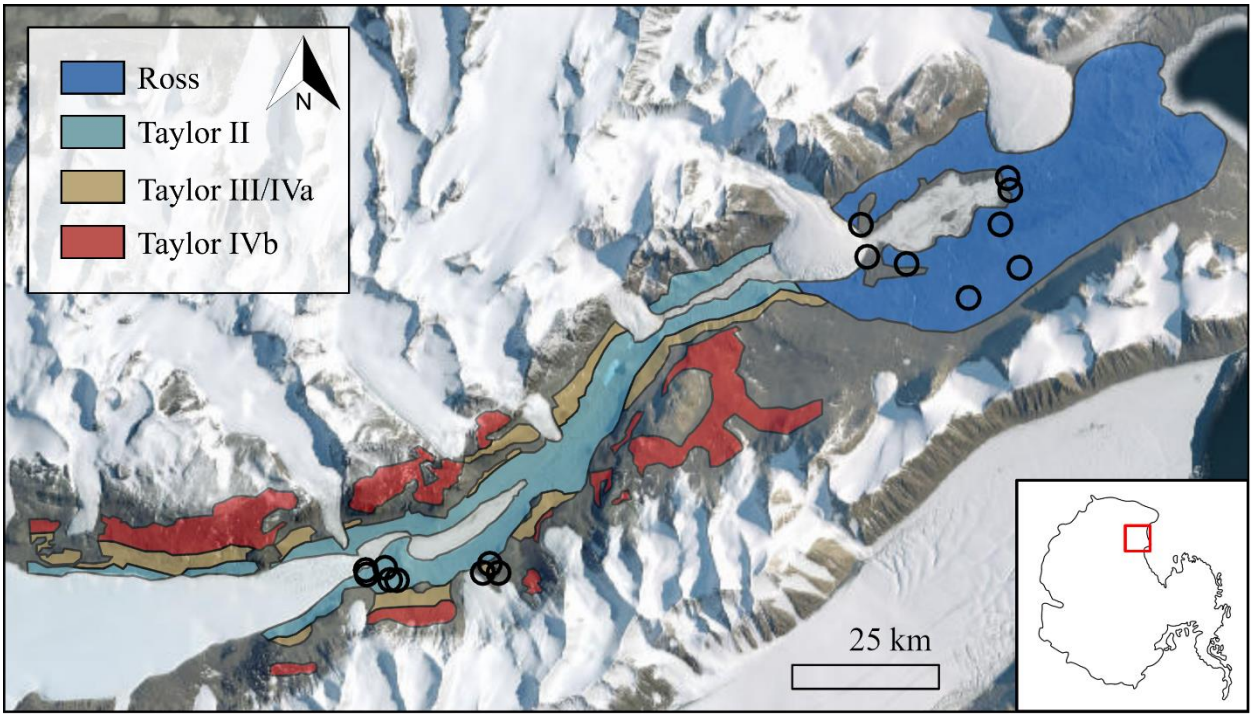

Figure 2.1. Map of eastern Taylor Valley with 16 field sites labeled with open black circles. Inset on bottom right identifies the McMurdo Dry Valleys, Antarctica with a red square. Ross, Taylor II, Taylor III/IVa, and Taylor IVb tills are delineated by color, modified from Bockheim et al. (2008). Esri basemap imagery © Earthstar Geographics.

Figure 2.2

Figure 2.2. Photos of a.) 0.5 x 0.5 m plot set up of dense black microbial mat alongside Crescent Stream (R07, Ross till), b.) dense black microbial mat alongside unnamed stream near the Taylor Glacier (T15, Taylor tills), and c.) dense orange microbial mat alongside unnamed stream near the Taylor Glacier (T14, Taylor tills). Photos taken by E. Osburn and S. Power.

Figure 2.3

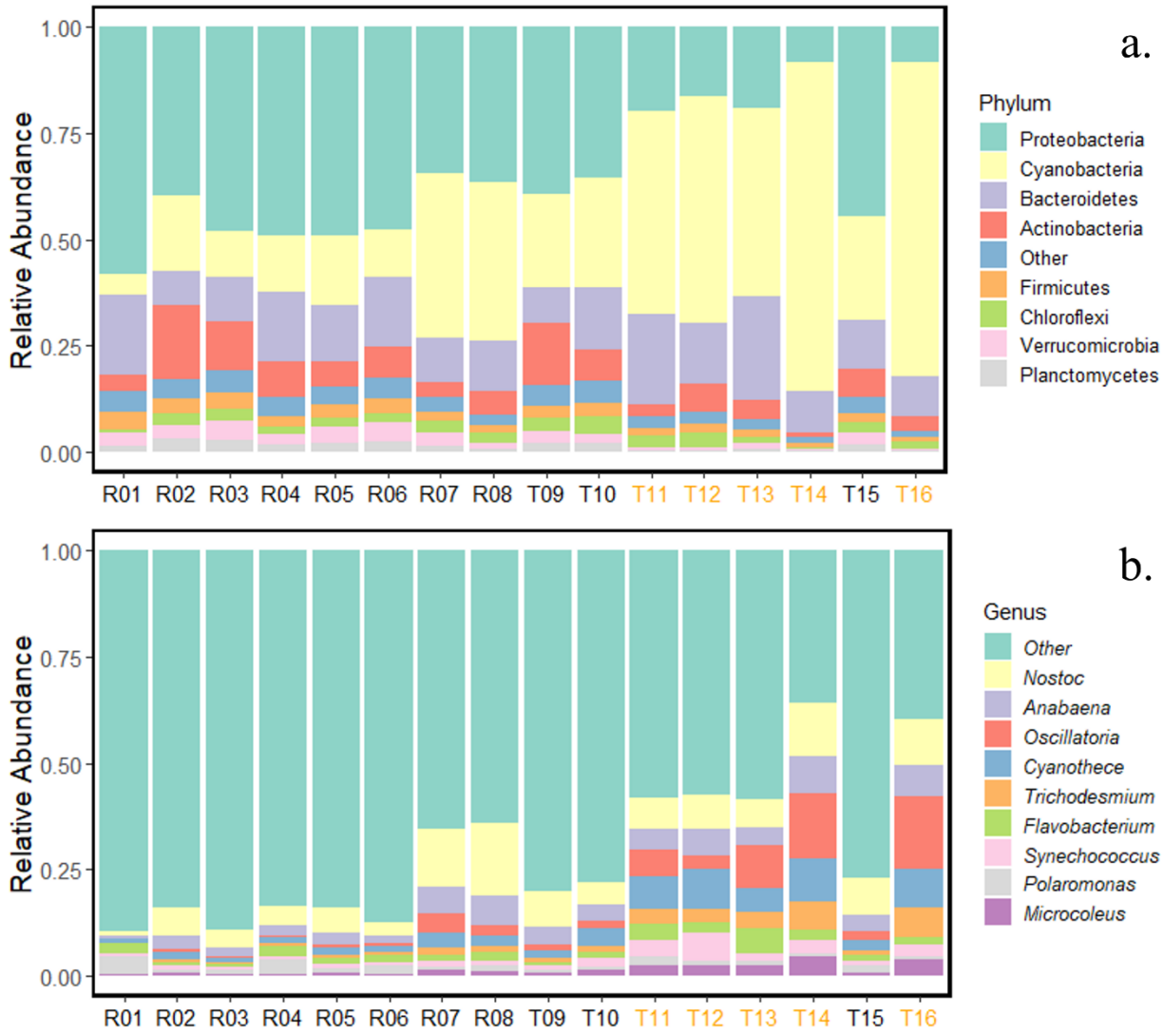

Figure 2.3. Relative abundance of a.) prokaryotic phyla and b.) prokaryotic genera identified within each of the 16 samples using the NCBI RefSeq sequence library. The remaining prokaryotic taxa of less than 1.4% are represented in "Other". Samples collected from the Ross till begin with "R" (*i.e.*, R01 - R08), and samples collected from the Taylor tills begin with "T" (*i.e.*, T09 - T16). The x-axis label colors represent whether the samples were collected from black or orange microbial mats based upon visual field survey.

Figure 2.4

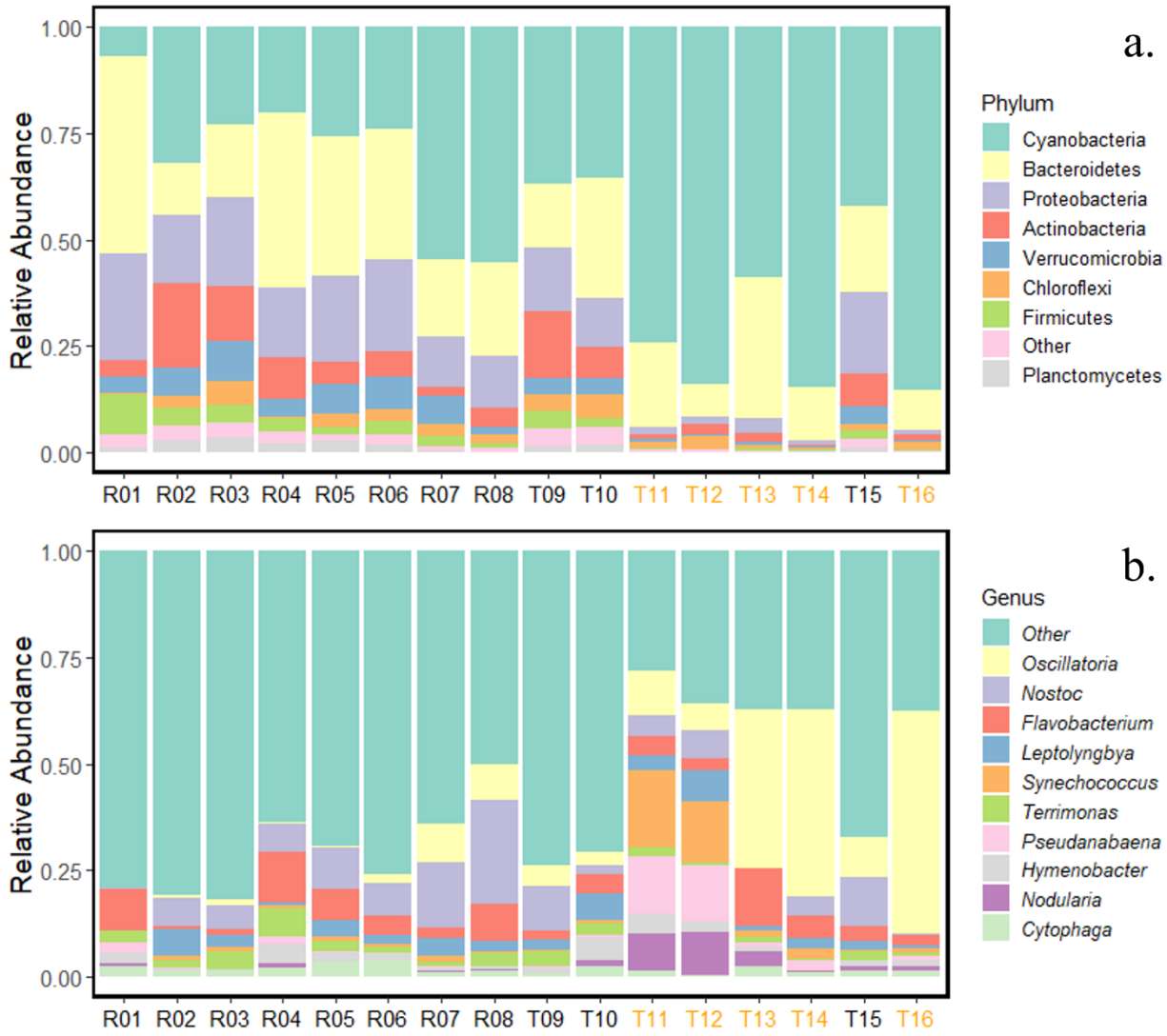

Figure 2.4. Relative abundance of a.) prokaryotic phyla and b.) prokaryotic genera identified within each of the 16 samples using the SILVA 138.1 sequence library. The remaining prokaryotic phyla and genera of less than 1% and 1.7%, respectively, are represented in "Other". Samples collected from the Ross till begin with "R" (*i.e.*, R01 - R08), and samples collected from the Taylor tills begin with "T" (*i.e.*, T09 - T16). The x-axis label colors represent whether the samples were collected from black or orange microbial mats based upon visual field survey.

Figure 2.5

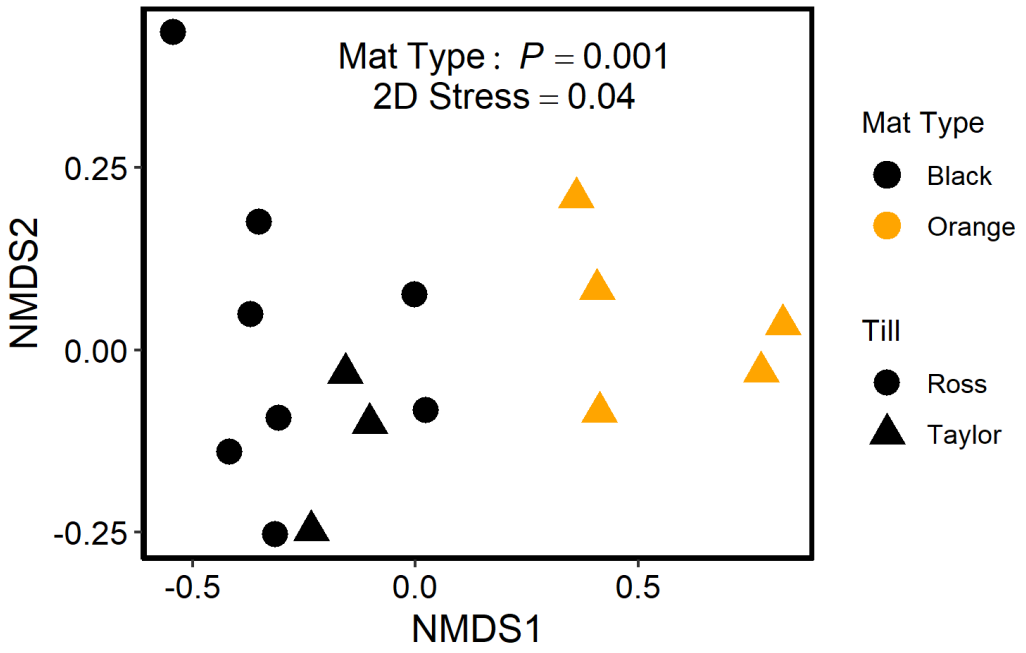

Figure 2.5. Non-metric multidimensional scaling (NMDS) ordination of the community composition (by genera) of each mat type using Bray-Curtis distances. Listed *P* value is mat type effect from PERMANOVA.

Figure 2.6

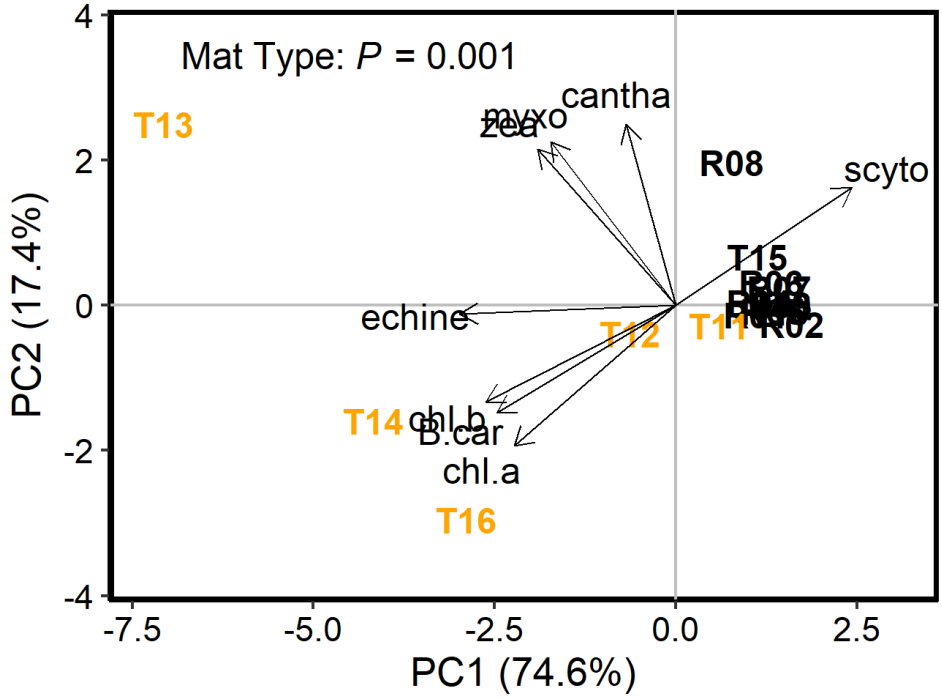

Figure 2.6. Principal components analysis ordination on correlation of the relative abundance of the pigments identified in the 16 microbial mat samples, where scyto is scytonemin, myxo is myxoxanthophyll, zea is zeaxanthin, chl.a is chlorophyll-a, chl.b is chlorophyll-b, B.car is β-carotene, cantha is canthaxanthin, and echine is echinenone. Samples collected from the Ross till begin with "R" (*i.e.*, R01 - R08), and samples collected from the Taylor tills begin with "T" (*i.e.*, T09 - T16). The label colors represent whether the samples were collected from black or orange microbial mats. Vectors represent correlations of the relative abundance of each pigment with PCA ordination axes (all displayed correlations are statistically significant, $P < 0.01$). Listed P value is mat type effect from PERMANOVA.

Figure 2.7

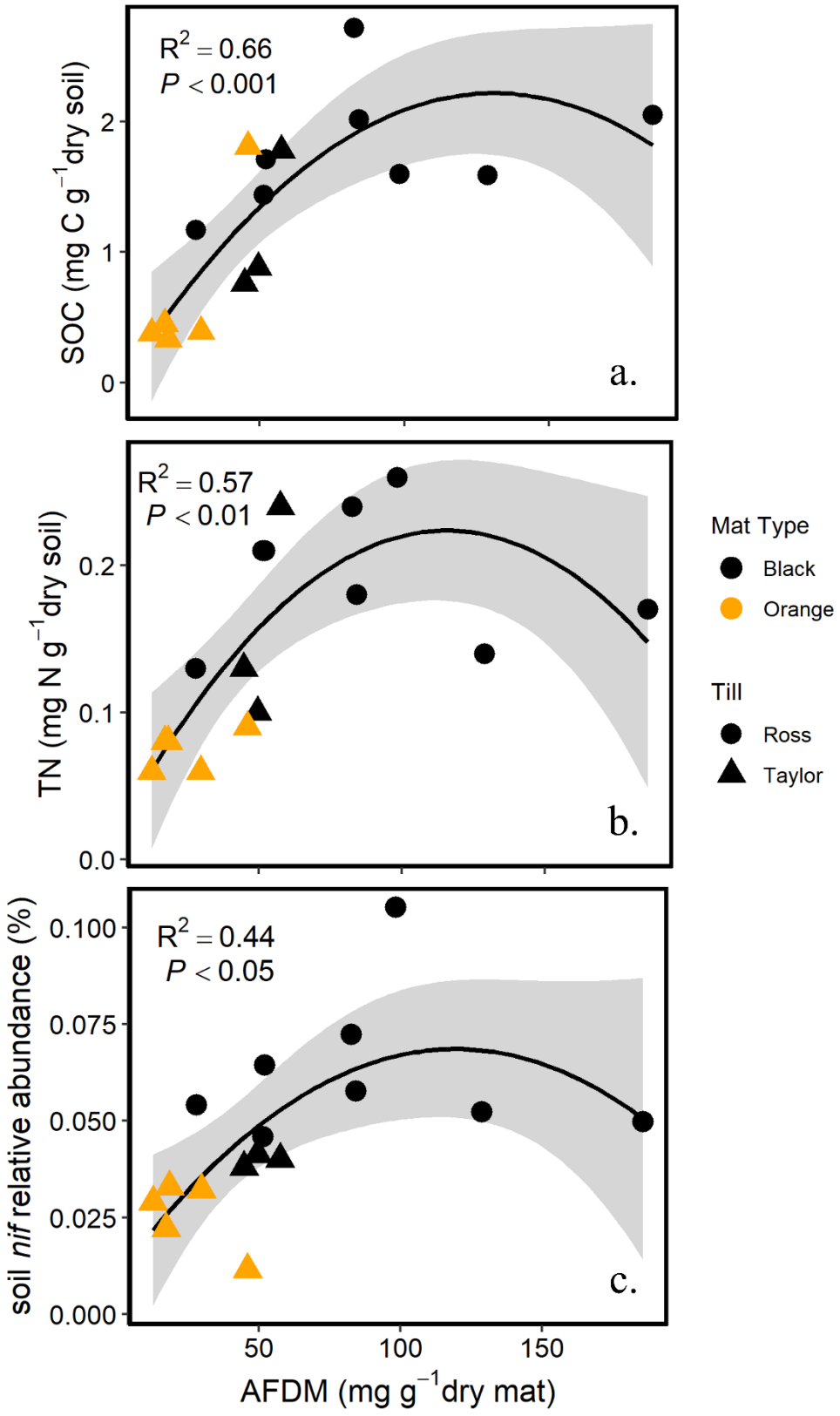
R² = 0.66
P < 0.001
SOC (mg C g⁻¹dry soil)
a.
R² = 0.57
P < 0.01
TN (mg N g⁻¹dry soil)
b.
R² = 0.44
P < 0.05
soil nif relative abundance (%)
c.
AFDM (mg g⁻¹dry mat)
Mat Type
Black
Orange
Till
Ross
Taylor

Figure 2.7. Polynomial regressions of a.) soil organic carbon, b.) total nitrogen, and c.) relative abundance of soil *nif* versus microbial mat organic matter content as AFDM. Symbol colors distinguish black and orange microbial mats, and symbol shape distinguish which till the mats were sampled on. 95% confidence interval of the regression line shown in gray.

Figure 2.8

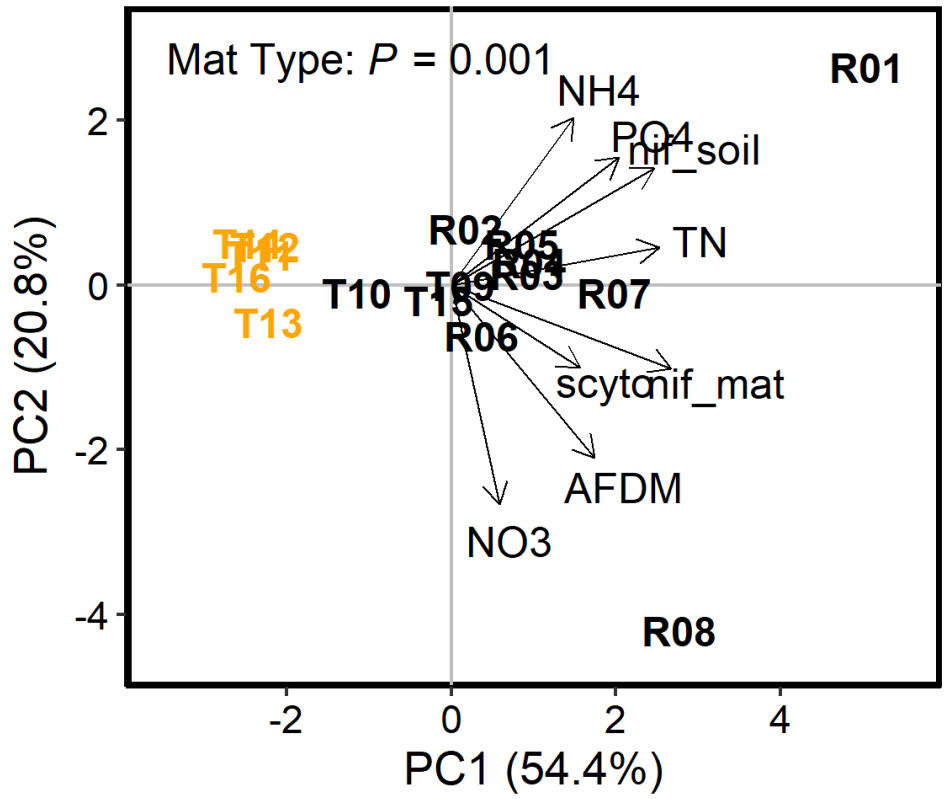

Figure 2.8. Principal components analysis ordination on correlation of the N and P availability of underlying soils, organic matter content as AFDM, *nif* gene relative abundance, and scytonemin concentration of the 16 microbial mat samples. Samples collected from the Ross till begin with "R" (*i.e.*, R01 - R08), and samples collected from the Taylor tills begin with "T" (*i.e.*, T09 - T16). The colors represent whether the samples were collected from black or orange microbial mats. Vectors represent correlations of each parameter with PCA ordination axes (all displayed correlations are statistically significant, $P < 0.05$, while NH4 is marginally significant, $P < 0.1$). Listed P value is mat type effect from PERMANOVA.

Figure 2.9

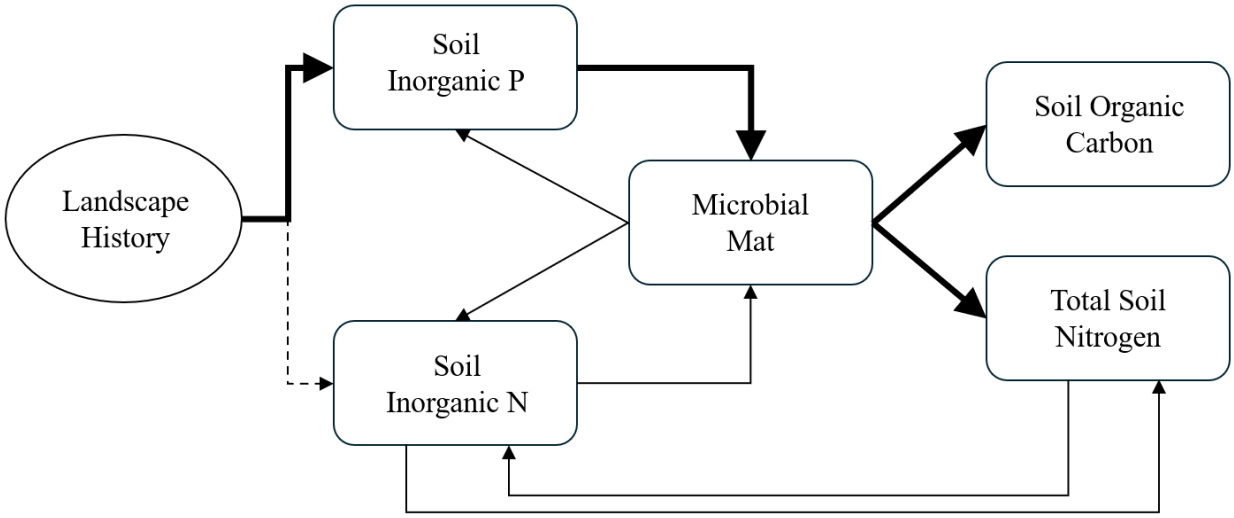

Figure 2.9. Conceptual model illustrating the hypothesized causal relationships between till composition, soil nutrients and organic matter, and microbial mats based upon my observations in this study. Arrows indicate material fluxes between stocks. Bold arrows indicate strong, positive relationships described in this study.

Tables

Table 2.1. Locations and description of the 16 sites used in this study. The general location identifies the closest identifiable landscape feature (note that samples were not collected from within stream channels), till composition name, and mat type based on visual assessment of the mat color.

Plot ID	Latitude S	Longitude E	General Location	Till	Mat Type
R01	-77.59846	163.26842	McKnight Creek	Ross	Black
R02	-77.61371	163.25754	Von Guerard Stream	Ross	Black
R03	-77.61382	163.04385	Canada Stream	Ross	Black
R04	-77.60246	163.27255	Aiken Creek	Ross	Black
R05	-77.62435	163.05362	Green Creek	Ross	Black
R06	-77.62669	163.11385	Delta Stream	Ross	Black
R07	-77.63781	163.20866	Crescent Stream	Ross	Black
R08	-77.62792	163.28668	Harnish/Relict Channel	Ross	Black
T09	-77.72765	162.46495	Hughes Glacier Pond	Taylor	Black
T10	-77.72767	162.48909	Hughes Glacier Pond	Taylor	Black
T11	-77.72469	162.47571	Hughes Glacier Pond	Taylor	Orange
T12	-77.73006	162.33351	Upper Wormherder Creek	Taylor	Orange
T13	-77.72599	162.31544	Lower Wormherder Creek	Taylor	Orange
T14	-77.72674	162.28580	near Taylor Glacier	Taylor	Orange
T15	-77.72820	162.28732	near Taylor Glacier	Taylor	Black
T16	-77.72993	162.32300	Middle Wormherder Creek	Taylor	Orange

Table 2.2. Pigments measured in microbial mat samples using high performance liquid chromatography. Detectable concentrations are denoted with “x”.

Pigments Measured	Detection
chlorophyllide-a	ND
chlorophyll c1&c2	ND
scytonemin	x
reduced scytonemin	x
19 butanoyloxyfucoxanthin	ND
fucoxanthin	ND
19 hexanoyloxyfucoxanthin	ND
9 cis neoxanthin	ND
violaxanthin	ND
diadinoxanthin	ND
antheraxanthin	ND
myxoxanthophyll	x
alloxanthin	ND
diatoxanthin	ND
monadoxanthin	ND
lutein	ND
zeaxanthin	x
gyroxanthin	ND
chlorophyll b	x
chlorophyll a	x
beta-carotene	x
canthaxanthin	x
echinenone	x

Table 2.3. Mean physicochemical variables for soils underlying microbial mats averaged by till composition: Ross till (n=8) and Taylor tills (n=8) with ± 1 standard deviation. GWC is gravimetric water content, EC is electrical conductivity, SOC is soil organic carbon, and TN is total nitrogen. One-way ANOVA tests were run between Ross and Taylor till soils for each parameter, and letters represent differences (measurements with dissimilar letters were significantly different from each other, $P < 0.05$).

	GWC g/g	**pH**	**EC** µS cm^{-1}	**NH_4^+** µg N g^{-1} dry soil	**NO_3^-** µg N g^{-1} dry soil	**PO_4^{3-}** µg P g^{-1} dry soil	**SO_4^{2-}** µg S g^{-1} dry soil	**Cl^-** µg Cl g^{-1} dry soil	**SOC** mg C g^{-1} dry soil	**TN** mg N g^{-1} dry soil
Ross Till	0.18 **a** ± 0.03	7.55 **a** ± 0.18	22.00 **a** ± 6.52	1.88 **a** ± 3.19	0.48 **a** ± 0.16	2.36 **a** ± 1.14	3.93 **a** ± 2.10	6.58 **a** ± 2.13	1.79 **a** ± 0.44	0.19 **a** ± 0.04
Taylor Tills	0.18 **a** ± 0.02	7.34 **b** ± 0.19	13.89 **a** ± 7.75	0.56 **a** ± 0.05	0.42 **a** ± 0.04	0.60 **b** ± 0.38	3.60 **a** ± 1.94	4.34 **a** ± 2.04	0.85 **b** ± 0.58	0.11 **b** ± 0.06

Table 2.4. Average ash-free dry mass and pigment concentrations averaged by microbial mat type: black mats (n=11) and orange mats (n=5) with ± 1 standard deviation. AFDM is ash-free dry mass, Scyto is scytonemin, Scyto-Red is reduced scytonemin, Myxo is myxoxanthophyll, Zea is zeaxanthin, Chl-a is chlorophyll-a, Chl-b is chlorophyll-b, B-Car is β-carotene, Cantha is canthaxanthin, and Echine is echinenone. One-way ANOVA tests were run between black and orange mats for each parameter, and letters represent differences (measurements with dissimilar letters were significantly different from each other, $P < 0.05$).

	AFDM mg g^{-1} dry mat	**Total Pigment Concentration** µg g^{-1} dry mat	**Scyto** µg g^{-1} dry mat	**Scyto-Red** µg g^{-1} dry mat	**Myxo** µg g^{-1} dry mat	**Zea** µg g^{-1} dry mat	**Chl-a** µg g^{-1} dry mat	**Chl-b** µg g^{-1} dry mat	**B-Car** µg g^{-1} dry mat	**Cantha** µg g^{-1} dry mat	**Echine** µg g^{-1} dry mat
Black Mat	78.5 **a** ± 43.6	267.5 **a** ± 129.5	225.3 **a** ± 112.9	38.5 **a** ± 17.0	0 **a** ± 0	0.005 **a** ± 0.006	2.67 **a** ± 1.85	0.02 **a** ± 0.04	0.011 **a** ± 0.004	0.75 **a** ± 0.79	0.26 **a** ± 0.28
Orange Mat	24.9 **b** ± 12.0	3.9 **b** ± 3.0	1.4 **b** ± 1.4	1.1 **b** ± 1.5	0.03 **b** ± 0.05	0.004 **a** ± 0.003	1.26 **a** ± 0.87	0.01 **a** ± 0.01	0.002 **b** ± 0.001	0.01 **a** ± 0.01	0.07 **a** ± 0.04

Table 2.5. Average nitrogen fixation gene abundance for black mats (n=11) and orange mats (n=5) with ± 1 standard deviation. Data are separated by those derived from metagenomic methods and qPCR methods. The measures of nitrogen fixation potential are represented by the relative abundance of all *nif* genes and gene abundance of *nifH* specifically. One-way ANOVA tests were run between black and orange mats for each parameter, and letters represent differences (measurements with dissimilar letters were significantly different from each other, $P < 0.05$).

	Metagenomic Method				**qPCR Method**	
	***nif* mat**	***nif* soil**	***nifH* mat**	***nifH* soil**	***nifH* mat**	***nifH* soil**
	nif gene relative abundance	*nif* gene relative abundance	*nifH* gene relative abundance	*nifH* gene relative abundance	# *nifH* genes g^{-1} wet mat	# *nifH* genes g^{-1} dry soil
Black Mat	0.103 **a** ± 0.051	0.056 **a** ± 0.018	0.0078 **a** ± 0.0067	0.0026 **a** ± 0.0023	3.8×10^7 **a** ± 2.8×10^7	1.2×10^7 **a** ± 8.1×10^6
Orange Mat	0.007 **b** ± 0.002	0.026 **b** ± 0.008	0.0001 **b** ± 0.0002	0.0001 **b** ± 0.0001	3.1×10^6 **b** ± 1.1×10^6	3.0×10^6 **b** ± 2.9×10^6

Table 2.6. Spearman correlation coefficients (ρ) between the inorganic phosphorus concentration of underlying soils and microbial mat parameters: AFDM, relative abundance of *nif*, and pigment concentration of chlorophyll-a, scytonemin, β-carotene, and canthaxanthin. Values in bold indicate statistically significant relationships, based on $P < 0.05$.

	AFDM	mat *nif*	Chl-a	Scyto	B-car	Cantha
PO_4^{3-}	**0.53** $P = 0.037$	**0.58** $P = 0.020$	**0.57** $P = 0.024$	0.50 $P = 0.051$	**0.63** $P = 0.010$	0.47 $P = 0.066$

CHAPTER 3 – Remotely characterizing photosynthetic biocrust in snowpack-fed microhabitats of Taylor Valley, Antarctica

Authors: Sarah N. Power, Mark R. Salvatore, Eric R. Sokol, Lee F. Stanish, Schuyler R. Borges, Byron J. Adams, and John E. Barrett

Published in *Science of Remote Sensing*

Power, S.N., Salvatore, M.R., Sokol, E.R., Stanish, L.F., Borges, S.R., Adams, B.A., Barrett, J.E. 2024. Remotely characterizing photosynthetic biocrust in snowpack-fed microhabitats of Taylor Valley, Antarctica. *Science of Remote Sensing*. 9, 100120.
https://doi.org/10.1016/j.srs.2024.100120

Abstract

Microbial communities are the primary drivers of carbon cycling in the McMurdo Dry Valleys of Antarctica. Dense microbial mats, consisting mainly of photosynthetic cyanobacteria, occupy aquatic areas associated with streams and lakes. Other microbial communities also occur at lower densities as patchy surface biological soil crusts (hereafter, biocrusts) across the terrestrial landscape. Multispectral satellite data have been used to model microbial mat abundance in high-density areas like stream and lake margins, but no previous studies have investigated the lower detection limits of biocrusts. Here, we describe remote sensing and field-based survey and sampling approaches to study the detectability and distribution of biocrusts in the McMurdo Dry Valleys. Using a combination of multi- and hyperspectral tools and spectral linear unmixing, we modeled the abundances of biocrust in eastern Taylor Valley. Our spectral approaches can detect low masses of biocrust material in laboratory microcosms down to biocrust concentrations of 1% by mass. These techniques also distinguish the spectra of biocrust from both surface rock and mineral signatures from orbit. We found that biocrusts are present throughout the soils of eastern Taylor Valley and are associated with diverse underlying soil communities. The densest biocrust communities identified in this study had total organic carbon

5x greater than the content of typical arid soils. The most productive biocrusts were located downslope of melting snowpacks in unique soil ecosystems that are distinct from the surrounding arid landscape. There are similarities between the snowpack and stream sediment communities (high diversity of soil invertebrates) as well as their ecosystem properties (*e.g.*, persistence of liquid water, high transfer of available nutrients, lower salinity from flushing) compared to the typical arid terrestrial ecosystem of the dry valleys. Our approach extends the capability of orbital remote sensing of photosynthetic communities out of the aquatic margins and into the drier soils which comprise most of this landscape. This interdisciplinary work is critical for measuring and monitoring terrestrial carbon stocks and predicting future ecosystem dynamics in this currently water-limited but increasingly dynamic Antarctic landscape, which is particularly climate-sensitive and difficult to access.

Introduction

Biocrusts, *i.e.*, soil aggregates containing communities of cyanobacteria, algae, moss, lichen, *etc*. on the surface of soil (Weber et al., 2022), inhabit all continents (Belnap et al., 2016), are estimated to cover 12% of the Earth's terrestrial surface (Rodriguez-Caballero et al., 2018), and play foundational roles in the ecosystems where they occur (Belnap et al., 2016). Biocrusts are distributed across hot and cold deserts and are oftentimes an important source, if not the primary source, of carbon (C) in these systems (Elbert et al., 2012). They perform key ecological functions, including photosynthesis, nitrogen fixation, nutrient cycling, and soil stabilization (Belnap, 2003), which are particularly important in ecosystems that lack vascular vegetation. Biocrusts may be more susceptible to climate change than previously thought (Finger-Higgens et al., 2022). Climate warming and precipitation variation appears to have already impacted some biocrust communities and will likely continue to result in biocrust degradation across ecosystems

(Finger-Higgens et al., 2022). Detecting and mapping biocrust is essential for monitoring these important soil communities in a changing climate.

In the McMurdo Dry Valleys (MDV) of Antarctica, microbial communities are the drivers of carbon cycling, particularly in and adjacent to lakes, ponds, and streams where dense microbial mats are abundant (Cary et al., 2010; Van Horn et al., 2016, Stone et al. *submitted*). However, less dense microbial communities also occur in drier soils outside the hydrological influence of glaciers, stream channels, or lakes in areas where snow or subsurface thaw are presumably the main sources of water. In such environments, which constitute most of the dry valley landscape, microbial communities are sparse, have high soil content, and are better described as biocrusts. Here, we define biocrusts as the communities which are present in drier areas away from streams and lakes, and although they can be quite similar morphologically to the microbial mats present in aquatic areas, biocrusts are typically less dense and patchily distributed among the terrestrial landscape where there are alternative sources of moisture, *e.g.*, snowpacks and groundwater seeps (Gooseff et al., 2013; Weber et al., 2022).

Previous studies of MDV microbial mat dynamics have primarily focused on the communities occurring close to or within the streams and lakes (*e.g.*, Alger et al., 1997). Soil environments outside of stream channels have traditionally been thought to support less visible biocrust biomass in comparison, so fewer studies have focused on these terrestrial communities. However, these terrestrial areas are far more spatially extensive than the aquatic environments in the MDV, and therefore, even sparse distributions and densities of biocrusts could sum to a considerable amount of total biomass. For example, the Lake Fryxell basin, excluding Lake Fryxell, is 53.55 km^2, while the cumulative stream area is approximately 2.58 km^2 (4.82%), determined via satellite imagery. The terrestrial landscape of this region occupies more than 20x

the surface area relative to ephemeral stream channels and lake margins, so although biocrusts are typically less dense than microbial mats, we anticipate soils of the MDV contain a considerable amount of carbon in and under these biocrusts (*e.g.*, Burkins et al., 2001). We suggest that the terrestrial regions of Taylor Valley may contain more cumulative biomass than the stream channels given their spatial extent. A systematic and scalable method is required to measure and monitor biocrust biomass over large spatial scales: remote sensing.

Assessing the detectability of biocrusts via remote sensing is a critical first step in estimating terrestrial carbon stocks in this region and examining controls over the distribution and activity of these soil communities. Our previous research has demonstrated the utility of multispectral satellites (*e.g.*, WorldView-2 and WorldView-3; WV-2 and WV-3) in detecting densely colonized microbial mats near streams in the Lake Fryxell basin region using spectral parameters and spectral linear unmixing models (Power et al., 2020; Salvatore, 2015; Salvatore et al., 2021, 2020). In addition to the strong photosynthetic signatures identified near stream channels and lake margins, we also observed enhanced spectral signatures indicative of photosynthetic activity in upland areas not connected to streams or lakes (Power et al., 2020). While remote sensing techniques have been demonstrated to be effective in regions of dense microbial mats, these techniques have not been specifically validated throughout the broader landscape where photosynthetic communities are much more dispersed and their resultant signatures are often much weaker and discontinuous. Therefore, this work tests the hypothesis that these observed spectral signatures outside of stream channels are associated with areas of increased soil productivity and not, for example, associated with spectral artifacts created by topographic or lithological variations.

Our objectives for this study are to assess the detectability of biocrust and examine the environments in which these unique communities are found in the MDV. By investigating the spatial distribution of biocrusts using orbital data, our work contributes in part to efforts in refining existing carbon budgets (*e.g.*, Barrett et al., 2006b; Burkins et al., 2001), predicting future carbon stocks, and examining controls over the distribution and activity of biocrusts in the MDV. Here, we present the first assessment of biocrust detectability in the MDV terrestrial landscape using a combination of laboratory hyperspectral spectroscopy, WorldView-2 and WorldView-3 multispectral satellite imagery, and *in-situ* soil and biocrust surveying and sampling.

Materials and Methods

Site description

The MDV are the largest contiguous ice-free area on the Antarctic continent, with approximately 4500 km^2 of exposed soil, stream, and lake ecosystems (Levy, 2013). Glacial meltwater during the austral summer (*i.e.*, 24 hours daylight) feeds streams that flow for an average of 4 - 9 weeks per year (Wlostowski et al., 2016). These streams drain into perennially ice-covered lakes along the floor of Taylor Valley. While dense microbial mats (mm – cm thick) occupy streams and lake margins (Figure 3.1a), biocrusts occur at lower densities as discontinuous mats in intermittently wet soils (Figure 3.1b, c). The microbial mats are dominated by cyanobacteria (*e.g.*, *Nostoc*, *Oscillatoria*, and *Phormidium*) and also contain chlorophyta (green algae) (Alger et al., 1997), various diatom species (Alger et al., 1997), and mosses which can also occur separately from microbial mats (*Bryum* spp. and *Hennediella* spp.; Pannewitz et al., 2003; Schwarz et al., 1992). While studies on biocrust composition in the MDV are lacking, the biocrusts here contain cyanobacteria and mosses based on visual identification and appear to

be dominated by *Nostoc* specifically. Communities of nematodes, rotifers, and tardigrades also inhabit the soils, sediments, and microbial mats of this region (Freckman and Virginia, 1997; Simmons et al., 2009a). Though, given the relatively low soil invertebrate biomass, grazing influences on microbial mats and biocrusts are thought to be minimal, making the MDV a simple system for studying biocrust and microbial mat dynamics.

Taylor Valley, one of several valleys in the MDV, spans from the McMurdo Sound of the Ross Sea in the east to the Taylor Glacier in the west. The eastern portion of Taylor Valley includes a dozen ephemeral glacial meltwater streams and Lake Fryxell, which have been the subject of numerous microbial mat studies (*e.g.*, Alger et al., 1997; Kohler et al., 2015; McKnight et al., 1998; Stanish et al., 2011). Due to proximity to the coast, eastern Taylor Valley also has the greatest relative humidity and the most shallow ice-cemented permafrost layers in the region, and therefore typically has higher soil water content (Bockheim et al., 2008; Doran et al., 2002; Obryk et al., 2020) and richer communities of soil invertebrates with greater biomass than other parts of Taylor Valley or neighboring Wright Valley (Adams et al., 2006; Barrett et al., 2007, 2006c; Courtright et al., 2001; Xue et al., 2023).

Spectral detection limit experiment

We created microcosms of biocrust material and bare soil (not containing biocrust) of varying percent (0 - 100%) biocrust by weight (g/g) in the laboratory and characterized these materials using hyperspectral reflectance techniques to quantify the potential detection limits of our remote sensing methods. The soil was collected from the Fryxell basin, and to minimize oversampling of the sensitive dry valley biocrust communities, we collected a *Nostoc*-dominated biocrust from a warm desert environment in Arizona, which has a similar spectrum as the dry valley biocrust (Figure S3.1). Both biocrust spectra contain absorption features at ~ 0.68, 1.19,

1.45, 1.78, and 1.93 μm, indicating that the major spectral characteristics between both types of biocrust are the same and therefore justify this analog material's appropriateness for our laboratory experiment. The biocrust and soil were separately ground into a homogenous fine particle size for hyperspectral analysis. This disaggregation process allows the biocrust to evenly distribute among the soil particles, and from a chemical and pigment perspective, the spectral characteristics of the biocrust remain largely unchanged after disaggregating. A known quantity of biocrust was mixed with a known quantity of soil to achieve the desired percent biocrust mixtures, and the mixtures were placed into a sample holder ~ 2.5 cm in diameter and 0.5 cm in depth. Sample mixtures were moistened with DI water and placed under a halogen lamp for several minutes, allowing time for the organisms to reactivate and begin photosynthesizing. We targeted a final water content for our wetted samples of approximately 0.25 GWC (g H_2O/g dry soil and biocrust material). Spectra were acquired using an Analytical Spectral Devices (ASD) FieldSpec4 high-resolution hyperspectral reflectance spectrometer set up for use in a stable lab environment. Data were collected between 350 and 2500 nm at a 1 nm sampling interval. A halogen lamp was used to illuminate the samples at 30° off-nadir and approximately 25 cm away, while reflectance was measured at nadir using the ASD's bare fiber optic cable roughly 3 cm above the sample surface with a 25° field of view projecting a 1.39 cm^2 spot size onto our samples. To minimize instrument noise, particularly at the longest and shortest wavelengths where the output of the halogen bulb is lowest, we averaged 50 individual spectra for each biocrust-soil combination produced in the lab. All data were then downsampled to WV-2 and WV-3 spectral resolutions for direct comparison to the respective orbital platforms. Linear mixtures of pure soil and biocrust spectra were also modeled for comparison to the spectra of those known physical mixtures to determine the nature of the observed spectral mixing

relationship, validating the ability to confidently translate this linear unmixing method to orbital data.

Orbital spectral collection and processing

Satellite images acquired during austral summers were used to identify photosynthetic signatures in upland terrestrial areas. WorldView-2 and WorldView-3 (DigitalGlobe, Inc.) are multispectral satellites in polar orbit with 8 multispectral bands at 1.84 m and 1.24 m nadir resolutions, respectively. Georeferenced data, validated using ground control points, were obtained from the University of Minnesota Polar Geospatial Center (PGC) through a cooperative agreement between the National Science Foundation (NSF) and National Geospatial-Intelligence Agency (NGA). These data were subsequently processed to atmospherically corrected surface reflectance using five spectral ground validation targets acquired in the field during the 2018-2019 austral summer, following methods from Salvatore et al. (2021). Band-specific linear relationships between top-of-atmosphere reflectance data and ground validation spectra were applied to the entirety of the satellite images to remove atmospheric contributions to the observed signal. These corrected surface reflectance data were used in several analyses and compared with ground-based surveys of soil chemical and biological properties detailed in the sections below.

Field site identification and in-situ environmental sample collection

We used vegetation indices, such as the Normalized Difference Vegetation Index parameter (NDVI; Tucker, 1979), to target locations of varying photosynthetic activity across the eastern Taylor Valley landscape. High NDVI values are typical of photosynthetic vegetation, which has a unique spectral signature of absorbance in the visible wavelengths (due to the activity of chlorophyll-a and other pigments) and strong reflectance in near-infrared regions due

to scattering and reflectance of long-wave radiation by cell walls. NDVI was calculated using spectral reflectance measurements acquired in the near-infrared (WV-2 Band 7, centered at 831 nm; WV-3 centered at 832 nm) and red (WV-2 Band 5, centered at 659 nm; WV-3 centered at 661 nm) using the Environment for Visualizing Images (ENVI, Harris Geospatial) software package.

Thirty locations with either consistently high NDVI values, consistently low NDVI values, or variable NDVI values were identified in eastern Taylor Valley outside of stream channels and lake margins (Figure 3.2) using three satellite images: a WV-3 image acquired on January 17, 2015 (1040010006846000), a WV-2 image acquired on January 19, 2018 (1030010077755100), and another WV-2 image acquired on December 11, 2018 (1030010089D13500). These 30 locations were selected to represent a range of potential photosynthetic activity and topographic features (*i.e.*, slope, aspect, and elevation) characterized using an airborne lidar-derived digital elevation model (DEM) at 1 m spatial resolution (Fountain et al., 2017). Depressions, rocky outcrops, sloped hills, and flat surfaces were all represented in our field locations. Overall, these locations were selected to maximize spatial coverage of ranges in photosynthetic activity and topography across the landscape.

We sampled, photographed, and documented relevant environmental conditions (*e.g.*, evidence of surface moisture, presence/absence of microbial mat, moss, or biocrust, presence of snowpacks, surface or lithological variations like dominant presence of oxidized granite) at each of these 30 locations in December of 2019. We collected a surface layer sample of soil or biocrust (if present) and rock from all sites for subsequent hyperspectral analysis in the laboratory using the same methods and laboratory set-up as previously described in Section 2.2. At 12 of the sites, we established 5 m x 5 m intensive sampling plots and collected 5 surface

layer soil or biocrust samples 128 cm^2 in area from each corner and center of the plots for pigment analysis (chlorophyll-a, scytonemin, and carotenoids) and organic matter content via ash-free dry mass (AFDM). We also collected underlying soil down to 10 cm below the surface for gravimetric water content (GWC), electrical conductivity (EC), pH, inorganic nitrogen (N) concentration in the form of ammonium (NH_4^+) and nitrate (NO_3^-), inorganic phosphorus (P) concentration in the form of phosphate (PO_4^{3-}), total organic carbon (TOC), total nitrogen (TN), and invertebrate abundance (see below). After the initial soil chemistry and invertebrate diversity and abundance analyses, samples were frozen at -20°C and transported to Virginia Tech and Northern Arizona University for remaining chemical and spectral analyses.

Analysis of environmental field samples

We estimated pigment concentration on the surface ~ 1 cm layer soil and biocrust samples using a trichromatic spectrophotometric method for chlorophyll-a, carotenoids, and scytonemin at 663, 490, and 384 nm, respectively (Garcia-Pichel and Castenholz, 1991). Throughout the process, care was taken to avoid exposing the samples to light. The samples were dried at 105°C for 24 hr, sieved through a 4 mm sieve, and extracted for 24 hr at ambient temperature in 90% unbuffered acetone using a 3.75:10 soil to solvent ratio, based on protocols from Couradeau et al. (2016) and the McMurdo Dry Valleys Long Term Ecological Research Program (MCM LTER) standard methods. After centrifugation, the extracts were analyzed on a spectrophotometer using 10 mL cuvettes. The absorbances contributed by each pigment were calculated using the trichromatic equations outlined in Garcia-Pichel and Castenholz (1991), and the pigment concentrations were calculated using the Beer-Lambert Law with the extinction coefficients of 89.7 L g^{-1} cm^{-1} for chlorophyll-a (Couradeau et al., 2016), 112.6 L g^{-1} cm^{-1} for scytonemin (Brenowitz and Castenholz, 1997), and 262 L g^{-1} cm^{-1} for carotenoids (Thrane et al.,

2015). Additionally, the surface layer soil and biocrust samples were measured for AFDM by weighing a known area of sample, combusting at 550°C for 24 hr using a muffle furnace, gently stirring samples halfway through combustion, and reweighing after cooling in a desiccator. Given the very low clay content of soils in this region (Barrett et al., 2006a), the rehydration of clays was assumed negligible, so we did not rewet samples.

Using the underlying 1-10 cm soil, we measured pH and electrical conductivity using a 1:2 and 1:5 soil to DI H_2O slurry with pH and conductivity probes, respectively (Barrett et al., 2004), and we measured gravimetric water content by mass lost after oven drying at 105°C for 24 hr. We also extracted inorganic N (NH_4^+ and NO_3^-) in 2 M potassium chloride and inorganic P (PO_4^{3-}) in 0.5 M sodium bicarbonate; inorganic N and P were measured on extracts using a Lachat QuikChem flow injection analyzer (Keeney and Nelson, 1982; Olsen and Sommers, 1982; Knepel, 2003; Prokopy, 1995). Additionally, we measured TOC and TN using an Elementar Vario MAX Cube analyzer after fumigating samples with concentrated hydrochloric acid to remove the influence of carbonates on TOC values (Ramnarine et al., 2011; Walthert et al., 2010; Fritsen et al., 2000).

Invertebrate abundance was enumerated using inverted light microscopy on soil solutions using a modified sugar-centrifugation extraction procedure described by Freckman and Virginia (1993). Nematode abundance is reported as the total number of live *Scottnema*, *Eudorylaimus,* and *Plectus* individuals, and total live rotifers and tardigrades per kg dry mass soil. Using R Statistical Software version 4.0.3 (R Core Team, 2017), a PCA on correlation was executed to visually compare plots in terms of their physicochemical properties. A MANOVA was performed to statistically assess whether there is a significant difference between the three plot types (biocrust, oxidized granite, soil) using physicochemical variables. An ANOVA was performed

next to assess which, if any, physicochemical variables are significantly different between the plot types.

Vegetation index analysis using orbital data

To examine variations in photosynthetic activity across our sampled locations in eastern Taylor Valley, we applied several vegetation indices to orbital data. The primary WV-2 image used in this analysis (103001009FA0AE00) was acquired on December 3, 2019, approximately three weeks before our field sampling campaign. In addition to NDVI, we also calculated the Simple Ratio Index (SR), the Red-Edge Simple Ratio Index (SRre), and the Normalized Pigment Chlorophyll Index (NPCI). SR and NPCI are effective in detecting dry biocrust communities from other arid regions (*e.g.*, the Colorado Plateau) with a portable spectroradiometer (Young and Reed, 2017). SR was calculated using the NIR and red bands, SRre was calculated using the NIR and red-edge bands, and NPCI was calculated using the red and coastal bands. Each of the parameter values were extracted from the four pixels centered at each of the plot locations, based on handheld GPS coordinates taken during sampling and visually confirming plot location via nearby boulders, snowpacks, *etc*. These values were averaged to estimate an average NDVI, SR, SRre, and NPCI value for each of the plots. Average reflectance values for each of the eight WV-2 bands were calculated for each plot as well. Using R Statistical Software version 4.0.3 (R Core Team, 2017), a correlation matrix was constructed with the vegetation indices and raw bands to investigate any significant relationships between these primary remote sensing data and biological parameters collected *in-situ* (AFDM and pigment concentration). A principal components analysis (PCA) on covariance was executed to visually compare plots in terms of their orbital reflectance spectra (raw bands B1 - B8). A multivariate analysis of variance (MANOVA) was performed to statistically assess whether there is a significant difference

between the three plot types (biocrust, oxidized granite, soil) using the multispectral bands. A univariate analysis of variance (ANOVA) was performed next to assess which, if any, spectral bands and vegetation indices (NDVI, SR, SRre, NPCI) are significantly different between the plot types. Plot 11 and plot 21 were excluded from these three statistical analyses because they were covered in snow and therefore their reflectance data skewed the analyses.

Spectral linear unmixing of orbital data

Spectral linear unmixing was used to model the spectral contribution of individual surface types, and therefore calculate the fractional abundance of each surface type per pixel (Lawson and Hanson, 1974; Adams et al., 1993; Ramsey and Christensen, 1998; Bioucas-Dias et al., 2012; Salvatore et al. 2020). Spectral unmixing uses a library of 'pure' spectral endmembers of each surface type to train the model by matching the measured spectral signature, while reducing the misfit between the measured and modeled spectra. Endmembers are limited to the number of spectral bands and degrees of freedom in the data that are being unmixed; therefore, we were constrained to eight or fewer endmembers for unmixing using the WV-2 and WV-3 satellites (Adams et al., 1993; Ramsey and Christensen, 1998). Our seven hyperspectral endmembers were derived through collection in the field, collection after laboratory preparation, or were modeled from field experiments. Six of these endmembers (black microbial mat, orange microbial mat #1 and #2, water, moss, and soil) were previously used in this region and are described in detail in Salvatore et al. (2021), and one additional endmember (an orange oxidized granite) was added for an updated emphasis on the terrestrial landscape and was collected during our field campaign and subsequently measured in the laboratory. This granite endmember is from a minor subunit of the broader Granite Harbour Intrusive Complex that outcrops near the top walls of Taylor Valley (Cox et al., 2012). X-ray diffraction confirmed the dominance of quartz

(~30%), plagioclase feldspar (~25%), alkali feldspar (~25%), and mafic and other ancillary phases (~20%), while VNIR reflectance spectroscopy indicated a crystalline Fe-oxide phase, likely goethite or hematite, at orbitally relevant wavelengths. As a result of these analyses, we refer to this endmember as "oxidized granite." All seven spectra were downsampled to WV-2 and WV-3 resolutions to create a spectral library that was used to unmix the entirety of each orbital image. Snow and ice were not included as spectral endmembers despite their pervasiveness across the landscape, because both snow and ice are known to exhibit significant VNIR spectral variability. For example, variations in snow crystallinity, grain size, liquid water content, and impurity content all have significant spectral influences (Warren, 1982). Instead, snow was identified in unmixed images using a combination of both high root-mean-square errors (RMSE) and high VNIR albedo.

Linear unmixing is less commonly used in the visible or near-infrared portions of the electromagnetic spectrum in more vertical ecosystems where multiple scattering can be significant, (*i.e*. between vegetation canopy layers). Here, however, we assume minimal spectral contributions from volumetric scattering with depth in the largely barren surface environments of the MDV where linear unmixing has been demonstrated successfully (Salvatore et al., 2021, 2020). Because of these assumptions and their demonstrated effectiveness in the past, we have selected linear unmixing as an appropriate method for this study (Peddle et al., 1999; Roberts et al., 1993; Salvatore et al., 2021, 2020).

An 'early season' December 21, 2021 WV-2 image (10300100CB9F3900) and a 'late season' January 21, 2015 WV-2 image (103001003ED2B400) were the primary images used in this unmixing analysis to capture potential seasonal variation in the spectral signatures of biocrusts and soils. The DaVinci software package was used to run the unmixing model, using

our seven spectral endmembers to linearly derive the areal abundance of these different surface components. The results include percent surface abundance as well as RMSE, which provides a measure of the goodness of fit between the input spectrum and the modeled spectrum. Abundance estimates from each of the endmembers were extracted from the 30 plot locations, incorporating a buffer to confidently capture the plot area (25 pixels per plot). RMSE were analyzed for each pixel-level abundance estimate, commonly ranging between ~ 0.1% to below 0.4%. However, certain pixels contained high RMSE and were attributed to being covered in snow, as verified by examining albedo estimates and the true-color WV-2 images. To account for the uncertainty imposed by snow in these areas, we filtered the abundance data by applying a threshold of RMSE >0.5%. Any pixels that contained RMSE >0.5% were removed from the analysis.

To qualitatively and quantitatively assess the unmixing model output for an early season and late season image, we selected 15 plots to examine abundances of the different surface types. These plots were visually categorized in the field as having either biocrust/incipient biocrust, soil, or oxidized granite (*i.e.*, 5 biocrust/incipient biocrust, 5 soil, and 5 oxidized granite plots). The orange microbial mat #1 and #2 endmember abundances were aggregated into a single orange mat group abundance, and we combined the soil endmember and water endmember abundances together as 'other abiotic' abundance. We compared our field measurements to our modeled total biocrust abundance, which was calculated as the sum of modeled black microbial mat, orange microbial mat, and moss abundance estimates for each pixel. While it is unlikely for all three of these microbial mat communities to co-occur in the environments we assessed outside of stream channels (Alger et al., 1997), summing all biological endmembers to create a "total biocrust abundance" parameter provides a quantitative assessment of the spectral

contributions of photosynthetic pigments and the reflective structure of living cells. Therefore, this parameter is effective for the purposes of distinguishing surfaces where photosynthetic signatures are present, and our efforts will help to quantify our abilities to derive the abundances of these communities remotely.

Albedo analysis of orbital data

We selected 13 cloud-free WorldView images acquired between 2009 and 2019 (six images acquired in December and seven images acquired in January) (Table S3.1) to determine how the landscape's albedo changes from the 'early season' to the 'late season' and to therefore examine the potential presence of ephemeral snowpacks in the vicinity of our study plots, which based upon our field surveys were often associated with visible biocrust communities. Moreover, the presence of snowpack can mask surface soil features, so it was necessary for our analyses to characterize snowpacks in the vicinity of our plots. The mean and standard deviation of each pixel in these suites of early and late season images can provide important information related to surface landscape features. For example, brightening of surfaces indicates the presence of salts or snow on the surface, while darkening typically indicates increased soil moisture. We assume that topographic variations resulting in variations in shadows are negligible on the valley floor for the purposes of this exercise. We predict that surfaces dominated by abiotic materials (granite and soil) will experience less variability in albedo over time than areas exhibiting increased photosynthetic and/or hydrological activity. After stacking the December and the January images, the average albedo and albedo standard deviation (SD) were calculated for each of the 25 pixels surrounding each plot's center. Plot-level average and SD albedo were then calculated for December and January, separately. These data were plotted against one another and

visualized based on identified surface type (biocrust, granite, soil) to analyze any associations with albedo and seasonality.

Results

Laboratory spectral validation study

Hyperspectral measurements of the soil biocrust microcosms exhibited significant chlorophyll absorption features at ~ 0.68 µm for all mixtures containing biocrust (Figure 3.3), including the lowest abundance sample of 1% biocrust by weight (g/g). Lab measurements of the two extreme spectra (100% soil and 100% biocrust) were downsampled to WorldView resolution to compare with the resolution of the orbital data available for the field plots and were used to unmix spectra of actual biocrust mixtures measured in the lab. There was a strong linear fit between the modeled and measured biocrust abundance with an R^2 of 0.99 and p-value < 0.001 (Figure 3.4). Mixtures of biocrust and soil combine linearly in VNIR spectral space in these ideal conditions, demonstrating how linear unmixing models can successfully predict biocrust abundance.

Field surveys and spectral analyses

We found that many of the high or variable NDVI locations occurred in areas near snowpacks and in the lee of hills or in depressions (*i.e.*, nivation hollows; Eveland et al., 2013), where biocrust cover over desert pavement was visually evident. One location in particular had visibly wet soils and dense biocrusts, plot 09 (Figure 3.5a, d, g). Percent coverage of up to 47% biocrust and average surface AFDM of 280 g m^{-2} of biocrust in plot 09 is similar to the lower range of densities reported for microbial mats on riparian sediments adjacent to nearby stream channels (Alger et al., 1997; Power et al., 2020; Salvatore et al., 2021). In contrast, several plots were extremely dry with no visible biocrust but had oxidized granite boulders and relatively high

NDVI from orbital data (Figure 3.5b, e, h). Hyperspectral VNIR measurements collected from the field plot samples exhibited clear spectral differences between plots with visible presence of biocrust, granite boulders, and typical desert pavement soil (Figure 3.5j, k, l). Additionally, some plots were visually characterized as having sparse, incipient biocrust with weak but significant chlorophyll absorptions (*e.g.*, P04, P11; Figure 3.6). We ranked each plot on biocrust presence as "not present", "possibly present", "likely present", and "present" based entirely on visual observations in the field, finding that plots where biocrust was present or was likely present had overall higher NDVI values using the hyperspectral VNIR measurements (Figure 3.7). Plots that were dominated by oxidized granite also had relatively high NDVI but lacked visible biocrust. The densest biocrust plot and the granite boulder plots had relatively high NDVI based on the hyperspectral data as well; however, the shapes of their spectral signatures are very different (*e.g.*, biocrust plot 09 and oxidized granite plot 20; Figure 3.5j, k; Figure S3.2).

In a PCA on covariance using the WV-2 band reflectance (B1 – B8), plot types are significantly differentiated using multispectral band data (MANOVA, p-value = 0.048) (Figure 3.8). Notably, the plots with oxidized granite are spectrally dissimilar from the biocrust and soil plots when all eight bands are used. It is also possible to distinguish among plot types using common vegetation indices (ANOVA; NDVI p-value < 0.001; SR p-value < 0.001; SRre p-value < 0.01; NPCI p-value < 0.01). Particularly, oxidized granite plots have significantly higher values for all vegetation indices compared to the biocrust and soil plots. In a correlation matrix between the vegetation indices, raw reflectance bands, and biological parameters (AFDM, chlorophyll, and scytonemin concentration), there are no significant relationships between these primary remote sensing data and biological parameters (Table S3.2).

Soil characterization

There was significant variation in pigments, organic matter, invertebrate populations, (Table 3.1) and in other physical and chemical variables (Table 3.2) among the plots. Notably, plot 09, with dense biocrust, had the highest abundances and diversity of soil invertebrates, hosting three nematode taxa (*Scottnema*, *Eudorylaimus*, and *Plectus*) in addition to tardigrades, rotifers, and ciliates, similar to the community composition found in soils near streams (Ayres et al., 2007; Simmons et al., 2009a; Treonis et al., 1999). While *Scottnema* was present in relatively high abundances throughout most plots (as has been previously reported for this area of Taylor Valley; Courtright et al., 2001), there were several plots (P22, 30, 31) without any invertebrates present where distinct soil chemistry (pH, nitrate, and electrical conductivity) likely created inhospitable conditions (*e.g.*, Barrett et al., 2004; Poage et al., 2008). The majority of samples had NH_4^+ concentration below detection except for plots 01, 09, 10, 22, 31, 33. Soil organic carbon and total nitrogen concentrations were higher than average compared to soils in this part of Taylor Valley (Barrett et al., 2007, 2006b) and may reflect the influence of moderate to dense biocrusts found in our most productive plots (Table 3.2). Importantly, dense biocrust plot 09 had the lowest electrical conductivity (indicator of soils that are regularly flushed by water), a more neutral pH, and a relatively higher concentration of ammonium, NH_4^+, (indicative of active microbial decomposition). Moreover, plot 09 had more than 5x the AFDM of the other plots on average. In a PCA on correlation, plot types are not significantly distinguished by physicochemical properties (MANOVA, p-value = 0.56) (Figure S3.3). However, NH_4^+ availability is significantly different among the plot types (ANOVA, p-value = 0.044) with dense biocrust most associated with increasing NH_4^+ availability.

Spectral linear unmixing of orbital data

The linear spectral unmixing analysis of an early season (Dec 21 2021) and late season (Jan 21 2015) image demonstrated consistency in surface cover estimates between the two images (Table 3.3). RMSE were relatively low except for areas that were snow covered (*i.e.*, also displayed high albedo values). Notably, these snowy areas often coincided with plots that were identified in the field as either having biocrust present or likely present (incipient biocrust). Half of locations with biocrust or incipient biocrust (n = 4 of 8) were snow covered during the early season image. The remaining locations with biocrust and incipient biocrust were all within 15-35 m of snowpacks, measured from the center of the plots. Among the remaining 22 plots identified as biocrust not present or possibly present, only 3 plots contained some pixels with RMSE > 0.5%. One of these plots contained some snow cover and lacked visible biocrust (P33), while the other two plots did not contain snow cover in the immediate area (P29, 30). Table 3.3 includes a subset of our 30 plots documenting the consistency of surface cover types between our two analyzed images, and also demonstrates the likely association between the presence of biocrust and snow cover.

Albedo analysis of orbital data

To identify any possible associations between biocrust cover and early season snowpack, the mean albedo and albedo SD were calculated for all plots among several December and January images (Figure 3.9). Locations that contained snow cover had greater mean albedo, primarily early in the season when snowpacks are most present, and greater albedo SD between images based on the seasonality of snow and surface soil moisture. All of the plots that contained visually conspicuous biocrust cover had higher mean albedo and albedo SD than typical soil or oxidized granite plots. While not *all* of our biocrust identified plots were associated with

variations in snow cover within the immediate area of the plots (note that biocrust can obtain moisture from groundwater seeps or melting subsurface ice as well), we do find that the brightest and most variable surfaces in our study area are all biocrust identified areas (Figure 3.9).

Discussion

Laboratory spectral detection of biocrust

Our laboratory spectral validation study demonstrated that biocrust present in soil microcosms is detectable at abundances as low as 1% by weight, and that spectral linear unmixing models can be used to successfully predict biocrust abundance. The absorption feature associated with photosynthetic pigments (~ 0.68 μm) is present in all biocrust microcosm mixtures, including the 1% biocrust microcosm where the feature is observable as well (Figure 3.3). When comparing the modeled biocrust abundance of each sample mixture to the actual measured biocrust abundance, there is a strong linear fit between the modeled and measured abundance with an R^2 of 0.99 (Figure 3.4). We have shown how, under ideal conditions, mixtures of biocrust and soil combine linearly in VNIR spectral space, allowing for linear unmixing models to accurately predict biocrust abundance. This detection method is successful over a range of abundances analogous to dense microbial mat communities associated with productive aquatic habitats (Power et al., 2020; Salvatore et al., 2021) and sparse biocrusts in the more typical arid soils of the MDV. Despite the known complexities associated with extrapolating these results to field and orbital data (*e.g.*, atmospheric contributions, variations in biotic and abiotic surface composition and moisture), the relationships derived in our laboratory analyses are successful in identifying and quantifying biocrust and can be modeled to approximate the distribution of microbial communities in the MDV.

Oxidized granite impedes use of vegetation indices

It was evident during our field surveying and sampling campaign that geological features are a significant factor in the detection of low density biocrusts in dry terrestrial environments. While the soils and dominant lithologies of the MDV have been widely characterized by previous investigators (*e.g.*, Bockheim et al., 2008), isolated outcrops or boulders of distinct composition have been shown to locally influence observed spectral signatures. For example, during our field campaign, several plots with high NDVI values were found to be predominantly covered by oxidized granitic boulders (Figure 3.5e, h). Despite their high NDVI values, these oxidized granite plots lack visible biocrust presence based on visual observation in the field (Figure 3.7) and had low AFDM and chlorophyll contents (Table 3.1), indicating that these relatively high NDVI values are not associated with photosynthesis. The hyperspectral data of the surface samples of all plots illustrated clear distinctions among the plots (Figure 3.6). For example, plots 20 and 29 were located within oxidized granite boulder fields and exhibit two broad absorption features associated with the presence of ferrous and ferric iron (Fe), centered near 0.67 μm and 0.94 μm, and resulting in a broad reflectance peak at approximately 0.74 μm (Figure 3.5k; Figure S3.2). While the hyperspectral shape of these granitic spectra is distinct from those of biocrust, NDVI does not effectively distinguish between them due to the granitic spectra containing an Fe-absorption feature at red wavelengths and thus an increase in reflectance in the NIR (Figure S3.2). This change in reflectance creates a slope that causes these granitic areas to have a high NDVI, despite not being correlated to indicators of photosynthetic activity (*e.g.*, chlorophyll or AFDM). While hyperspectral reflectance data can be used to distinguish these abiotic absorption features from those associated with biological activity,

simple multispectral parameters (*e.g.*, NDVI) are less capable of distinguishing between these different compositions and are therefore less reliable at detecting biocrust presence.

Biocrust distribution is associated with seasonal snowpacks

In contrast to soils with oxidized granites, several locations contained sparse, incipient biocrust, where it appeared that cyanobacteria colonies and potentially moss were emerging from wet desert pavement (Figure 3.1c). The locations identified as having biocrust present or likely present had relatively higher NDVI compared to the desert pavement locations not containing biocrust and which upon analyses were shown to have low chlorophyll concentrations and AFDM. Of particular interest, plot 09 hosted dense biocrust (Figure 3.5d, g) and diverse soil fauna (Table 3.1), similar in composition to the diversity found near stream and lake ecosystems (Ayres et al., 2007; Treonis et al., 1999). Plot 09 is outside of any stream channel or water track and is ~ 700 meters above the current elevation of Lake Fryxell. The only visible source of liquid water for plot 09 are a series of snowpacks immediately uphill and ~ 10 and 50 meters uphill (at the time of sampling and visible in multiple satellite images). While diverse invertebrate communities are common near aquatic environments in the Fryxell basin (Courtright et al., 2001; Freckman and Virginia, 1997), they have not been commonly reported for upland soils outside stream channels.

One well-documented landscape that exhibits similar biotic diversity to plot 09 is the Wormherder Creek wetland in western Taylor Valley on the south side of the west lobe of Lake Bonney (Harris et al., 2007; Simmons et al., 2009b; Nielsen et al., 2012). Unlike the soil biocrusts documented here (*e.g.*, plot 09), which are fed by the melt of relatively small snowpacks (<60 m in diameter), the Wormherder Creek wetland is fed intermittently by the melt of large snowpacks on the southern valley wall which create melt-water drainages that have

contributed to saturated soils and overland flow on at least 3 documented occasions (sufficiently warm and sunny summers) in the last thirty years (Lyons et al., 2005; Nielsen et al., 2012; Wlostowski et al., 2019; Stanish et al., 2012; Harris et al., 2007). Abundant microbial mats hosting diatom and invertebrate communities have been described in Wormherder Creek (Nielsen et al., 2012; Stanish et al., 2012; Simmons et al., 2009b). Both these snowpack-fed meltwater environments are examples of biological hotspots in an otherwise arid terrestrial landscape physically separated from the diverse communities within the annual ephemeral streams.

These snowpack-fed biological hotspots are distinct from the water track features described by Levy et al. (2011), which are narrow areas of subsurface hydrologic flow that route water downslope through soils above the ice table and lack overland flow. Water tracks are more saline in comparison to the surrounding landscape and therefore do not host conspicuous surface biocrust, microbial mats, or invertebrate communities (Kuentz et al., 2022; Levy et al., 2014, 2011). Therefore, biological activity in these snowpack areas is not driven solely by the presence of liquid water, but also suitable soil conditions as well.

A continuum of hydrological conditions exists: the arid terrestrial landscape, hypersaline water tracks, snowpack-fed microhabitats, snowpack-fed non-annual ephemeral wetlands, annual ephemeral streams, and lakes (Table 3.4). Plot 09 is compositionally and chemically more similar to near-stream environments than to the persistently dry and low organic matter soils that characterize most of this arid terrestrial landscape (Burkins et al., 2001; Barrett et al., 2006a). For example, plot 09 is wetter and less alkaline than the other soil plots with low or no biocrusts, which are representative of the arid soils described by Barrett et al. (2006a) and Campbell et al. (1998) (Table 3.2). Plot 09 also has the lowest electrical conductivity, which is an indicator that

soils are regularly flushed by water, and it has a relatively higher concentration of ammonium, NH_4^+, typical for biologically active soils with active turnover of organic matter (Barrett et al., 2009). Additionally, the concentration of soil organic C in this plot is more than 2x greater on average than previous reports for arid soils in Taylor Valley (Barrett et al., 2006b; Burkins et al., 2001) and closer to the concentrations of C in near-stream and lake sediments (Barrett et al., 2009). Moreover, the mass of carbon in the biocrust itself is 2-3x greater than that in the underlying surface soils (Burkins et al., 2001), indicating the importance of including biocrust estimates in regional carbon mass balances. Rather than viewing this landscape as simply aquatic or terrestrial units, a continuum of hydrological conditions exists, and these snowpack-fed landscapes constitute a unique component of the soil-sediment environment. Elucidating the factors contributing to the structure and function of these snowpack-associated environments is essential for refining our understanding of species distribution and organic C balance in the MDV.

Comparisons between multispectral and hyperspectral data

There are inherent limitations to multispectral data when they are used for detecting surfaces that are spectrally weaker and discontinuous, such as patchy biocrusts. When investigating our intensively sampled plots which had *in-situ* biological data collected (*i.e.*, AFDM, pigment content), there were no significant correlations between the biological parameters and multispectral vegetation indices and raw bands (Table S3.2). There were some correlations (*e.g.*, with B1, R ~ 0.73; and with B2, R ~ 0.64) that were driven by plot 09 with orders of magnitude higher AFDM and pigment concentration, but all significant correlations were lost when removing this dominant plot. Solely using these traditional multispectral indices

is inadequate for identifying patchy biocrust surfaces, specifically in areas with spectrally dominant surface geology, such as the MDV.

Hyperspectral reflectance measurements were essential in this study to understand the spectral complexities of our surface types. For example, plot 09 contained the most visibly dense biocrust in our field campaign and was spectrally unique with the highest NDVI measured from hyperspectral data in the laboratory (Figure 3.6). However, it did not always have the highest satellite-derived NDVI as expected; the oxidized granite areas sometimes had higher NDVI across images. This demonstrates the differences in spectral resolution between a hyperspectral reflectance spectrometer and a multispectral satellite, and also the differences in surface area of larger granitic surfaces compared to patchy biocrust surfaces when using satellite data. Additionally, this difference in plot 09 NDVI from hyperspectral laboratory measurements to multispectral orbital data could also in part be the result of fluctuating biological activity through time. For example, a 2019 WorldView-3 image shows higher NDVI at this location in January when the snow generally melts, the surrounding soils are moist, and the biocrust communities are likely active (Figure 3.5a). Barták et al. (2016) and Trnková and Barták (2017) both demonstrate the relationship between water content in black microbial mats, their photosynthetic activity, and their resultant spectral signatures. Their results indicate that there is a reduction in NDVI by roughly 50% from maximum photosynthetic signatures at roughly 55% relative water content (RWC) to complete desiccation at 0% RWC. These and other authors (*e.g.*, Salvatore et al., 2021) also note how burial by windblown sand can significantly mask the spectral signatures of dry mats and biocrusts. Together, these studies and our results demonstrate there are many factors that can influence the observed NDVI signature at multispectral resolutions beyond simply the

abundance of photosynthetic biomass, and hyperspectral data were necessary to elucidate these interactions.

However, incorporating all multispectral bands makes it possible to differentiate between the three plot types here (Figure 3.8). The gradient of plots from bare soil to denser biocrust along the raw WV-2 band reflectance vectors informs a detection threshold for biocrust around 47% cover or 280 g m^{-2} AFDM (plot 09). The oxidized granite plots are most spectrally dissimilar from the biocrust and soil plots. When using the vegetation indices calculated from the multispectral data, it is also possible to statistically distinguish among plot types. Though, the plots with the highest vegetation index values are those with the oxidized granite surfaces. It is evident through our analyses that surface geology in this environment can result in higher NDVI values, which is not indicative of biological activity, but are instead spectrally dominant areas in the wavelengths typically diagnostic for photosynthesis. Although hyperspectral data in the laboratory show that biocrust is identifiable and distinct from oxidized granite surfaces and typical soil surfaces, we are currently limited to multispectral resolution with available satellite data. While vegetation indices are also limited in the number of bands they incorporate and are shown here to be affected by surface geology, incorporating all eight multispectral bands proves useful in distinguishing biologically active surfaces. It is of particular importance to note that the overall success of our analyses was dependent on our ability to ground truth, which allows us to confidently link spectral data to what we saw and measured with boots on the ground.

Spectral linear unmixing models predict biocrust abundance

Moving beyond traditional remote sensing indices, we applied spectral linear unmixing models to WV-2 orbital data using spectral endmembers collected from the field with a hyperspectral reflectance spectrometer, including an oxidized granite endmember (Table 3.3).

The low RMSE associated with the unmixing of all surface types discussed here demonstrates that there are no clearly omitted spectral endmembers. Although our hyperspectral measurements outperform multispectral data in terms of biological detection, we are limited to multispectral bands with available satellite imagery. However, using multispectral orbital data, our results demonstrate how linear unmixing models perform better than vegetation indices, because they use all eight multispectral bands as opposed to only a few select bands. Specifically, there are clear spectral differences between oxidized granites and photosynthetic biocrust when all eight spectral bands are investigated, but these differences are lost when using vegetation parameters like NDVI. While some endmembers are less spectrally unique at multispectral resolutions in comparison to hyperspectral and can confuse the unmixing models at times, these models are still a far improvement over simple vegetation indices in detecting low density biocrusts and can be used to infer ecologically relevant properties of biocrust in this region. Most notably, our unmixing analyses with RMSE indicate that plots containing biocrust were all either snow covered or within 15-35 m of snowpacks during an early season (Dec 21 2021) WorldView-2 image (Table 3.3). This result suggests snowpacks are important sources of moisture sustaining biocrust community microhabitats in an otherwise arid terrestrial landscape, and therefore encourages further investigation.

Snowpacks as microhabitats for biocrusts and diverse soil communities

To identify associations between biocrust cover and early season snowpack, we visualized the mean albedo and albedo SD for all plots based on surface type among several December and January images (Table S3.1). We found that the brightest and most variable surface areas, where snow is present, were areas that were identified as biocrust visually in the field (Figure 3.9). There are biocrust areas that have lower mean and SD albedo and are likely

associated with other sources of moisture, like groundwater seeps or snow, which accumulates to a much lesser extent and melts earlier in the season. Among our plots, the highest and most variable albedo surfaces are associated with biocrust presence, indicating that these MDV biocrust habitats are likely associated with areas where snow accumulates early in the season, slowly melts later in the season, and supplies soil communities and biocrusts with sufficient moisture to sustain biological activity throughout the austral summers.

Snow is an important surface component of the Taylor Valley. Seasonal snow accumulates more on the eastern portion of the Taylor Valley closer to the coast (Eveland et al., 2012, 2013; Fountain et al., 2010). The Fryxell basin, where our study region is located, receives the greatest annual snowfall and has the highest interannual variability of snowfall within Taylor Valley (Myers et al., 2022). The Fryxell basin region received an average of 11.5 mm wet equivalent of snow accumulation from 1995 to 2017 between the months of August and May (Myers et al., 2022). While the magnitude of snowfall and snow accumulation is dependent on the variability of the frequency and intensity of storms and winds, snow is expected to collect in the same locations inter-annually because snow accumulation is most associated with variation in fine-scale topography (Eveland et al., 2012, 2013). Seasonal snow accumulates across a large portion of the Fryxell basin region. For example, prior research has shown accumulation covering an area of 10.29 km^2 (17.83% of the Fryxell basin delineated region) in late October of 2009 (Eveland et al., 2012). By mid-January of 2010, 93% of the snow accumulation was lost (Eveland et al., 2012), primarily due to sublimation given the arid environment but also due to snowmelt. For example, Gooseff et al. (2003) and Ayres et al. (2010) observed increases in soil moisture near snowpacks compared to the nearby dry soils. Eveland et al. (2012) also suggest that volumes of water that usually seem insignificant to some ecosystems may be an important

driver in structuring communities below snow in highly water-limited environments such as the MDV. Snow cover has also been shown to reduce temperature extremes in underlying soil and influence biogeochemical cycling and microbial activity in soils generally (Schimel et al., 2004; Van Horn et al., 2013).

Furthermore, we suggest that snowpacks commonly occurring throughout eastern Taylor Valley provide enough moisture for the development of biocrusts and underlying soil communities and likely create suitable microhabitats shielded from temperature extremes and intense UV-radiation. Given the broader spatial extent of the terrestrial landscape outside of stream channels and lake margins and the abundance of snowpacks, we anticipate that a considerable proportion of the valley-wide carbon budget is represented by biocrust communities. To refine the Taylor Valley carbon budget, future field work should incorporate more sampling and surveying of these snowpack areas to document the influence of snowpack variability on the dynamics of biocrust and soil microbial communities in the MDV. Given the strong interannual variability of snowfall and snow persistence in the Taylor Valley (Myers et al., 2022), the documented occurrence of anomalous weather events (Barrett et al., 2024), and the prediction that Antarctic coasts will experience more frequent and intense rainfall by the end of the century (Vignon et al., 2021), we encourage continued research on these biocrust microhabitats in this currently water-limited but increasingly dynamic landscape.

Conclusion

Here, we show that low density biocrusts are patchily distributed throughout the eastern Taylor Valley region in upland areas away from streams and lake margins. Seasonal snowpacks create microhabitats for these biocrust communities to successfully thrive in this otherwise harsh, desert environment. Soils beneath these biocrusts can support diverse soil fauna, similar in

community composition to soils immediately beside streams and lake margins. A continuum exists between aquatic and terrestrial environments where microhabitats are driven by snowpacks physically separate from streams that otherwise have ecosystem properties and biological diversity more similar to the local streams than the nearby arid soils. We suggest that these snowpack-fed microhabitats are unique ecosystems and a key ecological component to the region's carbon budget. Moreover, our work to study these microhabitats in further detail is ongoing (*e.g.*, Power et al., 2024), and we encourage other efforts as well.

Ground truthing is essential for detecting and mapping biocrust. Although geological surface composition can impede use of NDVI on soils, spectral linear unmixing methods are a practical alternative for successful biocrust detection. Our modeling efforts are currently the foundation of follow-up studies where further validation efforts in the field are needed to extrapolate the model and test our hypotheses about hydrological transitions and their influence on photoautotrophic communities. This work brings us closer in our efforts to refine the carbon budget for this region and to examine the controls over the distribution and activity of these critical soil communities. These remote sensing technologies are ideal for measuring ecosystem dynamics in Antarctic ecosystems, which are particularly climate-sensitive and difficult to access.

Data Availability Statement

All data presented in this study are archived in the Environmental Data Initiative (EDI) Data Repository (Power et al., 2023).

Funding Statement

This work was supported by the National Science Foundation (NSF) through grants #1637708 and #2224760 to the McMurdo Dry Valleys Long Term Ecological Research Project; NSF

through grant #1745053 to M. Salvatore, J. Barrett, and grant #1744849 to E. Sokol, L. Stanish; and the Virginia Space Grant Consortium 2020-2021 and 2021-2022 Fellowship Programs to S. Power.

Acknowledgements

We would like to acknowledge the Polar Geospatial Center for geospatial support and DigitalGlobe, Inc. for access to satellite imagery. We appreciate Antarctic Support Contractors and Air Center Helicopters for providing operational support in the field. We would also like to thank Ernest Osburn for assistance with ground truthing and sample collection in the field, and Bobbie Niederlehner and Maxwell Craddock for their assistance with laboratory analyses. Additionally, we acknowledge the two anonymous reviewers whose thoughtful feedback improved the clarity and organization of this manuscript.

References

Adams, B.J., Bardgett, R.D., Ayres, E., Wall, D.H., Aislabie, J., Bamforth, S., Bargagli, R., Cary, C., Cavacini, P., Connell, L., Convey, P., Fell, J.W., Frati, F., Hogg, I.D., Newsham, K.K., O'Donnell, A., Russell, N., Seppelt, R.D., Stevens, M.I., 2006. Diversity and distribution of Victoria Land biota. Soil Biol. Biochem. 38, 3003–3018. https://doi.org/10.1016/J.SOILBIO.2006.04.030

Adams, J.B., Smith M.O., and Gillespie A.R., 1993. Imaging spectroscopy: Interpretation based on spectral mixture analysis. In Topics in, edited by I. V. Remote Sensing, A. C. Remote Geochemical, M. Pieters, and P. A. J. Englert, 145–166. Cambridge: Cambridge University Press.

Alger, A.S., McKnight, D.M., Spalding, S.A., Tate, C.M., Shupe, G.H., Welch, K.A., Edwards, R., Andrews, E.D., House, H.R., 1997. Ecological Processes in a Cold Desert Ecosystem: The Abundance and Species Distribution of Algal Mats in Glacial Meltwater Streams in Taylor Valley, Antarctica. Institute of Arctic and Alpine Research Occasional Paper 51.

Ayres, E., Nkem, J.N., Wall, D.H., Adams, B.J., Barrett, J.E., Simmons, B.L., Virginia, R.A., Fountain, A.G., 2010. Experimentally increased snow accumulation alters soil moisture

and animal community structure in a polar desert. Polar Biol. 33, 897–907. https://doi.org/10.1007/s00300-010-0766-3

Ayres, E., Wall, D.H., Adams, B.J., Barrett, J.E., Virginia, R.A., 2007. Unique Similarity of Faunal Communities across Aquatic–Terrestrial Interfaces in a Polar Desert Ecosystem. Ecosystems 10, 523–535. https://doi.org/10.1007/s10021-007-9035-x

Barrett, J.E., Adams, B.J., Doran, P.T., Dugan, H.A., Myers, K.F., Salvatore, M.R., Power, S.N., Snyder, M.D., Wright, A.T., Gooseff, M.N., 2024. Response of a Terrestrial Polar Ecosystem to the March 2022 Antarctic Weather Anomaly. Earths Future 12, e2023EF004306. https://doi.org/10.1029/2023EF004306

Barrett, J.E., Gooseff, M.N., Takacs-Vesbach, C., 2009. Spatial variation in soil active-layer geochemistry across hydrologic margins in polar desert ecosystems. Hydrol. Earth Syst. Sci. Discuss. 6, 3725–3751. https://doi.org/10.5194/hessd-6-3725-2009

Barrett, J.E., Virginia, R.A., Hopkins, D.W., Aislabie, J., Bargagli, R., Bockheim, J.G., Campbell, I.B., Lyons, W.B., Moorhead, D.L., Nkem, J.N., Sletten, R.S., Steltzer, H., Wall, D.H., Wallenstein, M.D., 2006a. Terrestrial ecosystem processes of Victoria Land, Antarctica. Soil Biol. Biochem. 38, 3019–3034. https://doi.org/10.1016/J.SOILBIO.2006.04.041

Barrett, J.E., Virginia, R.A., Lyons, W.B., McKnight, D.M., Priscu, J.C., Doran, P.T., Fountain, A.G., Wall, D.H., Moorhead, D.L., 2007. Biogeochemical stoichiometry of Antarctic Dry Valley ecosystems. J. Geophys. Res. 112. https://doi.org/10.1029/2005JG000141

Barrett, J.E., Virginia, R.A., Parsons, A.N., Wall, D.H., 2006b. Soil carbon turnover in the McMurdo Dry Valleys, Antarctica. Soil Biol. Biochem. 38, 3065–3082. https://doi.org/10.1016/j.soilbio.2006.03.025

Barrett, J.E., Virginia, R.A., Wall, D.H., Cary, S.C., Adams, B.J., Hacker, A.L., Aislabie, J.M., 2006c. Co-variation in soil biodiversity and biogeochemistry in northern and southern Victoria Land, Antarctica. Antarct. Sci. 18, 535. https://doi.org/10.1017/S0954102006000587

Barrett, J.E., Virginia, R.A., Wall, D.H., Parsons, A.N., Burkins, M.B., 2004. Variation in Biogeochemistry and Soil Biodiversity across Spatial Scales in a Polar Desert Ecosystem. Ecology 85, 3105–3118.

Barták, M., Hazdrová, J., Skácelová, K., Hájek, J., 2016. Dehydration-induced responses of primary photosynthetic processes and spectral reflectance indices in Antarctic Nostoc

commune. Czech Polar Rep. 6, 87–95. https://doi.org/10.5817/cpr2016-1-9

Belnap, J., 2003. The world at your feet: desert biological soil crusts. Front. Ecol. Environ. 1, 181–189. https://doi.org/10.1890/1540-9295(2003)001[0181:TWAYFD]2.0.CO;2

Belnap, J., Weber, B., Büdel, B., 2016. Biological Soil Crusts as an Organizing Principle in Drylands, in: Weber, B., Büdel, B., Belnap, J. (Eds.), Biological Soil Crusts: An Organizing Principle in Drylands. Springer International Publishing, pp. 3–13.

Bioucas-Dias, J.M., Plaza, A., Dobigeon, N., Parente, M., Du, Q., Gader, P., Chanussot, J., 2012. Hyperspectral unmixing overview: Geometrical, statistical, and sparse regression-based approaches. IEEE Journal of Selected Topics in Applied Earth Observations and Remote Sensing. https://doi.org/10.1109/JSTARS.2012.2194696

Bockheim, J.G., Prentice, M.L., McLeod, M., 2008. Distribution of glacial deposits, soils, and permafrost in Taylor Valley, Antarctica. Arct. Antarct. Alp. Res. 40, 279–286. https://doi.org/10.1657/1523-0430(06-057)[BOCKHEIM]2.0.CO;2

Brenowitz, S., Castenholz, R.W., 1997. Long-term effects of UV and visible irradiance on natural populations of a scytonemin-containing cyanobacterium (Calothrix sp.). FEMS Microbiol. Ecol. 24, 343–352. https://doi.org/10.1016/S0168-6496(97)00075-5

Burkins, M.B., Virginia, R.A., Wall, D.H., 2001. Organic carbon cycling in Taylor Valley, Antarctica: quantifying soil reservoirs and soil respiration. Glob. Chang. Biol. 7, 113–125. https://doi.org/10.1046/j.1365-2486.2001.00393.x

Campbell, I.B., Claridge, G.G.C., Campbell, D.I., Balks, M.R., 1998. The soil environment of the McMurdo dry valleys, Antarctica, in: Ecosystem Dynamics in a Polar Desert: The Mcmurdo Dry Valleys, Antarctica, Antarctic Research Series. American Geophysical Union, Washington, D. C., pp. 297–322. https://doi.org/10.1029/ar072p0297

Cary, S.C., McDonald, I.R., Barrett, J.E., Cowan, D.A., 2010. On the rocks: the microbiology of Antarctic Dry Valley soils. Nat. Rev. Microbiol. 8, 129–138. https://doi.org/10.1038/nrmicro2281

Couradeau, E., Karaoz, U., Lim, H.C., Nunes Da Rocha, U., Northen, T., Brodie, E., Garcia-Pichel, F., 2016. Bacteria increase arid-land soil surface temperature through the production of sunscreens. Nat. Commun. https://doi.org/10.1038/ncomms10373

Courtright, E.M., Wall, D.H., Virginia, R.A., 2001. Determining habitat suitability for soil invertebrates in an extreme environment: The McMurdo Dry Valleys, Antarctica. Antarct.

Sci. 13, 9–17. https://doi.org/10.1017/S0954102001000037

Cox, S.C., Turnbull, I.M., Isaac, M.J., Townsend, D.B., Lyttle, B.S., 2012. Geology of Southern Victoria Land, Antarctica. Institute of Geological and Nuclear Sciences 1:250 000 Geological Map.

Doran, P.T., McKay, C.P., Clow, G.D., Dana, G.L., Fountain, A.G., Nylen, T., Lyons, W.B., 2002. Valley floor climate observations from the McMurdo dry valleys, Antarctica, 1986–2000. J. Geophys. Res. 107, 4772. https://doi.org/10.1029/2001JD002045

Elbert, W., Weber, B., Burrows, S., Steinkamp, J., Büdel, B., Andreae, M.O., Pöschl, U., 2012. Contribution of cryptogamic covers to the global cycles of carbon and nitrogen. Nat. Geosci. 5, 459–462. https://doi.org/10.1038/ngeo1486

Eveland, J., Gooseff, M.N., Lampkin, D.J., Barrett, J.E., Takacs-Vesbach, C., 2012. Spatial and temporal patterns of snow accumulation and aerial ablation across the McMurdo Dry Valleys, Antarctica. Hydrol. Process. 27. https://doi.org/10.1002/hyp.9407

Eveland, J.W., Gooseff, M.N., Lampkin, D.J., Barrett, J.E., Takacs-Vesbach, C.D., 2013. Seasonal controls on snow distribution and aerial ablation at the snow-patch and landscape scales, McMurdo Dry Valleys, Antarctica. The Cryosphere 7, 917–931. https://doi.org/10.5194/tc-7-917-2013

Finger-Higgens, R., Duniway, M.C., Fick, S., Geiger, E.L., Hoover, D.L., Pfennigwerth, A.A., Van Scoyoc, M.W., Belnap, J., 2022. Decline in biological soil crust N-fixing lichens linked to increasing summertime temperatures. Proc. Natl. Acad. Sci. U. S. A. 119, e2120975119. https://doi.org/10.1073/pnas.2120975119

Fountain, A.G., Fernandez-Diaz, J.C., Obryk, M., Levy, J., Gooseff, M., Van Horn, D.J., Morin, P., Shrestha, R., 2017. High-resolution elevation mapping of the McMurdo Dry Valleys, Antarctica, and surrounding regions. Earth System Science Data 9, 435–443. https://doi.org/10.5194/essd-9-435-2017

Fountain, A.G., Nylen, T.H., Monaghan, A., Basagic, H.J., Bromwich, D., 2010. Snow in the McMurdo Dry Valleys, Antarctica. Int. J. Climatol. 30, 633–642. https://doi.org/10.1002/joc.1933

Freckman, D.W., Virginia, R.A., 1997. Low-diversity antarctic soil nematode communities: Distribution and response to disturbance. Ecology 78, 363–369. https://doi.org/10.1890/0012-9658(1997)078[0363:LDASNC]2.0.CO;2

Freckman, D.W., Virginia, R.A., 1993. Extraction of nematodes from Dry Valley Antarctic soils. Polar Biol. 13, 483–487. https://doi.org/10.1007/BF00233139

Fritsen, C.H., Grue, A.M., Priscu, J.C., 2000. Distribution of organic carbon and nitrogen in surface soils in the McMurdo Dry Valleys, Antarctica. Polar Biol. 23, 121–128. https://doi.org/10.1007/s003000050017

Garcia-Pichel, F., Castenholz, R.W., 1991. Characterization and Biological Implications of Scytonemin, a Cyanobacterial Sheath Pigment. J. Phycol. 27, 395–409. https://doi.org/10.1111/j.0022-3646.1991.00395.x

Gooseff, M.N., Barrett, J.E., Doran, P.T., Fountain, A.G., Lyons, W.B., Parsons, A.N., Porazinska, D.L., Virginia, R.A., Wall, D.H., 2003. Snow-Patch Influence on Soil Biogeochemical Processes and Invertebrate Distribution in the McMurdo Dry Valleys, Antarctica. Arct. Antarct. Alp. Res. 35, 91–99.

Gooseff, M.N., Barrett, J.E., Levy, J.S., 2013. Shallow groundwater systems in a polar desert, McMurdo Dry Valleys, Antarctica. Hydrogeol. J. 21, 171–183. https://doi.org/10.1007/s10040-012-0926-3

Harris, K.J., Carey, A.E., Berry Lyons, W., Welch, K.A., Fountain, A.G., 2007. Solute and isotope geochemistry of subsurface ice melt seeps in Taylor Valley, Antarctica. GSA Bulletin 119, 548–555. https://doi.org/10.1130/B25913.1

Keeney, D.R., Nelson, D.W., 1982. Nitrogen—Inorganic forms. In A.L. Page (ed.). Methods of soil analysis. Chemical and microbiological properties. Agronomy 9 (2): 643-698. Am. Soc. of Agron., Madison, WI.

Knepel, K., 2003. Determination of Nitrate in 2M KCl soil extracts by Flow Injection Analysis. QuikChem Method 12-107-04-1-B. Lachat Instruments, Loveland, CO.

Kohler, T.J., Stanish, L.F., Crisp, S.W., Koch, J.C., Liptzin, D., Baeseman, J.L., McKnight, D.M., 2015. Life in the Main Channel: Long-Term Hydrologic Control of Microbial Mat Abundance in McMurdo Dry Valley Streams, Antarctica. Ecosystems 18, 310–327. https://doi.org/10.1007/s10021-014-9829-6

Kuentz, L., Levy, J., Salvatore, M., 2022. Timing and duration of ephemeral Antarctic water tracks and wetlands using high temporal–resolution satellite imagery, high spatial–resolution satellite imagery, and ground-based sensors in the McMurdo Dry Valleys. Arct. Antarct. Alp. Res. 54, 538–561. https://doi.org/10.1080/15230430.2022.2123858

Lawson, C.L., Hanson, R.J., 1974. Solving least squares problems. Prentice-Hall, Englewood Cliffs, N.J.

Levy, J.S., 2013. How big are the McMurdo Dry Valleys? Estimating ice-free area using Landsat image data. Antarct. Sci. 25, 119–120. https://doi.org/10.1017/S0954102012000727

Levy, J.S., Fountain, A.G., Gooseff, M.N., Barrett, J.E., Vantreese, R., Welch, K.A., Berry Lyons, W., Nielsen, U.N., Wall, D.H., 2014. Water track modification of soil ecosystems in the Lake Hoare basin, Taylor Valley, Antarctica. Antarct. Sci. 26, 153–162. https://doi.org/10.1017/S095410201300045X

Levy, J.S., Fountain, A.G., Gooseff, M.N., Welch, K.A., Lyons, W.B., 2011. Water tracks and permafrost in Taylor Valley, Antarctica: Extensive and shallow groundwater connectivity in a cold desert ecosystem. Bulletin of the Geological Society of America 123, 2295–2311. https://doi.org/10.1130/B30436.1

Lyons, W.B., Welch, K.A., Carey, A.E., Doran, P.T., Wall, D.H., Virginia, R.A., Fountain, A.G., Csath, B.M., Tremper, C.M., 2005. Groundwater seeps in Taylor Valley Antarctica: an example of a subsurface melt event. Ann. Glaciol. 40, 200–206. https://doi.org/10.3189/172756405781813609

McKnight, D.M., Alger, A., Tate, C., Shupe, G., Spaulding, S., 1998. Longitudinal Patterns in Algal Abundance and Species Distribution In Meltwater Streams In Taylor Valley, Southern Victoria Land, Antarctica, in: Ecosystem Dynamics in a Polar Desert: The McMurdo Dry Valleys, Antarctica. American Geophysical Union, pp. 109–127. https://doi.org/10.1029/AR072p0109

Myers, M.E., Doran, P.T., Myers, K.F., 2022. Valley-floor snowfall in Taylor Valley, Antarctica, from 1995 to 2017: spring, summer and autumn. Antarct. Sci. 34, 325–335. https://doi.org/10.1017/S0954102022000256

Nielsen, U.N., Wall, D.H., Adams, B.J., Virginia, R.A., Ball, B.A., Gooseff, M.N., McKnight, D.M., 2012. The ecology of pulse events: insights from an extreme climatic event in a polar desert ecosystem. Ecosphere 3, art17. https://doi.org/10.1890/ES11-00325.1

Obryk, M.K., Doran, P.T., Fountain, A.G., Myers, M., McKay, C.P., 2020. Climate From the McMurdo Dry Valleys, Antarctica, 1986–2017: Surface Air Temperature Trends and Redefined Summer Season. J. Geophys. Res. D: Atmos. 125, e2019JD032180. https://doi.org/10.1029/2019JD032180

Olsen, S.R., Sommers, L.E., 1982. Phosphorus. In A.L. Page (ed.) Methods of soil analysis. Chemical and microbiological properties. Agronomy 9 (2): 403-430. Am. Soc. of Agron., Madison, WI.

Pannewitz, S., Green, T.G.A., Scheidegger, C., Schlensog, M., Schroeter, B., 2003. Activity pattern of the moss Hennediella heimii (Hedw.) Zand. in the Dry Valleys, Southern Victoria Land, Antarctica during the mid-austral summer. Polar Biol. 26, 545–551. https://doi.org/10.1007/s00300-003-0518-8

Peddle, D.R., Hall, F.G., Ledrew, E.F., 1999. Spectral mixture analysis and geometric-optical reflectance modeling of boreal forest biophysical structure. Remote Sens. Environ. 67, 288–297. https://doi.org/10.1016/S0034-4257(98)00090-X

Poage, M.A., Barrett, J.E., Virginia, R.A., Wall, D.H., 2008. The influence of soil geochemistry on nematode distribution, Mcmurdo Dry Valleys, Antarctica. Arct. Antarct. Alp. Res. 40, 119–128. https://doi.org/10.1657/1523-0430(06-051)[POAGE]2.0.CO;2

Power, S.N., Salvatore, M.R., Sokol, E.R., Stanish, L.F., Barrett, J.E., 2020. Estimating microbial mat biomass in the McMurdo Dry Valleys, Antarctica using satellite imagery and ground surveys. Polar Biol. 43, 1753–1767. https://doi.org/10.1007/s00300-020-02742-y

Power, S.N., Salvatore, M.R., Adams, B.J., Barrett, J.E., 2023. Hyperspectral reflectance values and biophysicochemical properties of biocrusts and soils in the Fryxell Basin, McMurdo Dry Valleys, Antarctica (2019). [Dataset] Environmental Data Initiative. https://doi.org/10.6073/pasta/a34f2a95ddae3f471fea0cab90a1e287

Power, S.N., Thomas, V.A., Salvatore, M.R., Barrett, J.E., 2024. Habitat suitability of biocrust communities in a cold desert ecosystem. Ecol. Evol. 14, e11649. https://doi.org/10.1002/ece3.11649

Prokopy, W.R., 1995. Phosphorus in 0.5 M sodium bicarbonate soil extracts. QuikChem Method 12-115-01-1-B. Lachat Instruments, Milwaukee, WI.

R Core Team (2017) R: A language and environment for statistical computing. R Foundation for Statistical Computing, Vienna, Austria. http://www.R-project.org

Ramnarine, R., Voroney, R., Wagner-Riddle, C., Dunfield, K., 2011. Carbonate removal by acid fumigation for measuring the δ13C of soil organic carbon. Can. J. Soil Sci. 91, 247–250. https://doi.org/10.1139/CJSS10066

Ramsey, M.S., Christensen, P.R., 1998. Mineral abundance determination: Quantitative

deconvolution of thermal emission spectra. Journal of Geophysical Research 103, 577–596. https://doi.org/10.1029/97JB02784

Roberts, D.A., Smith, M.O., Adams, J.B., 1993. Green vegetation, nonphotosynthetic vegetation, and soils in AVIRIS data. Remote Sens. Environ. 44, 255–269. https://doi.org/10.1016/0034-4257(93)90020-X

Rodriguez-Caballero, E., Belnap, J., Büdel, B., Crutzen, P.J., Andreae, M.O., Pöschl, U., Weber, B., 2018. Dryland photoautotrophic soil surface communities endangered by global change. Nat. Geosci. 11, 185–189. https://doi.org/10.1038/s41561-018-0072-1

Salvatore, M.R., 2015. High-resolution compositional remote sensing of the Transantarctic Mountains: application to the WorldView-2 dataset. Antarct. Sci. 27, 473–491. https://doi.org/10.1017/S095410201500019X

Salvatore, M.R., Barrett, J.E., Borges, S.R., Power, S.N., Stanish, L.F., Sokol, E.R., Gooseff, M.N., 2021. Counting Carbon: Quantifying Biomass in the McMurdo Dry Valleys through Orbital & Field Observations. Int. J. Remote Sens. 42, 8597–8623. https://doi.org/10.1080/01431161.2021.1981559

Salvatore, M.R., Borges, S.R., Barrett, J.E., Sokol, E.R., Stanish, L.F., Power, S.N., Morin, P., 2020. Remote characterization of photosynthetic communities in the Fryxell basin of Taylor Valley, Antarctica. Antarct. Sci. 1–16. https://doi.org/10.1017/S0954102020000176

Schimel, J.P., Bilbrough, C., Welker, J.M., 2004. Increased snow depth affects microbial activity and nitrogen mineralization in two Arctic tundra communities. Soil Biol. Biochem. 36, 217–227. https://doi.org/10.1016/j.soilbio.2003.09.008

Schwarz, A.M.J., Green, T.G.A., Seppelt, R.D., 1992. Terrestrial vegetation at Canada Glacier, Southern Victoria Land, Antarctica. Polar Biol. 12, 397–404. https://doi.org/10.1007/BF00243110

Simmons, B.L., Wall, D.H., Adams, B.J., Ayres, E., Barrett, J.E., Virginia, R.A., 2009a. Terrestrial mesofauna in above-and below-ground habitats: Taylor Valley, Antarctica. Polar Biol. 32, 1549–1558. https://doi.org/10.1007/s00300-009-0639-9

Simmons, B.L., Wall, D.H., Adams, B.J., Ayres, E., Barrett, J.E., Virginia, R.A., 2009b. Long-term experimental warming reduces soil nematode populations in the McMurdo Dry Valleys, Antarctica. Soil Biol. Biochem. 41, 2052–2060.

https://doi.org/10.1016/j.soilbio.2009.07.009

Stanish, L.F., Nemergut, D.R., McKnight, D.M., 2011. Hydrologic processes influence diatom community composition in Dry Valley streams. J. North Am. Benthol. Soc. 30, 1057–1073. https://doi.org/10.1899/11-008.1

Stanish, L.F., Kohler, T.J., Esposito, R.M.M., Simmons, B.L., Nielsen, U.N., Wall, D.H., Nemergut, D.R., McKnight, D.M., 2012. Extreme streams: flow intermittency as a control on diatom communities in meltwater streams in the McMurdo Dry Valleys, Antarctica. Can. J. Fish. Aquat. Sci. 69, 1405–1419. https://doi.org/10.1139/f2012-022

Stone, M., Devlin, S., Hawes, I., Welch, K.A., Gooseff, M.N., Takacs-Vesbach, C.D., Morgan-Kiss, R.M., Adams, B.J., Barrett, J.E., Priscu, J.C., Doran, P.T., *Submitted for publication*. McMurdo Dry Valley lake edge "moats": the ecological intersection between terrestrial and aquatic polar desert habitats.

Thrane, J.-E., Kyle, M., Striebel, M., Haande, S., Grung, M., Rohrlack, T., Andersen, T., 2015. Spectrophotometric Analysis of Pigments: A Critical Assessment of a High-Throughput Method for Analysis of Algal Pigment Mixtures by Spectral Deconvolution. PLoS One 10, e0137645. https://doi.org/10.1371/journal.pone.0137645

Treonis, A., Wall, D., Virginia, R., 1999. Invertebrate biodiversity in Antarctic Dry Valley soils and sediments. Ecosystems 2, 482–492. https://doi.org/10.1007/s100219900096

Trnková, K., Barták, M., 2017. Desiccation-induced changes in photochemical processes of photosynthesis and spectral reflectance in Nostoc commune (Cyanobacteria, Nostocales) colonies from polar regions. Phycological Res. 65, 44–50. https://doi.org/10.1111/pre.12157

Tucker, C.J., 1979. Red and Photographic Infrared Linear Combinations for Monitoring Vegetation. Remote Sens. Environ. 8, 127–150. https://doi.org/10.1016/0034-4257(79)90013-0

Van Horn, D.J., Van Horn, M.L., Barrett, J.E., Gooseff, M.N., Altrichter, A.E., Geyer, K.M., Zeglin, L.H., Takacs-Vesbach, C.D., 2013. Factors Controlling Soil Microbial Biomass and Bacterial Diversity and Community Composition in a Cold Desert Ecosystem: Role of Geographic Scale. PLoS One 8, e66103. https://doi.org/10.1371/journal.pone.0066103

Van Horn, D.J., Wolf, C.R., Colman, D.R., Jiang, X., Kohler, T.J., McKnight, D.M., Stanish, L.F., Yazzie, T., Takacs-Vesbach, C.D., 2016. Patterns of bacterial biodiversity in the

glacial meltwater streams of the McMurdo Dry Valleys, Antarctica. FEMS Microbiol. Ecol. 92. https://doi.org/10.1093/femsec/fiw148

Vignon, É., Roussel, M.-L., Gorodetskaya, I.V., Genthon, C., Berne, A., 2021. Present and future of rainfall in Antarctica. Geophys. Res. Lett. 48. https://doi.org/10.1029/2020gl092281

Walthert, L., Graf, U., Kammer, A., Luster, J., Pezzotta, D., Zimmermann, S., Hagedorn, F., 2010. Determination of organic and inorganic carbon, δ 13 C, and nitrogen in soils containing carbonates after acid fumigation with HCl. J. Plant Nutr. Soil Sci. 173, 207–216. https://doi.org/10.1002/jpln.200900158

Warren, S.G., 1982. Optical Properties of Snow. Review of Geophysics and Space Physics 20, 67–89.

Weber, B., Belnap, J., Büdel, B., Antoninka, A.J., Barger, N.N., Chaudhary, V.B., Darrouzet-Nardi, A., Eldridge, D.J., Faist, A.M., Ferrenberg, S., Havrilla, C.A., Huber-Sannwald, E., Malam Issa, O., Maestre, F.T., Reed, S.C., Rodriguez-Caballero, E., Tucker, C., Young, K.E., Zhang, Y., Zhao, Y., Zhou, X., Bowker, M.A., 2022. What is a biocrust? A refined, contemporary definition for a broadening research community. Biol. Rev. Camb. Philos. Soc. 97, 1768–1785. https://doi.org/10.1111/brv.12862

Wlostowski, A.N., Gooseff, M.N., McKnight, D.M., Jaros, C., Lyons, W.B., 2016. Patterns of hydrologic connectivity in the McMurdo Dry Valleys, Antarctica: a synthesis of 20 years of hydrologic data. Hydrol. Process. 30, 2958–2975. https://doi.org/10.1002/hyp.10818

Wlostowski, A.N., Schulte, N.O., Adams, B.J., Ball, B.A., Esposito, R.M.M., Gooseff, M.N., Lyons, W.B., Nielsen, U.N., Virginia, R.A., Wall, D.H., Welch, K.A., McKnight, D.M., 2019. The hydroecology of an ephemeral wetland in the McMurdo dry valleys, Antarctica. J. Geophys. Res. Biogeosci. 124, 3814–3830. https://doi.org/10.1029/2019jg005153

Xue, X., Adhikari, B.N., Ball, B.A., Barrett, J.E., Miao, J., Perkes, A., Martin, M., Simmons, B.L., Wall, D.H., Adams, B.J., 2023. Ecological stoichiometry drives the evolution of soil nematode life history traits. Soil Biol. Biochem. 177, 108891. https://doi.org/10.1016/j.soilbio.2022.108891

Young, K.E., Reed, S.C., 2017. Spectrally monitoring the response of the biocrust moss Syntrichia caninervis to altered precipitation regimes. Sci. Rep. 7, 1–10. https://doi.org/10.1038/srep41793

Figures

Figure 3.1

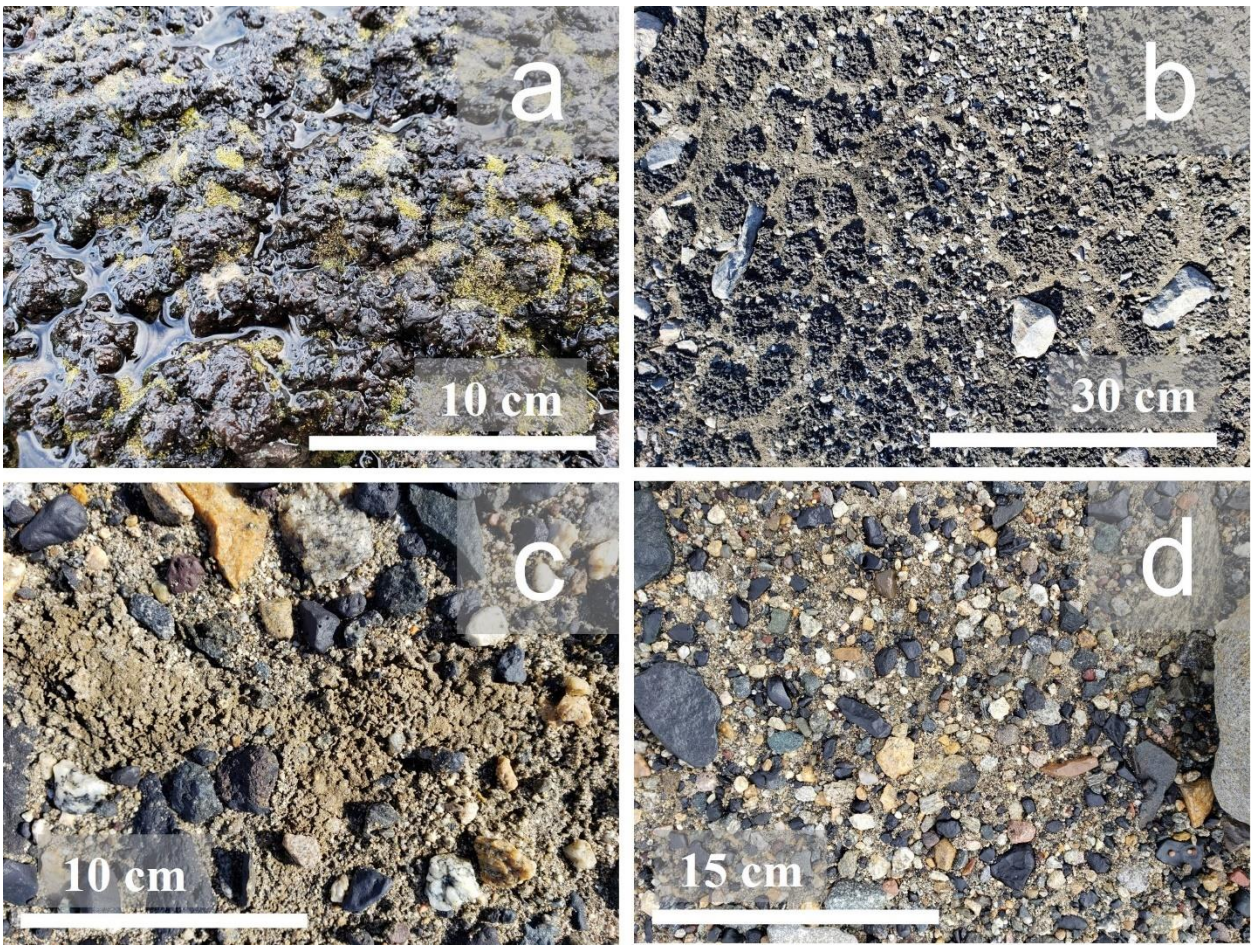

Figure 3.1. Photos of (a) dense, wet microbial mat in the Canada Flush (see Power et al. 2020); (b) dense biocrust downhill from snowpack (plot 09); (c) sparse, incipient biocrust in moist depression (plot 26); and (d) representative low productivity desert pavement (plot 31). Photographs taken by S. Power.

Figure 3.2

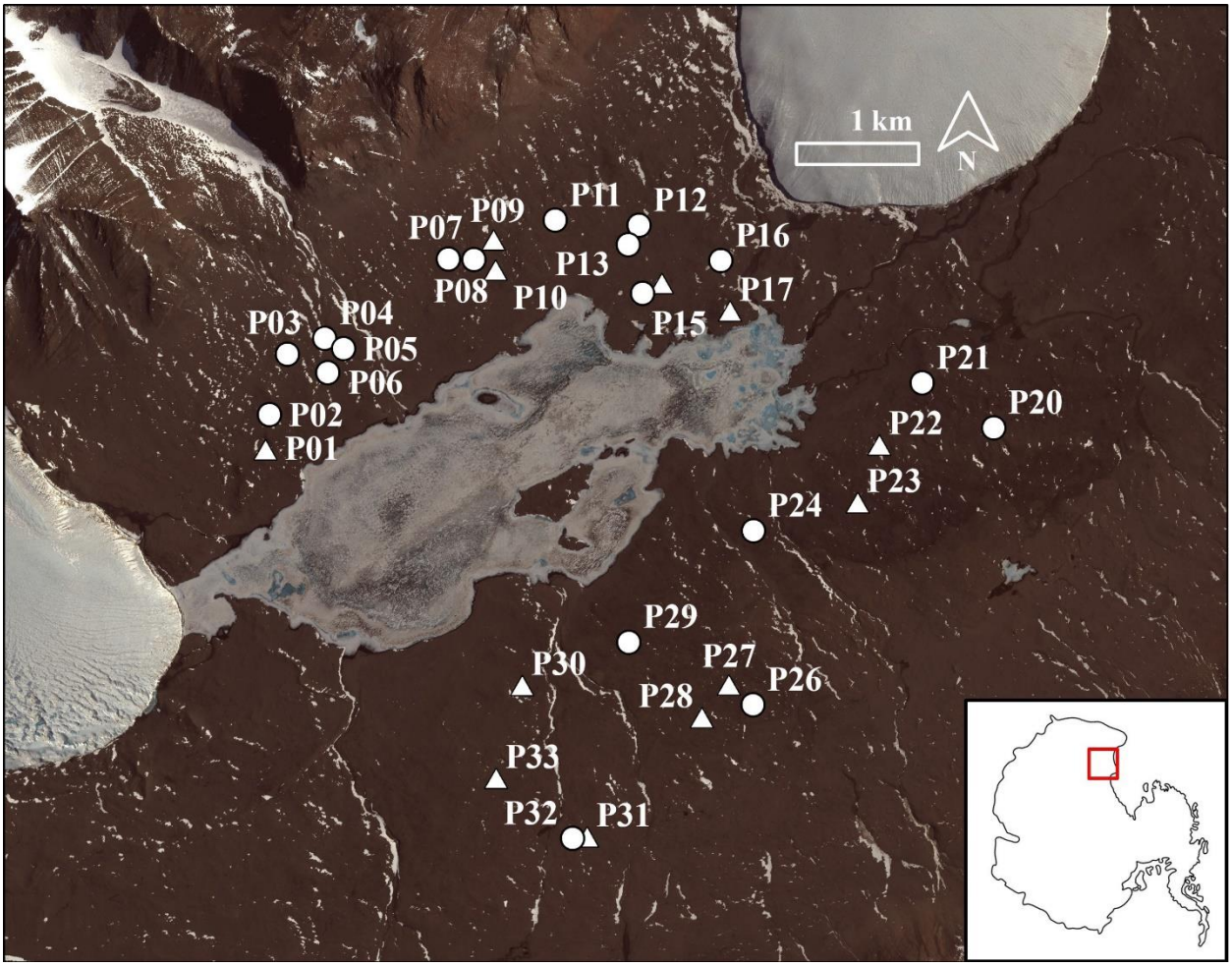

Figure 3.2. True color image of the Lake Fryxell basin with the 30 sampling locations labeled. The 12 intensively sampled plots are denoted by triangles. Inset on the bottom right corner identifies the McMurdo Dry Valleys, Antarctica with a red square. WV-2 imagery (1030010089D13500) © Dec 11 2018 DigitalGlobe, Inc.

Figure 3.3

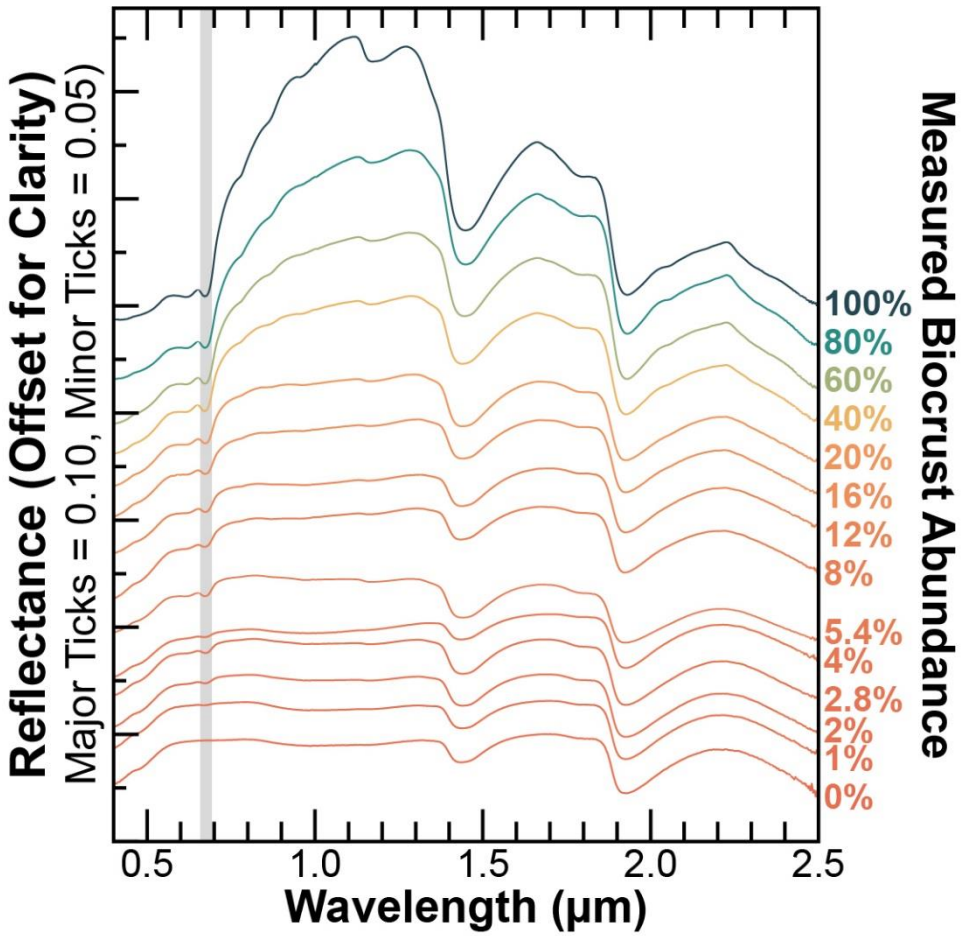

Figure 3.3. Hyperspectral signatures of wetted laboratory mixtures of soil and biocrust at varying abundances. Reflectance offset to distinguish each spectra separately. Listed percentages indicate measured biocrust by weight. Chlorophyll absorption feature identifiable at ~ 0.68 μm, denoted by vertical gray bar.

Figure 3.4

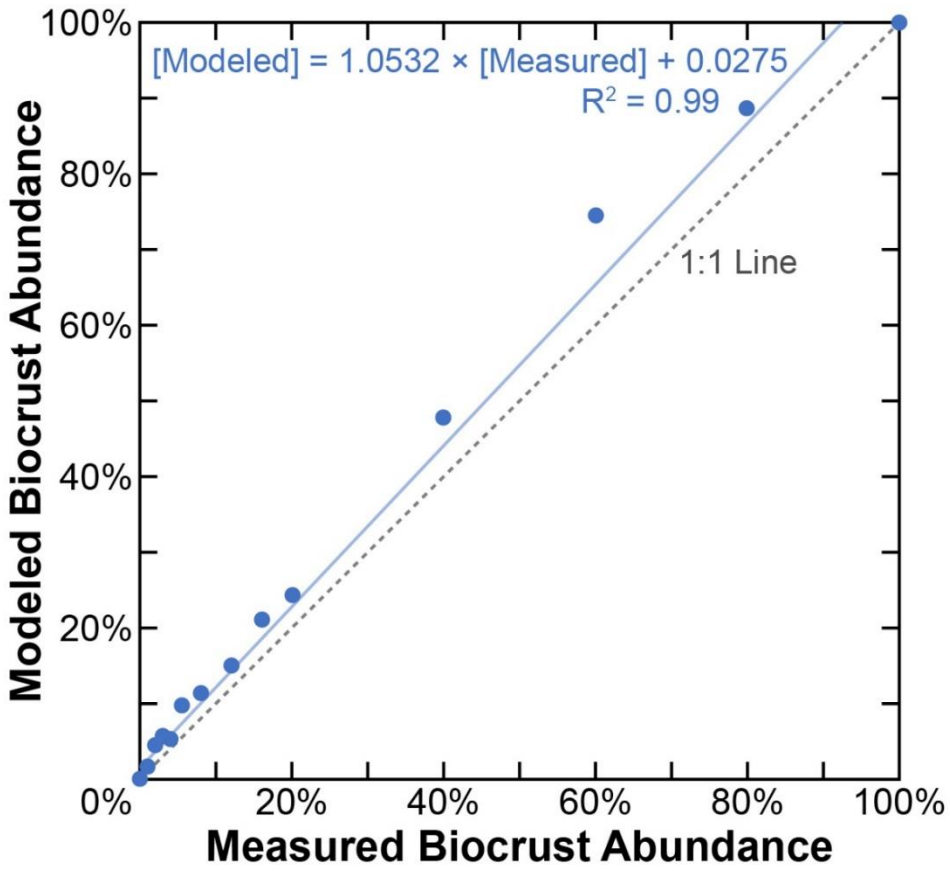

Figure 3.4. Scatterplot showing modeled vs. measured biocrust abundance determined in laboratory experiment. Highly significant fit ($R^2 = 0.99$, p-value < 0.001) between modeled (spectral linear unmixing) and measured biocrust abundance using laboratory mixtures of soil and biocrust.

Figure 3.5

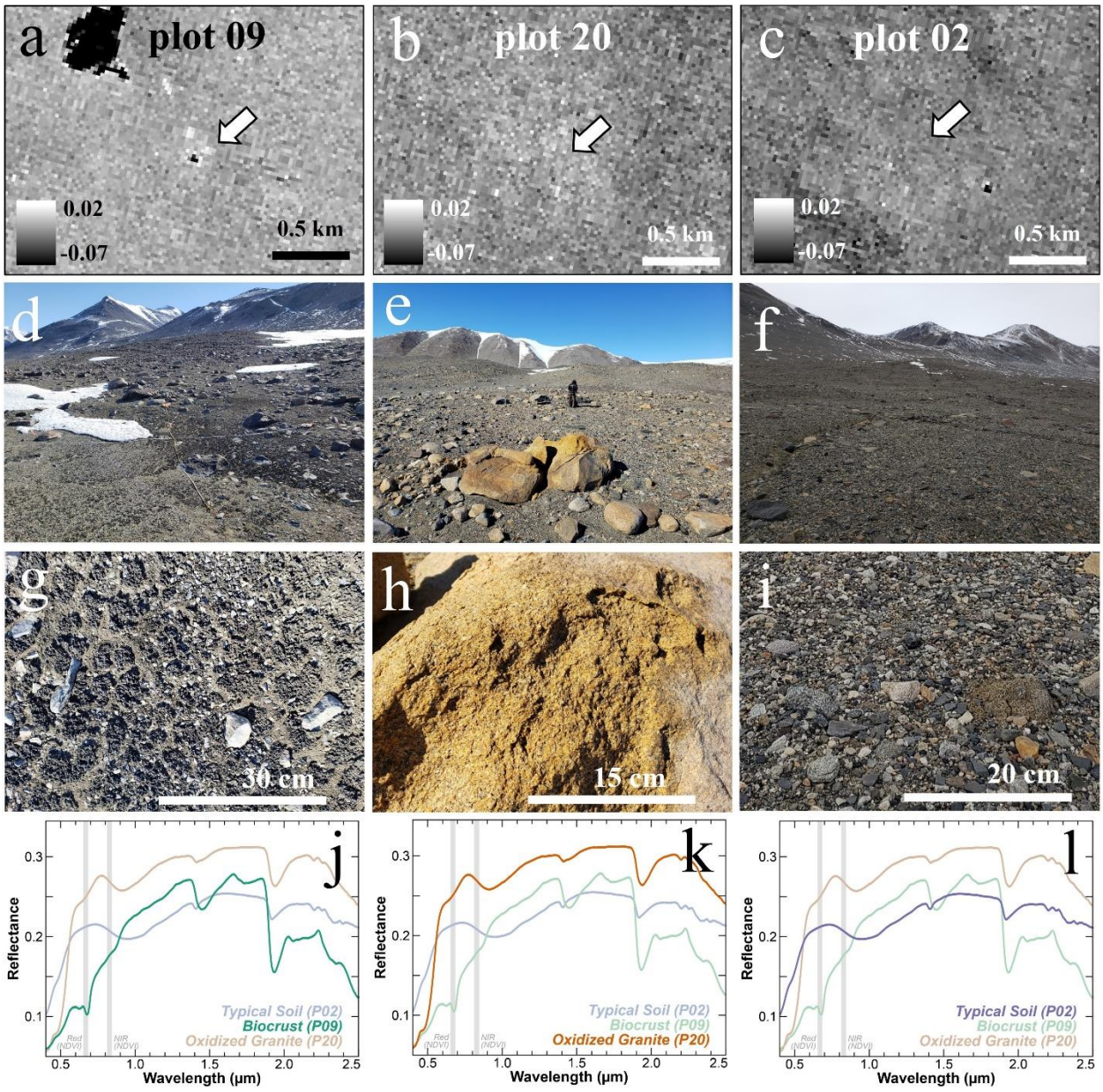
a
plot 09
0.02
-0.07
0.5 km
b
plot 20
0.02
-0.07
0.5 km
c
plot 02
0.02
-0.07
0.5 km
d
e
f
g
30 cm
h
15 cm
i
20 cm
j
k
l
Reflectance
Wavelength (μm)
Typical Soil (P02)
Biocrust (P09)
Oxidized Granite (P20)
Red (NDVI)
NIR (NDVI)

Figure 3.5. Orbital NDVI images of (a) relatively high NDVI area of plot 09, (b) relatively high NDVI area of plot 20, and (c) relatively low NDVI area of plot 02. Landscape photos of (d) dense biocrust downhill from snowpack (plot 09), (e) oxidized, weathered granite boulder field (plot 20), and (f) typical low productivity desert pavement (plot 02). Close up photos of the (g) dense biocrust, (h) oxidized, weathered granite, and (i) typical desert pavement. Hyperspectral reflectance signature of (j) plot 09 biocrust, (k) plot 20 oxidized granite, and (l) plot 02 typical soil with each separate spectra transparent in background. Gray bars outline the region of NDVI calculation (steeper slope illustrates higher NDVI). Photographs taken by S. Power. WV-3 imagery (10400100485D6900) © Jan 26 2019 DigitalGlobe, Inc.

Figure 3.6

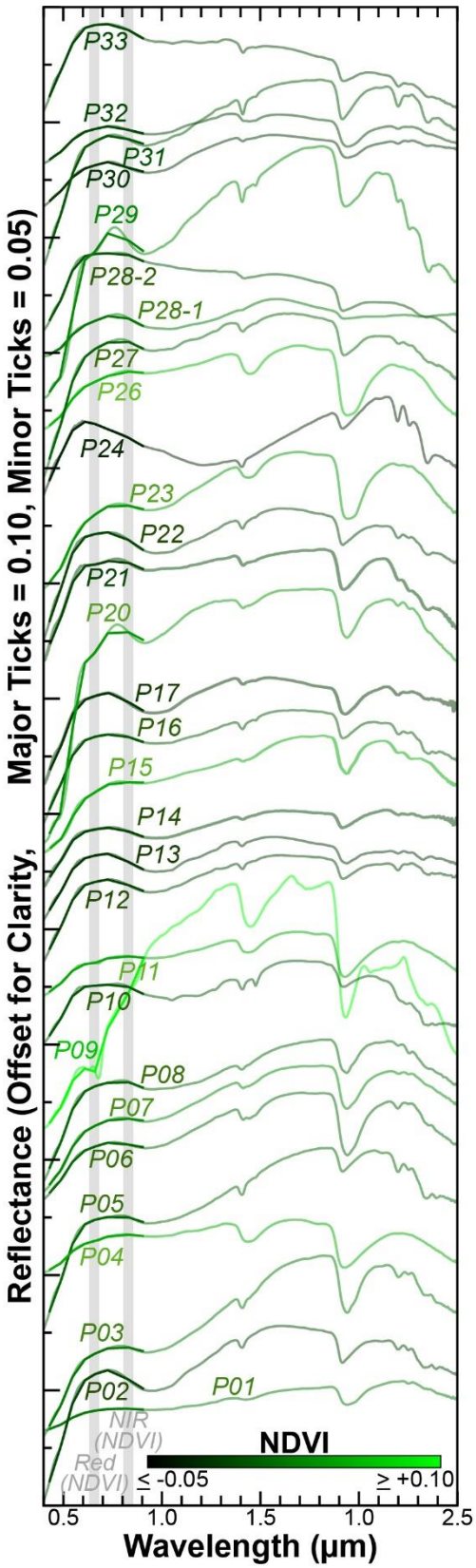
P33
P32
P31
P30
P29
P28-2
P28-1
P27
P26
P24
P23
P22
P21
P20
P17
P16
P15
P14
P13
P12
P11
P10
P09
P08
P07
P06
P05
P04
P03
P02
P01
NIR (NDVI)
Red (NDVI)
NDVI
≤ -0.05
≥ +0.10
0.5
1.0
1.5
1.0
2.5
Wavelength (µm)
Reflectance (Offset for Clarity, Major Ticks = 0.10, Minor Ticks = 0.05)

Figure 3.6. Spectra acquired from each plot's surface soil or biocrust sample using a hyperspectral imaging spectrometer. Spectra downsampled to WV-2 resolution are shown in bold in the NDVI identified region of the spectrum with gray bars. Bright green spectra indicate higher NDVI.

Figure 3.7

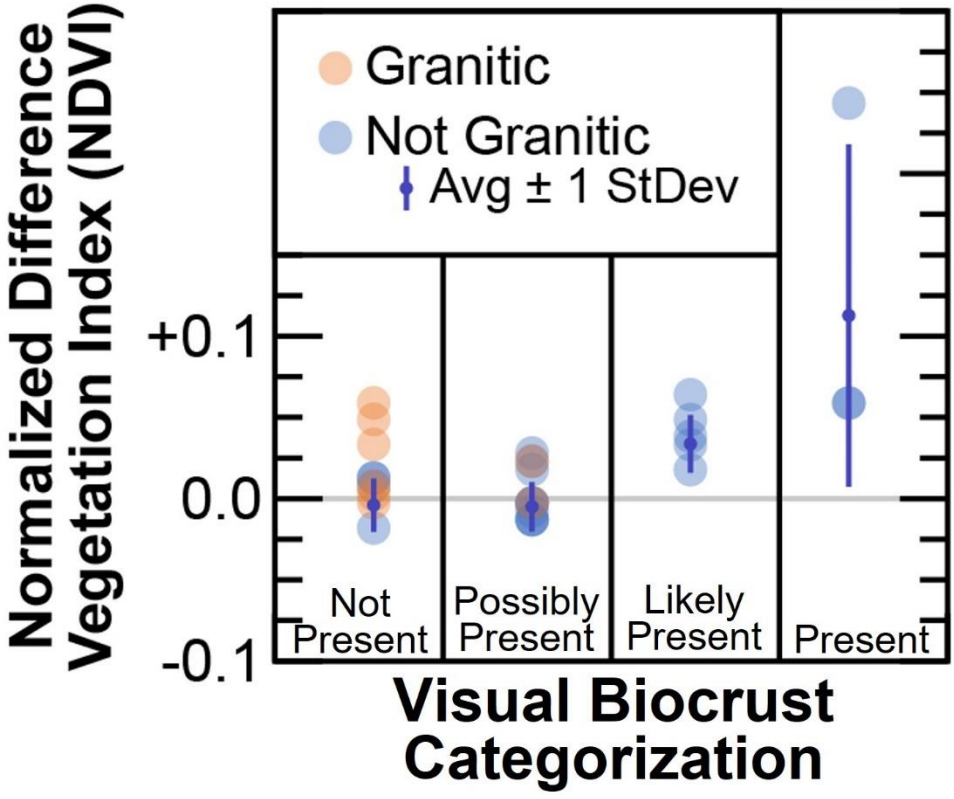

Figure 3.7. Confidence in biocrust presence at each plot location, based on human interpretation in the field, compared to hyperspectral NDVI measurements acquired from samples transferred to and measured in the laboratory. Visually identified oxidized granite dominated plots are denoted in orange and the remaining plots (biocrust or typical soil) are denoted in blue.

Figure 3.8

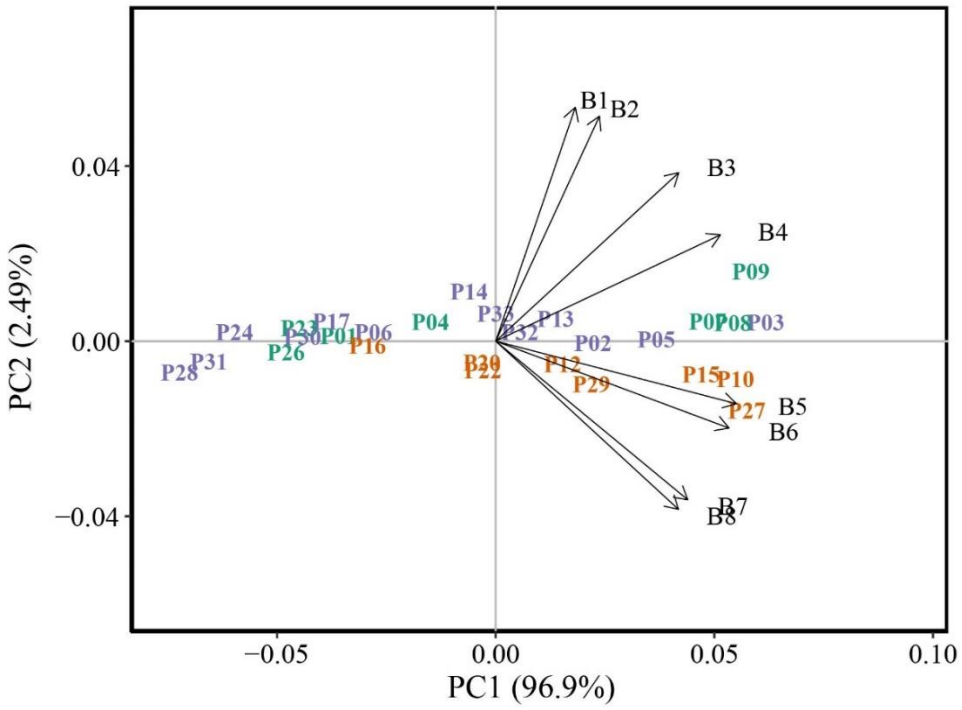

Figure 3.8. Principal components analysis ordination on covariance of 28 plots (2 plots excluded due to snow coverage). Plots with ground cover consisting mainly of oxidized granite are shown in orange, biocrust and incipient biocrust in green, and typical soil in purple. Plots shown in green are categorized as biocrust "present" or "likely present" based on our visual biocrust categorization. Vectors represent correlations of WorldView-2 band reflectance (B1 - B8) with PCA ordination axes (all displayed correlations are significant, $p < 0.001$). Spectral data were acquired by the WV-2 satellite on Dec 03, 2019.

Figure 3.9

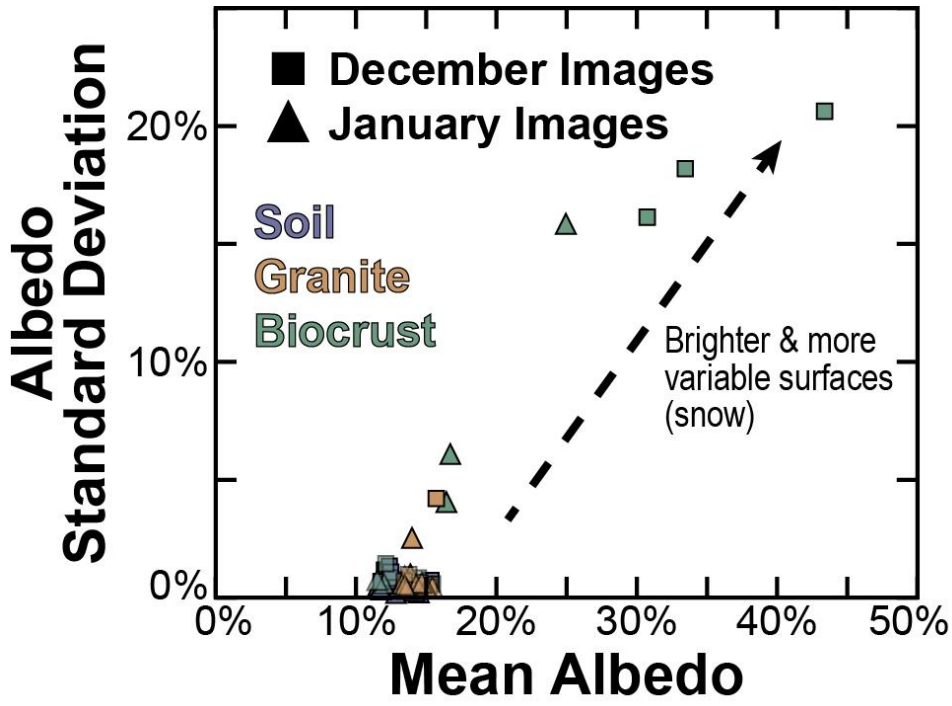

Figure 3.9. Mean and standard deviation albedo of early season December and late season January WorldView-2 and -3 images at each of the 30 plots locations. Colors indicate surface type of plot. Biocrust plots include those which were identified in the field as having visually conspicuous biocrust present or likely present (incipient biocrust).

Tables

Table 3.1. Biological variables averaged (n = 5) ± 1 standard deviation from each of the 12 intensively sampled plots. Invertebrates are counted as the number of total-living.

Plot ID	AFDM (mg cm^{-2})	Chlorophyll (μg cm^{-2})	Carotenoid (μg cm^{-2})	Scytonemin (μg cm^{-2})	Nematodes (# kg^{-1} dry soil)	Rotifers (# kg^{-1} dry soil)	Tardigrades (# kg^{-1} dry soil)
P01	5.35 ± 2.81	0.009 ± 0.006	0.062 ± 0.030	0.864 ± 0.693	362 ± 804	0 ± 0	2 ± 5
P09	28.29 ± 21.62	4.974 ± 5.698	2.141 ± 2.500	77.395 ± 89.278	1102 ± 735	30 ± 38	1822 ± 2144
P10	2.12 ± 0.49	0.007 ± 0.002	0.031 ± 0.009	0.331 ± 0.109	1453 ± 1405	32 ± 31	2 ± 4
P14	4.06 ± 1.06	0.006 ± 0.006	0.063 ± 0.030	0.800 ± 0.314	959 ± 1990	0 ± 0	0 ± 0
P17	3.90 ± 0.79	0.005 ± 0.003	0.040 ± 0.016	0.683 ± 0.231	449 ± 756	0 ± 0	0 ± 0
P22	2.19 ± 0.95	0.005 ± 0.002	0.027 ± 0.004	0.285 ± 0.049	0 ± 0	0 ± 0	0 ± 0
P23	2.99 ± 0.89	0.002 ± 0.002	0.040 ± 0.026	0.399 ± 0.271	85 ± 179	0 ± 0	0 ± 0
P27	3.18 ± 1.12	0.006 ± 0.003	0.032 ± 0.013	0.432 ± 0.186	168 ± 354	0 ± 0	0 ± 0
P28	2.55 ± 0.51	0.003 ± 0.002	0.033 ± 0.017	0.379 ± 0.165	495 ± 595	2 ± 5	0 ± 0
P30	3.46 ± 0.57	0.005 ± 0.003	0.036 ± 0.023	0.272 ± 0.184	0 ± 0	0 ± 0	0 ± 0
P31	3.87 ± 0.77	0.007 ± 0.002	0.037 ± 0.013	0.309 ± 0.122	0 ± 0	0 ± 0	0 ± 0
P33	2.61 ± 0.84	0.004 ± 0.003	0.019 ± 0.003	0.137 ± 0.054	875 ± 1288	0 ± 0	0 ± 0

Table 3.2. Physical and chemical variables averaged (n = 5) ± 1 standard deviation from each of the 12 intensively sampled plots where "GWC" refers to gravimetric water content, "EC" electrical conductivity, "TOC" total organic carbon, and "TN" total nitrogen.

				NH_4^+	**NO_3^-**	**PO_4^{3-}**	**TOC**	**TN**
Plot ID	**GWC** (g/g)	**EC** ($\mu S\ cm^{-1}$)	**pH**	$\mu g\ N\ g^{-1}$ dry soil	$\mu g\ N\ g^{-1}$ dry soil	$\mu g\ P\ g^{-1}$ dry soil	$mg\ C\ g^{-1}$ dry soil	$mg\ N\ g^{-1}$ dry soil
P01	0.06 ± 0.03	2330 ± 2318	8.4 ± 1.3	0.12 ± 0.19	57.87 ± 60.82	3.56 ± 0.54	0.309 ± 0.08	0.112 ± 0.05
P09	0.06 ± 0.04	70 ± 37	8.5 ± 0.7	0.09 ± 0.19	0.86 ± 0.36	3.12 ± 0.66	1.24 ± 0.34	0.176 ± 0.04
P10	0.02 ± 0.00	112 ± 50	9.9 ± 0.4	0.02 ± 0.04	0.002 ± 0.01	4.47 ± 5.93	0.405 ± 0.08	0.119 ± 0.04
P14	0.06 ± 0.02	2311 ± 1819	8.6 ± 0.7	0 ± 0	48.30 ± 43.83	12.19 ± 6.15	1.14 ± 0.55	0.203 ± 0.07
P17	0.02 ± 0.01	1095 ± 654	8.8 ± 0.5	0 ± 0	65.79 ± 71.17	5.85 ± 2.65	0.497 ± 0.19	0.115 ± 0.04
P22	0.05 ± 0.02	2152 ± 786	9.5 ± 0.6	0.02 ± 0.03	65.51 ± 51.13	18.65 ± 10.70	1.11 ± 0.58	0.178 ± 0.06
P23	0.02 ± 0.01	907 ± 283	9.6 ± 0.6	0 ± 0	13.43 ± 7.04	3.34 ± 0.40	0.272 ± 0.07	0.081 ± 0.02
P27	0.03 ± 0.04	656 ± 523	8.4 ± 0.3	0 ± 0	4.32 ± 5.95	2.71 ± 1.07	0.495 ± 0.16	0.097 ± 0.02
P28	0.08 ± 0.09	515 ± 440	8.9 ± 0.5	0 ± 0	5.17 ± 7.02	3.00 ± 2.03	0.529 ± 0.28	0.099 ± 0.02
P30	0.04 ± 0.03	2347 ± 2602	9.0 ± 0.8	0 ± 0	33.40 ± 46.07	3.70 ± 1.70	0.364 ± 0.21	0.111 ± 0.06
P31	0.05 ± 0.02	2431 ± 1757	8.2 ± 0.3	0.01 ± 0.01	27.68 ± 22.36	1.70 ± 0.52	0.275 ± 0.09	0.074 ± 0.02
P33	0.02 ± 0.00	130 ± 67	9.6 ± 0.3	0.03 ± 0.05	0.12 ± 0.27	2.30 ± 0.88	0.352 ± 0.11	0.085 ± 0.02

Table 3.3. Modeled abundance of total biocrust, oxidized granite, and remaining abiotic endmembers at a select number of plots visually identified by the surface type. 'Other abiotic' is the combination of the soil and water endmember abundances. An 'early season' and a 'late season' WV-2 image were selected for the spectral linear unmixing: Dec 21 2021 and Jan 21 2015, respectively. Specific pixels were excluded from the abundance average (n = 25 per plot) if the RMSE > 0.5%, common for snow covered areas.

Plot ID	Surface Type Present	Dec 21 2021 'Early Season' Modeled Abundance (%)			Average % RMSE	% Excluded Pixels	Jan 21 2015 'Late Season' Modeled Abundance (%)			Average % RMSE	% Excluded Pixels
		Biocrust	Oxidized Granite	Other Abiotic			Biocrust	Oxidized Granite	Other Abiotic		
P02	soil	0.6	2.4	97.0	0.302	0	1.7	9.4	88.9	0.240	0
P04	biocrust	-	-	-	5.000	100	8.4	11.0	80.6	0.260	0
P09	biocrust	-	-	-	5.863	100	16.5	11.3	72.2	0.200	0
P10	ox. granite	9.5	39.9	50.6	0.181	0	2.5	52.1	45.3	0.150	0
P11	biocrust	-	-	-	5.297	100	4.2	1.7	94.1	0.190	0
P14	soil	0.6	4.9	94.4	0.303	0	0.4	5.5	94.1	0.260	0
P17	soil	2.7	6.9	90.4	0.309	0	1.3	12.0	86.7	0.220	0
P20	ox. granite	7.4	50.2	42.4	0.203	0	1.9	49.6	48.4	0.170	0
P22	ox. granite	5.8	40.2	54.0	0.160	0	2.1	69.4	28.6	0.170	0
P23	incipient biocrust	0.4	23.5	76.0	0.226	0	0.0	33.9	66.1	0.220	0
P26	incipient biocrust	7.7	29.1	63.2	0.201	0	12.2	1.0	86.8	0.241	0
P27	ox. granite	2.2	27.0	70.9	0.168	0	4.3	20.9	74.8	0.224	0
P29	ox. granite	16.7	39.3	44.0	0.308	24	17.8	39.3	42.9	0.303	16
P30	soil	3.5	25.8	70.8	0.226	4	0.8	24.4	74.8	0.262	0
P31	soil	7.6	25.8	66.6	0.231	0	3.3	8.9	87.7	0.276	0

Table 3.4. Continuum of hydrological conditions in Taylor Valley, Antarctica.

Landscape Feature	**Water Abundance**	**Salinity**	**Biological Activity**
Arid Terrestrial Landscape	Low	Low-High	Low
Hypersaline Water Tracks	Medium	High	Low
Snowpack-Fed Microhabitats	Low-Medium	Low-Medium	Medium
Snowpack-Fed Non-Annual Ephemeral Wetlands	Medium	Low-Medium	Medium
Annual Ephemeral Streams	Medium-High	Low	Medium-High
Lakes	High	Low	High

Supplemental Figures

Figure S3.1

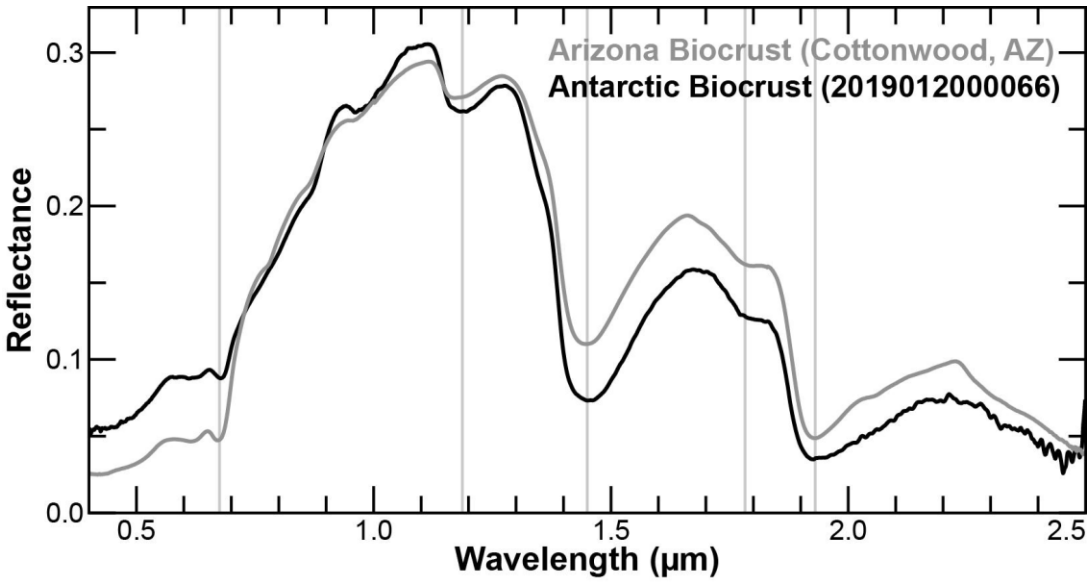

Figure S3.1. Spectral comparison of Antarctic biocrust to Arizona biocrust sample used in laboratory spectral unmixing analysis. Gray vertical bars denote the presence of corresponding absorption features of similar location (~ 0.68, 1.19, 1.45, 1.78, and 1.93 µm).

Figure S3.2

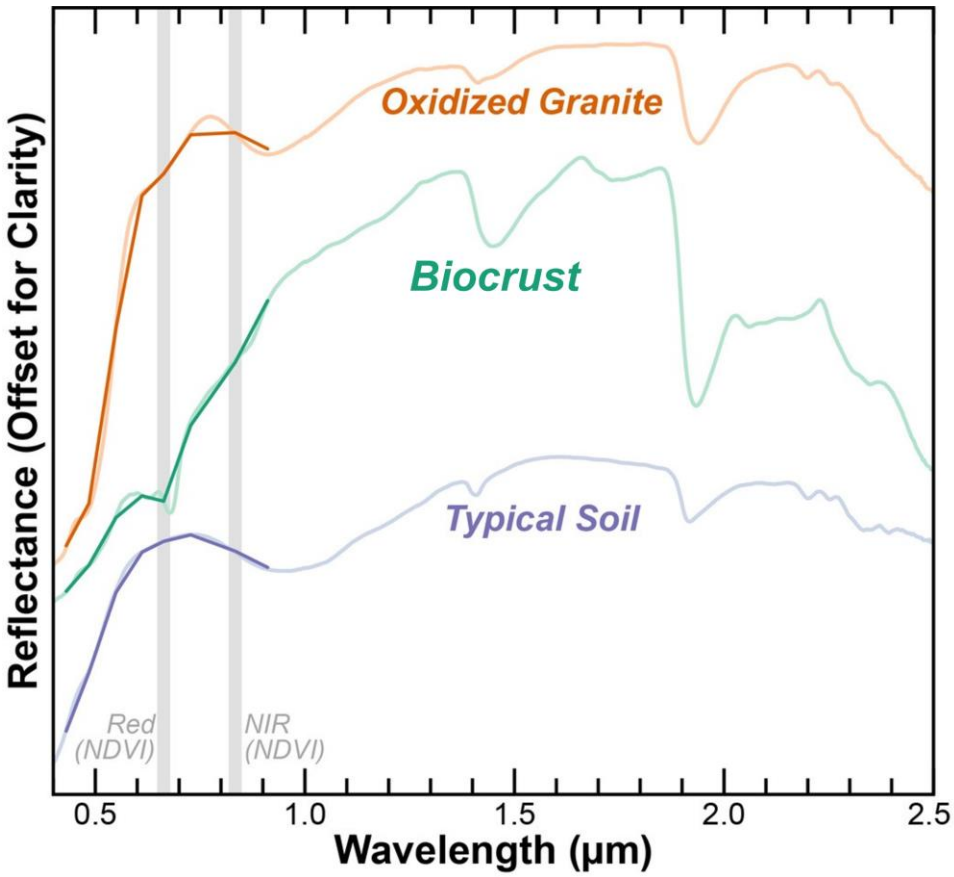

Figure S3.2. Three spectral signatures illustrating relatively high NDVI from biocrust (plot 09) and oxidized granite (plot 20), and low NDVI from typical soil (plot 02). Spectra downsampled to WV-2 resolution are shown in bold. Gray bars outline the region of NDVI calculation.

Figure S3.3

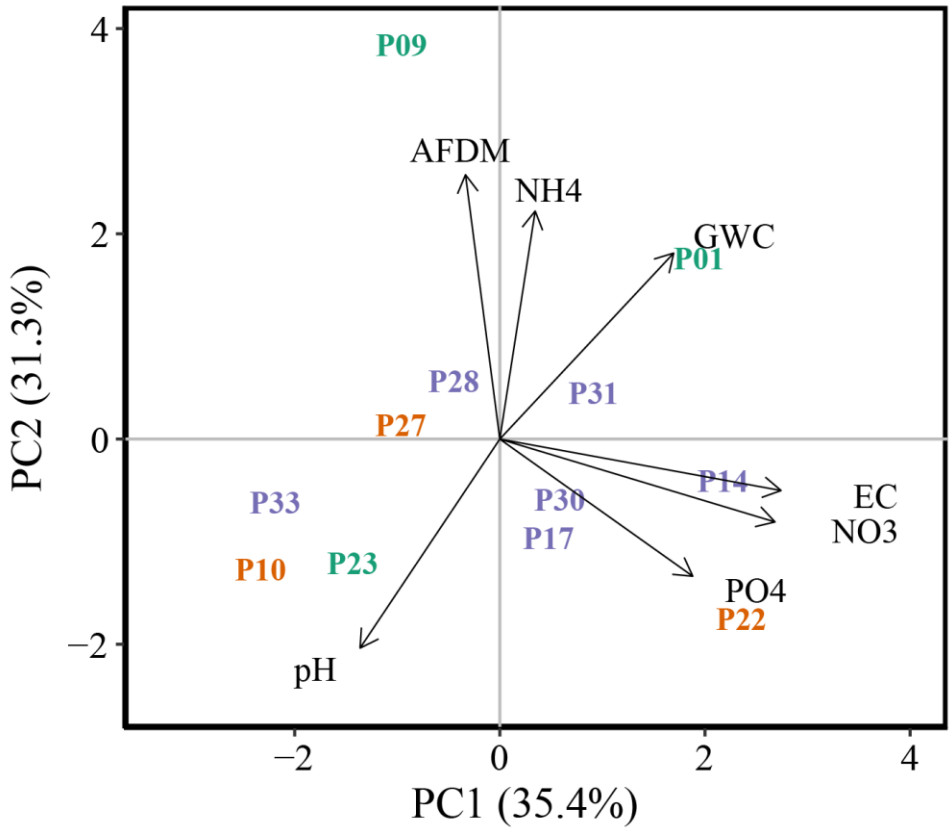

Figure S3.3. Principal components analysis ordination on correlation of the 12 intensively sampled plots. Plots with ground cover consisting mainly of oxidized granite are shown in orange, biocrust and incipient biocrust in green, and typical soil in purple. Plots shown in green are categorized as biocrust "present" or "likely present" based on our visual biocrust categorization. Vectors represent correlations of soil habitat variables with PCA ordination axes (all displayed correlations are significant, $p < 0.05$).

Supplemental Tables

Table S3.1. WorldView images used in albedo analysis.

Month	Image Acquisition	Image ID
December	12/25/2009 18:40:39	1030010003085D00
	12/25/2009 21:59:36	1030010003A9F300
	12/19/2010 20:55:06	1030010008A27200
	12/11/2018 21:00:21	1030010089D13500
	12/3/2019 20:20:55	103001009FA0AE00
	12/1/2015 21:15:44	1040010015737400
January	1/5/2013 21:30:30	103001001D642400
	1/21/2015 19:51:58	103001003ED2B400
	1/23/2015 20:17:49	103001003CD3ED00
	1/25/2017 21:14:28	10300100648C3100
	1/22/2015 20:12:31	1040010007721800
	1/28/2017 21:00:46	104001002855C000
	1/26/2019 21:46:20	10400100485D6900

Table S3.2. Correlation matrix of biological parameters (AFDM, chlorophyll-a, scytonemin content), vegetation indices (NDVI, SR, SRre, NPCI), and the 8 WorldView bands for the 12 intensively sampled plots, excluding plot 09 which some correlations were entirely driven by. There are no significant relationships between the biological parameters and the multispectral indices or raw bands from these plots.

	AFDM	**Chl-a**	**Scyto**	**NDVI**	**SR**	**SRre**	**NPCI**	**B1**	**B2**	**B3**	**B4**	**B5**	**B6**	**B7**	**B8**
AFDM	1.00														
Chl-a	0.58	1.00													
Scyto	0.78	0.49	1.00												
NDVI	-0.42	0.27	-0.17	1.00											
SR	-0.42	0.27	-0.17	1.00	1.00										
SRre	-0.32	0.30	-0.02	0.86	0.86	1.00									
NPCI	-0.44	0.13	-0.32	0.76	0.77	0.87	1.00								
B1	-0.17	0.26	0.13	0.41	0.41	0.49	0.32	1.00							
B2	-0.14	0.26	0.10	0.46	0.46	0.57	0.45	0.97	1.00						
B3	-0.30	0.24	-0.04	0.62	0.62	0.73	0.65	0.92	0.96	1.00					
B4	-0.34	0.23	-0.10	0.70	0.70	0.78	0.74	0.87	0.92	0.99	1.00				
B5	-0.36	0.24	-0.10	0.72	0.73	0.83	0.80	0.82	0.89	0.98	0.99	1.00			
B6	-0.39	0.24	-0.13	0.77	0.77	0.82	0.80	0.81	0.87	0.97	0.99	1.00	1.00		
B7	-0.38	0.26	-0.12	0.80	0.80	0.87	0.83	0.78	0.84	0.95	0.98	0.99	1.00	1.00	
B8	-0.36	0.29	-0.13	0.81	0.82	0.85	0.82	0.77	0.84	0.94	0.98	0.99	0.99	1.00	1.00

CHAPTER 4 – Habitat suitability of biocrust communities in a cold desert ecosystem

Authors: Sarah N. Power, Valerie A. Thomas, Mark R. Salvatore, and John E. Barrett

Published in *Ecology and Evolution*

Power, S.N., Thomas, V.A., Salvatore, M.R., Barrett, J.E. 2024. Habitat suitability of biocrust communities in a cold desert ecosystem. *Ecology and Evolution*, 14, e11649. https://doi.org/10.1002/ece3.11649

Abstract

Drylands are unique among terrestrial ecosystems in that they have a significant proportion of primary production facilitated by non-vascular plants such as colonial cyanobacteria, moss, and lichens, *i.e.*, biocrusts, which occur on and in the surface soil. Biocrusts inhabit all continents, including Antarctica, an increasingly dynamic continent on the precipice of change. Here, we describe *in-situ* field surveying and sampling, remote sensing, and modeling approaches to assess the habitat suitability of biocrusts in the Lake Fryxell basin of Taylor Valley, Antarctica, which is the main site of the McMurdo Dry Valleys Long Term Ecological Research Program. Soils suitable for the development of biocrusts are typically wetter, less alkaline, and less saline compared to unvegetated soils. Using random forest models, we show that gravimetric water content, electrical conductivity, and snow frequency are the top predictors of biocrust presence and biomass. Areas most suitable for the growth of dense biocrusts are soils associated with seasonal snow patches. Using geospatial data to extrapolate our habitat suitability model to the whole basin predicts that biocrusts are present in 2.7×10^5 m^2 and contain 11 - 72 Mg of aboveground carbon, based on 90% probability of occurrence. Our study illustrates the synergistic effect of combining field and remote sensing data for understanding the distribution and biomass of biocrusts, a foundational community in the carbon balance of this region.

Extreme weather events and changing climate conditions in this region, especially those influencing snow accumulation and persistence, could have significant effects on the future distribution and abundance of biocrusts and therefore soil organic carbon storage in the McMurdo Dry Valleys.

Introduction

Drylands, Earth's largest biome (Schimel 2010), cover approximately 45% of the Earth's land surface (Prăvălie, 2016) and store about 32% of the global soil organic carbon (C) pool (Plaza et al., 2018). Among these dryland ecosystems are unique phototrophic communities growing on the surface soil. Biological soil crusts (*i.e*., biocrusts) are soil bio-aggregates containing communities of cyanobacteria, algae, moss, and lichen (Weber et al, 2022), inhabit all continents (Belnap et al., 2016), cover 12% of the Earth's terrestrial surface (Rodriguez-Caballero et al., 2018), and play foundational roles in the ecosystems where they occur, such as stabilizing soil, influencing soil hydrology, governing nutrient cycles, and supporting biodiversity hotspots (Belnap et al., 2016). Biocrusts are considered ecosystem engineers since they modulate the availability of resources and therefore modify, maintain, and create habitats for other terrestrial species (Barrera et al., 2022). Moreover, biocrusts are often the primary source of fixed carbon in some drylands (Elbert et al., 2012).

Drylands are particularly sensitive to climate change and are projected to become even drier (Allan and Douville, 2024; Feng and Zhang, 2015; Prăvălie, 2016). Climate change, especially changes in precipitation and soil disturbances, is predicted to decrease biocrust abundance by 25 - 40% within the next 60 years (Finger-Higgens et al., 2022; Rodriguez-Caballero et al., 2018). Additionally, changes in weather and climate patterns have already caused vegetation shifts in drylands (Schlaepfer et al., 2017) and may have complex impacts on

biocrust distribution and abundance, *e.g.*, decline in vascular vegetation sometimes creates more available surface area for biocrust expansion (Chen et al., 2020).

The polar desert environment of continental Antarctica also hosts biocrusts, primarily consisting of cyanobacteria, bryophytes, algae, and lichen (Büdel and Colesie, 2014; Colesie et al., 2014; Green and Broady, 2001). Although sporadic in occurrence, biocrusts develop where there is a regular water supply (*e.g.*, from melting snow), as well as shelter and sunlight (Green and Broady, 2001; Kennedy, 1993). Biocrusts often occur in micro-niches where snow drifts accumulate and persist – typically in shallow depressions, on the lee side of boulders, and within the microtopography of periglacial features (Cannone and Guglielmin, 2010; Green and Broady, 2001). Cyanobacteria-dominated biocrusts occur in the wettest areas, and bryophyte-dominated biocrusts are more common along the margins of consistent water sources, typically as *Bryum-Hennediella heimii* communities, with drier mosses often colonized by lichens (Büdel and Colesie, 2014; Green and Broady, 2001; Schwarz et al., 1992). Antarctic biocrusts form sheltered microhabitats associated with diverse soil fauna, hosting nematodes, tardigrades, rotifers, and ciliates (Green and Broady, 2001; Colesie et al., 2014; Power et al., 2024). They have also been shown to increase soil fertility (Barrera et al., 2022). For example, some cyanobacteria taxa fix atmospheric nitrogen to usable nitrogen forms for other organisms (Kohler et al., 2018), and biocrusts are a source of leached organic matter into the soils as well (Colesie et al., 2014; Power et al., 2024). This is an essential function of Antarctic biocrusts in particular, since the terrestrial environment of continental Antarctica is overall nutrient poor with low diversity. Biocrusts also stabilize soils, particularly the stems and rhizoids of moss aggregate soil particles (Colesie et al., 2014), as has been extensively shown in non-Antarctic deserts as well (Belnap and Büdel, 2016).

The McMurdo Dry Valleys are the largest ice-free area on the Antarctic continent (Levy

2013) and are one of Earth's coldest and driest deserts with mean annual temperatures between -15 and -30°C and less than 50 mm water equivalent of snowfall annually (Obryk et al., 2020; Fountain et al., 2010). The Lake Fryxell basin in eastern Taylor Valley hosts the most productive soils in the McMurdo Dry Valleys and supports patchily distributed biocrust communities across the terrestrial landscape (Barrett et al., 2007; Power et al., 2024). This region also has the greatest snow accumulation, highest relative humidity, and the shallowest ice-cemented permafrost layers in the Taylor Valley, and therefore has higher soil moisture content (Bockheim et al., 2008; Doran et al., 2002; Myers et al., 2022; Obryk et al., 2020). Recent work suggests that melting of seasonal snow patches is the primary source of liquid water to biocrust communities outside the glacial flow paths of meltwater streams and endorheic lakes (Power et al., 2024; Thapa-Magar et al., *in review*).

Like other dryland ecosystems, Antarctica's climate is changing, and its unique vegetation is already responding (Colesie et al., 2023; Robinson et al., 2003). Predictions for the outlook of Antarctica's vegetation are multifaceted, as vegetation responses to changes in temperature, water availability, and snow, for example, are complex and taxa-specific, and as climate trends are different in maritime and continental Antarctica, likely leading to dissimilar vegetation responses among the two bioregions (Colesie et al., 2023). Increasingly dynamic weather and general climate warming are predicted for the McMurdo Dry Valleys region (Fountain et al., 2014; Nielsen et al., 2023; Obyrk et al., 2020), and recent observations have illustrated significant responses of terrestrial and aquatic ecosystems to extreme weather events (Barrett et al., 2024; Gooseff et al., 2017). More variable climate and dynamic weather will likely influence the distribution and abundance of biocrusts in the McMurdo Dry Valleys in unknown ways. Therefore, understanding the controls of biocrust distribution is the essential first

step in elucidating the impacts of climate change on the base of the McMurdo Dry Valleys soil ecosystem and organic C balance.

Here, we describe the distribution and abundance of biocrust communities occupying soil environments in the Lake Fryxell basin outside of stream channel and lake margin environments (Figure 4.1). We used a combination of *in-situ* field surveying and sampling, remote sensing, and machine learning algorithms to: 1.) assess the main drivers of biocrust distribution and biomass, 2.) model the distribution of biocrust presence and biomass, and 3.) estimate the total surface organic C content of biocrusts across soils of the Lake Fryxell basin of Taylor Valley, Antarctica. This initial assessment is essential to ultimately characterize and monitor biocrust distribution and habitat suitability as a baseline against a changing regional climate.

Materials and Methods

Sampling locations were identified in the Lake Fryxell basin using multispectral satellite data to select sites over a range of soil moisture contents and biocrust cover. These sites were visited, surveyed, and sampled, and physical and chemical characteristics of biocrust and surface soil were measured in the laboratory. Potential predictors of biocrust presence and biomass include these field survey-based variables and geospatial raster variables which were extracted from each site using digital elevation models (DEM) and multispectral satellite data. A series of random forest algorithms were developed to assess the top predictors of biocrust presence/absence and ash-free dry mass (AFDM). Maps of biocrust presence and AFDM were created for the Lake Fryxell basin, and projections of aboveground organic C were estimated.

Field site selection

We identified 64 sites for ground truthing of satellite imagery and surveying and sampling of surface soils (Figure 4.2). These sites were selected to cover a range of predicted

moisture content and predicted biocrust abundance using high spatial resolution WorldView-2 and -3 multispectral satellite imagery (Maxar Technologies, Inc.). WorldView-2 and -3 are in polar orbit with 8 multispectral bands in the visible and near-infrared regions at 1.84 m and 1.24 m spatial resolutions at nadir, respectively. The predicted moisture content model used was derived from albedo measurements relative to long-term baseline surface albedos (Salvatore et al., 2023), and the predicted biocrust abundance model used was derived from spectral linear unmixing models (Power et al., 2024; Salvatore, 2015; Salvatore et al., 2020, 2021). The moisture content model used was a product of 21 WorldView-2 and -3 images (see table A1, Salvatore et al., 2023), and the biocrust abundance model was based on the spectral unmixing of a WorldView-3 image (10400100485D6900) acquired Jan 26, 2019. In ArcGIS Pro, we used conditional statements to identify pixels of a variety of conditions (*i.e*., wet, dry, barren, and/or abundant). We intentionally identified coordinates of areas covering a range of predicted moisture content and biocrust abundance and spatially spread throughout the Lake Fryxell basin (Figure 4.2).

In-situ surveying and sampling

The 64 locations identified using multispectral satellite imagery, representing a range of predicted moisture content and biocrust abundance, were visited between December 20 to 25, 2022. Sites were photographed and surface features and conditions (*e.g*., snow patch presence, moisture status, *etc*.) were documented. In particular, the presence or absence of biocrust was documented based on visual observation and assessment using the contemporary definition presented in Weber et al. (2022). Sites were noted as having biocrust absent, incipient biocrust present (*e.g*., sparse or emerging colonies), or dense biocrust present. Additionally, we differentiated the biocrusts between bryophyte-dominated and cyanobacteria-dominated

biocrusts (Figure 4.1), and noted the presence of lichen, hypoliths, or other photosynthetic communities near or part of the biocrusts. Incipient biocrusts were identified as areas with emerging colonies entrained within the sediment of the desert pavement surface. These incipient biocrusts appeared as cohesive cyanobacteria filaments either as part of dry and flaky surface layers or moist and firm connected surface layers. We considered biocrust as *present* at both dense sites where biomass covered large proportions of the survey areas as well as much sparser and patchier sites as well. Surface soil or biocrust was collected from bare desert pavement (128 cm^2) or with a brass cork borer (2.27 cm^2), respectively, at each site for subsequent pigment analysis (chlorophyll-a, scytonemin, and carotenoids) and organic matter content as AFDM. Samples were collected from representative areas of the landscape. Underlying soil to 10 cm depth was also collected at each site for subsequent analysis of gravimetric water content (GWC), pH, electrical conductivity (EC), inorganic nitrogen (N) and phosphorus (P) concentration, soil organic carbon (SOC), and total nitrogen (TN). Samples were kept frozen at -20°C in complete darkness until subsequent analyses were performed.

Laboratory analyses

We measured pigment concentration on the surface ~ 1 cm layer soil and biocrust samples using a trichromatic spectrophotometric method for chlorophyll-a, carotenoids, and scytonemin at 663, 490, and 384 nm, respectively (Garcia-Pichel and Castenholz, 1991). The dried samples were prepared by extracting the pigments in 90% unbuffered acetone for 24 hr using a 3.75:10 soil to solvent ratio for samples which contained zero or minimal biocrust and a 0.5:10 biocrust to solvent ratio for samples containing dense biocrust. Details regarding sample preparation, analysis using spectrophotometer, and pigment calculation are written in Power et al. (2024). Additionally, the surface layer soil and biocrust samples were measured for AFDM by

weighing a known area of sample, oven drying, weighing, and then combusting at 550°C for 24 hr using a muffle furnace, gently stirring samples halfway through combustion, and reweighing after cooling in a desiccator.

pH and electrical conductivity were measured in the underlying soil samples using a 1:2 and 1:5 soil to DI H_2O slurry, respectively, and GWC was determined as the mass of water lost after oven drying at 105°C for 24 hr. We also extracted inorganic N (NH_4^+ and NO_3^-) in 2 M potassium chloride and inorganic P (PO_4^{3-}) in 0.5 M sodium bicarbonate. Inorganic N and P were measured on extracts using a Lachat flow injection analyzer (Knepel, 2003; Prokopy, 1995). Additionally, we measured SOC and TN using an Elementar Vario MAX Cube analyzer after fumigating samples with concentrated hydrochloric acid to remove the influence of carbonates on SOC values (Walthert et al., 2010). SOC and TN were expressed as g C m^{-2} and g TN m^{-2} using a bulk density estimate of 1.6 g dry soil cm^{-3} (Levy and Schmidt, 2016) for estimation of soil organic matter stocks (0 – 10 cm).

Habitat description and characterization

Since many of the physical and chemical properties of the soil were highly skewed (Figure S4.1), a Wilcoxon Rank Sum test was performed in R Statistical Software version 4.1.2 to assess differences between sites that contained biocrust and those that did not (R Core Team, 2021). Potential predictor variables of biocrust measured from samples collected in the field include both physical (GWC and EC) and chemical properties (pH, NH_4^+, NO_3^-, PO_4^{3-}, SOC and TN). Other potential predictors of biocrust were selected using remotely derived datasets. These include aspect, slope, and elevation collected from a high resolution DEM (Fountain et al., 2017), a rasterized GWC layer developed for this region by Salvatore et al. (2023) using 21 WorldView-2 and -3 images (see table A1, Salvatore et al., 2023), and a rasterized snow

frequency layer also developed for this region using albedo thresholds with the same 21 images (Salvatore et al., 2023) over the course of the austral summer (see also, Thapa-Magar et al., *in review*) (Figure S4.2). Snow frequency was calculated as the percentage of the 21 WorldView-2 and -3 images that indicate snow at each pixel relative to those images that do not indicate snow at each pixel (*e.g.*, 0% representing no snow observed in any of the images analyzed and 100% representing snow observed in all the images analyzed).

Machine learning algorithm development

A series of classification and regression models were developed for predicting biocrust presence and AFDM using MATLAB's classification and regression learner with an out-of-bag (OOB) approach. Binary classification models were developed using biocrust presence and absence (based on visual survey) as the response variables and separately the field survey and rasterized geospatial variables as predictor variables. Regression models were also developed using AFDM as the response variable and using the same predictor variables as indicated above. MATLAB's classification learner tested 40+ different models (*e.g.*, decision trees, support vector machines, nearest neighbors, Bayes classifiers, ensemble classifiers, neural networks) to assess whether our data could be successfully trained to classify data, as did MATLAB's regression learner (*e.g.*, linear regression, regression trees, support vector machines, kernel approximation, ensembles of trees, neural networks), assessing whether our data could train regression models for prediction. Results from the classification and regression learner are presented as Supplemental Text.

For our study, we chose to concentrate on the random forest algorithms and apply those to map predictions since these are widely used and understood in the species distribution modeling and geospatial communities (Cerrejón et al., 2020; Evans et al., 2011; Qiu et al., 2023).

We ran a series of random forest models: 1.) classification models for predicting biocrust presence and absence, and 2.) regression models for predicting biocrust AFDM. These models were informed by "field survey" data, "geospatial raster" data, or "hybrid" approach that included both field and remotely sensed data. The quality of the models was evaluated using OOB predictions on the training data rather than setting aside test data; therefore, all data were used in training the models. All random forest models presented in this paper were developed using the R package ModelMap (Freeman and Frescino, 2009), which provides an interface between the randomForest (Liaw and Wiener, 2002) and PresenceAbsence packages (Freeman and Moisen, 2008), in R Statistical Software (v4.1.2; R Core Team, 2021).

Predicting biocrust presence/absence with random forest models

Presence or absence of biocrust observed at the 64 sites was the binary response variable, and the predictor variables were the field survey data measured for each site and the rasterized geospatial data calculated for each site as well, modeled separately and together (hybrid). The number of trees in the models were optimized based on the OOB error. The outputs included model accuracy, OOB error, area under the receiver operating characteristic curve (AUC), relative influence of the predictor variables, and confusion matrices which provided class errors. AUC scores range from 0 to 1 and are used to evaluate model performance; the closer the AUC score is to 1, the greater the prediction accuracy of the model (Elith et al., 2006; Hosmer and Lemeshow, 2000). The relative influence of the predictor variables is based on the mean decrease in accuracy, which expresses how much accuracy the model loses by excluding each variable, and the mean decrease in Gini, which is a measure of how each variable contributes to the homogeneity of the nodes and leaves in the model. These are both measures of variable importance; the variables with the greatest mean decrease in accuracy and greatest mean

decrease in Gini are considered the most important variables in predicting biocrust presence/absence.

Predicting biocrust AFDM with random forest models

We chose to model AFDM, which provides information beyond whether a biocrust is present or not, but *how much* biomass is present, and can therefore be used to estimate carbon stocks. AFDM measured at the 64 sites was the continuous response variable in 2 random forest models using data from the field surveys and the rasterized geospatial data as the predictor variables. The number of trees in the models were optimized based on the OOB error. The outputs included measures of the relative influence of the predictor variables and observed versus predicted AFDM, which were used to calculate model R^2 and root mean square error (RMSE). The relative influence of the predictor variables is based on the percent increase in mean square error (MSE), which is a measure of the increase in error from randomly permuting each predictor, and the increase in node purity, which is based on changes in node purity from splitting on the variable. These are also both measures of variable importance; the variables with the greatest percent increase in MSE and greatest increase in node purity are considered the most important variables in predicting biocrust AFDM.

Mapping biocrust presence and AFDM

Maps of predicted biocrust presence were created using random forest models with geospatial predictors in the R package ModelMap (Freeman and Frescino, 2009). ModelMap provides an interface between the raster package to read and predict over raster data (Hijmans 2023). Files of the detailed prediction surface images were created in R and opened in ArcGIS Pro for subsequent analysis and map production. Symbology thresholds for each map were created by presenting either a high likelihood of biocrust presence (> 70%) or relatively dense

AFDM locations (> 150 g m^{-2}). The resultant prediction map is the mean of all the trees, since the model for AFDM had a continuous response.

The presence/absence probability and AFDM models were used to estimate the area biocrusts are likely present within and basin-wide aboveground C content in terrestrial environments of the Lake Fryxell basin, *i.e.*, outside of stream channels and lake margins. Using ArcGIS Pro, the number of pixels containing a 90% probability of biocrust occurrence was determined and divided by the total number of pixels, providing a percentage of the Lake Fryxell basin that have biocrusts present. Multiplying the number of pixels that contain biocrusts with 90% certainty by the individual pixel area (~ 15 m^2) resulted in the area of the Lake Fryxell basin that are predicted to have biocrusts present. The modeled AFDM of all pixels containing a 90% probability of biocrust occurrence was extracted from ArcGIS Pro. The range of these AFDM predictions was used to bracket a range of C (g C m^{-2}) likely contained in biocrusts for the Lake Fryxell basin study area. Aboveground C content of this range was calculated as 53% of the AFDM, assuming organic matter is 53% C by weight (Wetzel 1983). This AFDM range was then multiplied by the total area that biocrusts were present in (2.7 x 10^5 m^2).

Results

Biocrust field surveys

Of the 64 sites visited, 17 contained visually conspicuous biocrust (Table 4.1), including dense or incipient morphologies, and 47 lacked visually discernible biocrust presence. The biocrusts identified and sampled were predominantly bryophyte-dominated and cyanobacteria-dominated biocrusts (Figure 4.1, Table 4.1). The bryophyte communities were primarily dark moss (likely *Bryum* spp.; Schwarz et al., 1992), and one site contained red moss (likely *Hennediella heimii*; Pannewitz 2003). Sparse yellow and orange lichen were noted on some of

the bryophyte-dominated biocrusts. The cyanobacteria-dominated biocrusts were predominantly black *Nostoc* spp. with active, green-pigmented algae layers below the dark-pigmented surface layer of some samples. The incipient biocrust communities contained emerging colonies of cohesive cyanobacteria filaments. Hypoliths were commonly found around the areas of biocrusts and incipient biocrusts, as previously identified in this region (*e.g.*, Cowan et al., 2010). Many surveyed sites containing biocrust lacked snow cover at the time of sampling but had microtopographic features suggesting the presence of snow previously or earlier in the season (*e.g.*, depressions, alluvial-like features where snow melt moves surface soil downslope). These areas were confirmed with WorldView-2 and -3 imagery to often contain early season snow cover in other seasons.

Soil physical and biochemical properties

Sites supporting biocrust had significantly higher concentrations of chlorophyll-a, scytonemin, and carotenoid pigments in surface soils compared to sites lacking biocrust, with scytonemin the most abundant pigment among all sites (Table 4.2). Surface organic matter content in the form of AFDM ranged from 16.1 g m^{-2} to 773 g m^{-2} and was highest in the biocrust sites and consistently lower in the sites lacking biocrust (Table 4.2). Soils supporting biocrust had higher moisture content, lower alkalinity, and lower EC compared to sites lacking biocrust (Table 4.2). Most of the soil variables had frequency distributions that were highly right-skewed, roughly following power-law frequency distributions, which are common in ecological data (Bak 1996). EC data were particularly right-skewed, due to several sites having very high EC, > 5000 µS/cm (Figure S4.1). For example, site 25, one of the sites supporting incipient biocrusts, had exceptionally high EC (~ 15,000 µS/cm), inorganic N, and amongst the highest SOC and TN values. While NH_4^+ and TN were not significantly different between sites

containing biocrust and those lacking biocrust, SOC was significantly higher and PO_4^{3-} and NO_3^- were significantly lower in sites containing surface biocrust (Table 4.2). Two dense biocrust sites in particular had high SOC concentrations of 5.58 and 5.60 mg C g^{-1} dry soil (Figure S4.1), equating to ~ 900 g C m^{-2} in the surface 10 cm of soil.

Biocrust presence/absence and AFDM model performance

The field survey model predicting biocrust presence using exclusively field survey derived variables had an overall accuracy of 87.5% (OOB error 12.5%), with class errors of 2.1% for absent and 41% for present (Figure 4.3b), and an AUC of 0.86. The confusion matrix indicates the field survey model underpredicts the presence of biocrust (Figure 4.3b). GWC and EC were the most important variables when predicting biocrust presence in the field survey model, when comparing the mean decrease in accuracy (Figure 4.3a) and pH and EC were the most important when comparing the mean decrease in Gini (Figure S4.3a).

The geospatial raster model predicting biocrust presence using exclusively remote sensing derived variables performed with 84% accuracy (16% OOB error) and an AUC of 0.80. Snow frequency and rasterized GWC were the most important variables when predicting biocrust presence in the geospatial raster model, when comparing the mean decrease in accuracy and Gini (Figure 4.3c, S4.3b). The class errors were 4.2% for absent and 47% for present, with the confusion matrix indicating the model underpredicts the presence of biocrust (Figure 4.3d).

A hybrid model predicting biocrust presence using both field survey and geospatial rasterized variables performed with the overall highest accuracy, 91% (OOB error of 9%), and AUC, 0.89. Field-based GWC and EC were the most important variables when predicting biocrust presence in the hybrid model, followed by snow frequency, aspect, and pH according to the mean decrease in accuracy and Gini assessments (Figure 4.3e, S4.3c). The class errors were

2.1% for absent and 29% for present (Figure 4.3f), indicating the hybrid model is more accurate when predicting areas where biocrust is absent, and it slightly underpredicts the presence of biocrust based on the confusion matrix.

The geospatial raster model predicting AFDM using exclusively remote sensing derived data had an R^2 of 0.32 and RMSE of 14.6, with a slight underprediction of AFDM based on the observed vs. predicted AFDM plot (Figure 4.4b). Snow frequency and slope were the most important variables when predicting AFDM in the geospatial raster model, when comparing the percent increase in MSE assessment (Figure 4.4a), and snow frequency and aspect were the most important variables when comparing the increase in node purity (Figure S4.4a).

The hybrid model predicting AFDM using both field survey and geospatial raster variables performed well with an R^2 of 0.56 and RMSE of 12.2, with a slight underprediction of AFDM based on the observed vs. predicted AFDM plot (Figure 4.4d). The most important variables predicting AFDM in the hybrid model were EC and snow frequency, when comparing the percent increase in MSE and node purity assessments (Figure 4.4c, S4.4b).

Biocrust maps and carbon estimates

The predicted distribution of biocrust in the Lake Fryxell basin (Figure 4.5) at 90% probability occurred within 2.7×10^5 m^2. These areas of high probability of biocrust occurrence often coincided with areas of seasonal snow cover (*e.g.,* Figure 4.6). The map of AFDM density follows a similar geographic pattern (Figure S4.5). Using both maps, we predict that areas with 90% probability of biocrust presence contain between 11 and 72 Mg of C in aboveground biocrust in 0.6% of the terrestrial Lake Fryxell basin landscape, excluding the masked-out glaciers, lake, streams, and perennial snow areas.

Discussion

Our models predict that biocrusts occur in 2.7 x 10^5 m^2 or in 0.6% of the arid terrestrial landscape of the Lake Fryxell basin (a conservative estimate based on 90% probability of presence), typically alongside and below seasonal snow patches (Figure 4.5, 4.6). Physical and chemical analyses of the surface soils showed that biocrust sites are significantly different from unvegetated sites, especially for pigments and organic matter content (Table 4.2), illustrating the influence of biocrusts on soils. Field survey-based data and remotely sensed data were both reliable predictors of biocrust presence and biomass, although hybrid models generated the most robust models. Remote sensing data are essential in informing our understanding of long-term dynamics of snow (one of the most important predictors of biocrust occurrence and biomass) and are therefore essential in understanding the distribution of biocrusts and predicting their sensitivity to climate change. However, field sampling is an important complement to remote sensing efforts by highlighting important soil properties (*e.g.*, EC) that are currently missing from our remote sensing capabilities. Our study illustrates the synergistic effect of combining field and remote sensing data for understanding and predicting ecological dynamics.

Primary drivers of biocrust distribution and biomass

The conditions that promote the densest microbial mats in the McMurdo Dry Valleys, *e.g.*, as found in the Canada Glacier Antarctic Specially Protected Area 131, are associated with wet to intermittently saturated soils that are often sheltered from foehn winds (Antarctic Treaty ASPA 131 Management Plan https://www.ats.aq/documents/recatt%5Catt683_e.pdf; Power et al., 2020). Here, we explicitly focused on the spatial distribution and drivers of lower density biocrust, which we found are also associated with moist conditions and sheltered within depressional features and snow patches. Random forest models provided robust, conservative

predictions of biocrust presence and biomass (AFDM), *i.e.*, they underpredict biocrust presence and biomass. All random forest classification models predicting biocrust presence performed with 'excellent' accuracy based on their AUC scores (Hosmer and Lemeshow, 2000), and the regression models predicting biocrust AFDM performed well with acceptable RMSE and R^2 values. While several variables were significant in our models, GWC, EC, and snow frequency were the strongest predictors of biocrusts, confirmed by two separate measures of evaluating variable importance per model (Figure 4.3, 4.4, S4.3, S4.4). GWC is a more important variable in the models predicting biocrust presence (Figure 4.3) compared to those predicting biocrust AFDM, where EC and snow frequency were more important (Figure 4.4). Modeling AFDM provides information beyond whether a biocrust is present or not – it informs about the mass or density of the biocrust present. While GWC is important when predicting biocrust presence, we found that high frequency of snow cover and low EC are the habitat characteristics driving the densest biocrust sites (Figure 4.4).

We found that snow is an essential driver of biocrust presence and biomass in the Taylor Valley, evidenced by our random forest models, but also more simply by strong positive correlations between snow frequency and AFDM, chlorophyll-a, and SOC (Table S4.1), confirming the importance snow presence has on biocrusts and the underlying soil C. In the McMurdo Dry Valleys, snow patches are documented to increase surrounding soil moisture compared to nearby snow-free soils (Ayers et al., 2010; Eveland et al., 2012; Gooseff et al., 2003). The microtopography of periglacial features, shallow depressions, and the lee side of boulders collect snow drifts that accumulate in the winter and slowly melt in the summer months, sustaining biocrust communities (Cannone and Guglielmin, 2010; Green and Broady, 2001; Kappen et al., 1990). While dense and perennial snow covers have been shown to reduce the

survival and growth of some lichen (*e.g.*, "snowkill"; Sancho et al., 2017), the seasonal snow patches that slowly melt during the summer often sustain dense bryophyte- and cyanobacteria-dominated biocrusts (Kappen et al., 1990; Power et al., 2024). Shallow layers of snow (~ 15 cm or less) allow sufficient light penetration for photosynthesis, and Antarctic vegetation below have been shown to remain active (Kappen et al., 1991). Snow patches provide benefits beyond moisture availability, and therefore serve as preferential microhabitats for biocrusts and other organisms in Antarctica (Kappen 1985; Power et al., 2024) and other ecosystems outside of Antarctica (Hao et al., 2020; Hui et al., 2022; Ladrón de Guevara and Maestre, 2022; Yang et al., 2023; Zhang et al., 2021). For example, snow cover reduces temperature extremes in underlying soil (Schimel et al., 2004), supplies nutrient inputs (Wright et al., 2024), and likely provides refuge for biocrusts from both aeolian scouring during common extreme wind events (*e.g.*, Beane, 2021; Nylen et al., 2004; Obryk et al., 2020) and intense UV-radiation (*e.g.,* Bernhard and Stierle, 2020; Farman et al., 1985; McKnight et al., 1999).

Water availability is essential, but it is not the sole environmental factor controlling the distribution and abundance of photosynthetic life in Antarctica (Kennedy 1993). The interaction of water and soluble salts can create wet, salty sites that are inhospitable to biocrusts, likely because of the physiological stress associated with salts, as has been documented in the “water track” environments of the McMurdo Dry Valleys (Kuentz et al., 2022; Levy et al., 2014, 2011). For example, dense biocrust sites with the highest AFDM values (> 400 g m^{-2}) all had EC under 55 µS cm^{-1}, while the average EC for sites without biocrust was 1700 µS cm^{-1}. This interaction of salt and water is modulated by the topography and the timing of snow melt and permafrost thaw. For example, the frequency of melt events influences how often the soils and salts are hydrated, while topographic conditions influence whether those salts are flushed downhill. There is wide

variation in GWC and EC, for example, within the sites containing biocrust and those not containing biocrust (Figure S4.1). Site 25 is an ecological outlier with low AFDM but high SOC, and exceptionally high EC (~ 15,000 uS/cm) and nitrate concentrations. Several of our study sites that lacked biocrust had sufficiently high GWC (Figure S4.1); indicating that while water is essential for the development of biocrust, other factors can limit establishment and growth (*e.g.*, exposure, insufficient nutrients, or excess salts). Other landscape factors like aspect and slope also contribute significantly to the random forest models predicting AFDM. For example, south facing slopes in the Lake Fryxell basin receive less intense solar radiation (Dana et al., 1998) and therefore likely have higher soil water content and greater seasonal snow accumulation.

Some of the top predictors for biocrust presence (*i.e.*, snow and gravimetric water content) can be remotely measured via satellite imagery and, therefore, can be incorporated into models of landscape-scale biocrust distribution. However, there are important field-based geochemical variables, especially EC, that are not yet remotely measurable from satellite imagery and, therefore, could not be included in our geospatial-based models. Weaker performance of the geospatial-based models in comparison to the field survey-based models is likely due to the absence of important edaphic variables. Future work incorporating geochemical data into these geospatial models will likely improve model performance (*e.g.*, resistivity surveys using airborne instruments, Gutterman et al., 2023), and therefore improve accuracy into our prediction maps used for monitoring biocrust communities in a changing climate.

Contribution of biocrusts to carbon budget

Globally, biocrusts and other cryptogams (*i.e.*, plants that have no true flowers or seeds,) contain approximately 4.9 Pg of C or ~1% of the C content of terrestrial vegetation (Elbert et al., 2012), which includes other organisms beyond the contemporary definition of biocrusts (*e.g.*,

organisms growing in or on rocks, leaves, and wood) (Weber et al., 2022). This small fraction belies the local importance of biocrusts where they are sometimes the primary source of C in arid ecosystems. At a glance, the terrestrial landscape of the Taylor Valley appears barren and devoid of vegetation outside of the lakes and ephemeral streams which host dense microbial mats (Alger et al., 1997; Kohler et al., 2015; Stone et al., 2024). However, biocrusts occupy the soils in microhabitats suitable for their growth and contain a significant amount of C, influencing the organic matter content of the underlying soils as well (Power et al., 2024).

We estimate a range of biocrust biomass of 40 – 265 g C m^{-2} in pixels with a greater than 90% probability of biocrust occurrence, which scales to 11 – 72 Mg of aboveground biocrust C in the Lake Fryxell basin. Our models used to map biocrusts and AFDM likely underpredict the presence and biomass of biocrust but represent a first attempt at including these types of communities in regional C budgets. Scalable and systematic estimates of aboveground C are limited for this region, primarily due to the logistical challenges of conducting Antarctic field work. Early work by Burkins et al. (2001) estimated an average of 150 g C m^{-2} for the top 20 cm of soils in the Taylor Valley, in which they note that soils occupy over 95% of the non-glacial landscape. We found that soils hosting biocrusts contained, on average, 228 g C m^{-2} in the top 10 cm and soils lacking biocrusts contained 85 g C m^{-2} on average, bracketing the SOC estimates in Burkins et al. (2001). When combining the aboveground biocrust C estimate of all areas in the Lake Fryxell basin predicted with 90% probability to contain biocrust (40 - 265 g C m^{-2}) and the average belowground C from biocrust sites measured *in-situ* (228 g C m^{-2}), we estimate a total range of 268 - 493 g C m^{-2} in areas containing biocrust.

Remote sensing tools are essential in characterizing ecological processes at landscape scales. More recently with the advancements in remote sensing technologies and applications,

remote assessments of aboveground biomass in the Lake Fryxell basin have been conducted (Power et al., 2020; Salvatore et al., 2021), primarily validated for use in the aquatic environments of dense microbial mats, while some have focused on characterizing the surrounding soil landscape (Power et al., 2024). Power et al. (2020) estimated C stocks of 21.7 Mg in the Canada Glacier Antarctic Specially Protected Area alone, which is considered one of the most diverse and productive environments in Taylor Valley (Schwarz et al., 1992). Salvatore et al. (2021) estimated 757 Mg of C in the Lake Fryxell basin, using a model derived primarily from observations from soils and sediments near stream channels and lake margins, possibly overestimating C when extrapolating out to the drier terrestrial landscapes. These recent estimates of aboveground biomass in the Lake Fryxell basin included dense microbial mats from aquatic landscapes and are therefore much greater than ours reported here, which were produced from models specifically designed for the drier terrestrial landscape. Our estimate of 11 – 72 Mg C in biocrusts occupying drier landscapes of the Lake Fryxell basin suggests that a significant portion of the valley-wide C budget lies outside the conventionally studied aquatic flow-paths.

The future of Antarctic biocrusts in a changing climate

Climate change is likely to tip arid ecosystems, and cold deserts in particular, out of stable states (Reed et al., 2016; Wall 2007). The distribution of Antarctic biocrusts and their role on the local C cycle are sensitive to changes in local and regional climate (*e.g.*, Cannone et al., 2021; Colesie et al., 2023; Convey and Peck, 2019; Robinson et al., 2003; Siegert et al., 2019). Specifically, future snow dynamics are particularly important in the survival and distribution of Antarctic vegetation (Colesie et al., 2023; Green et al., 2011; Tarca et al., 2022). Increases in precipitation from the occurrence of extreme snowfall events in coastal Antarctica (Turner et al., 2019) in contrast to regional drying trends in continental Antarctica (Robinson et al., 2018)

illustrates how climate variability is region-specific in the Antarctic and is nonetheless anticipated to impact vegetation in varying ways (Colesie et al., 2023). There is strong interannual variability of snow accumulation and snow persistence in the McMurdo Dry Valleys (Myers et al., 2022), an increasingly dynamic region on the precipice of change (Colesie et al., 2023; Gooseff et al., 2017; Levy et al., 2018; Obryk et al., 2020; Wall 2007). For example, in the McMurdo Dry Valleys, recent climate variation has included an extended cooling period (Doran et al., 2002; Obryk et al., 2020), summer floods (Gooseff et al., 2017), the first records of rainfall in Taylor Valley, and an autumnal heatwave (Barrett et al., 2024) which are likely to influence the distribution and activity of biocrust communities (Colesie et al., 2023). Antarctic coastal regions are also predicted to experience more frequent and intense rainfall by the end of the century (Vignon et al., 2021). These changing weather and climate patterns could have drastic implications for the distribution and abundance of biocrust communities. Predicting how increasingly dynamic weather and future climate will impact terrestrial ecosystems and carbon balance in terrestrial Antarctica will require this improved understanding of the environmental drivers of soil biocrust communities.

Data Availability Statement

All data presented in this study are archived in the Environmental Data Initiative (EDI) Repository (Power, Salvatore, Adams, & Barrett 2024).

Ethics Statement

Permission to enter the Canada Glacier Antarctic Specially Protected Area (ASPA 131) and sample soil and biocrust was given by the National Science Foundation Division of Polar Programs through Antarctic Conservation Act Permit.

Funding Statement

Funding for this work was provided by several awards from the National Science Foundation: #OPP-1637708 and most recently #OPP-2224760 for Long Term Ecological Research, and #OPP-2046260 to M. Salvatore.

Acknowledgements

We acknowledge the Polar Geospatial Center for geospatial support, Maxar Technologies, Inc. for access to satellite imagery, and Antarctic Support Contractors and Air Center Helicopters for providing operational support in the field. We appreciate Meredith Snyder and Jesse Jorna for their assistance with ground truthing and sample collection in the field and sample processing in the Crary Laboratory at McMurdo Station. We would also like to thank Bobbie Niederlehner for her expertise with analytical chemistry techniques back home, and we wish her a wonderful, well-deserved retirement. Finally, we gratefully acknowledge Dr. Claudia Colesie and one anonymous reviewer whose thoughtful feedback improved this manuscript.

References

Allan, R. P., & Douville, H., 2023. An even drier future for the arid lands. Proceedings of the National Academy of Sciences of the United States of America, 121, e2320840121. https://doi.org/10.1073/pnas.2320840121

Alger, A.S., McKnight, D.M., Spalding, S.A., Tate, C.M., Shupe, G.H., Welch, K.A., Edwards, R., Andrews, E.D., House, H.R., 1997. Ecological Processes in a Cold Desert Ecosystem: The Abundance and Species Distribution of Algal Mats in Glacial Meltwater Streams in Taylor Valley, Antarctica. Institute of Arctic and Alpine Research Occasional Paper 51.

Ayres, E., Nkem, J.N., Wall, D.H., Adams, B.J., Barrett, J.E., Simmons, B.L., Virginia, R.A., Fountain, A.G., 2010. Experimentally increased snow accumulation alters soil moisture and animal community structure in a polar desert. Polar Biol. 33, 897–907. https://doi.org/10.1007/s00300-010-0766-3

Bak, P., 1996. How nature works: the science of self-organized criticality. Springer, New York,

New York, USA. https://doi.org/10.1007/978-1-4757-5426-1

Barrera, A., Acuña-Rodríguez, I.S., Ballesteros, G.I., Atala, C., Molina-Montenegro, M.A., 2022. Biological Soil Crusts as Ecosystem Engineers in Antarctic Ecosystem. Front. Microbiol. 13, 755014. https://doi.org/10.3389/fmicb.2022.755014

Barrett, J.E., Virginia, R.A., Lyons, W.B., McKnight, D.M., Priscu, J.C., Doran, P.T., Fountain, A.G., Wall, D.H., Moorhead, D.L., 2007. Biogeochemical stoichiometry of Antarctic Dry Valley ecosystems. J. Geophys. Res. 112. https://doi.org/10.1029/2005JG000141

Barrett, J.E., Adams, B.J., Doran, P.T., Dugan, H.A., Myers, K.F., Salvatore, M.R., Power, S.N., Snyder, M.D., Wright, A.T., Gooseff, M.N., 2024. Response of a Terrestrial Polar Ecosystem to the March 2022 Antarctic Weather Anomaly. Earths Future 12, e2023EF004306. https://doi.org/10.1029/2023EF004306

Beane, S.J., 2021. Hydrologic Response to Foehn Winds in the McMurdo Dry Valleys, Southern Victoria Land, Antarctica (Masters Thesis). University of Colorado at Boulder.

Belnap, J., Weber, B., Büdel, B., 2016. Biological Soil Crusts as an Organizing Principle in Drylands, in: Weber, B., Büdel, B., Belnap, J. (Eds.), Biological Soil Crusts: An Organizing Principle in Drylands. Springer International Publishing, pp. 3–13. https://doi.org/10.1007/978-3-319-30214-0_1

Belnap, J., Büdel, B., 2016. Biological Soil Crusts as Soil Stabilizers, in: Weber, B., Büdel, B., Belnap, J. (Eds.), Biological Soil Crusts: An Organizing Principle in Drylands. Springer International Publishing, Cham, pp. 305–320. https://doi.org/10.1007/978-3-319-30214-0_16

Bernhard, G., Stierle, S., 2020. Trends of UV Radiation in Antarctica. Atmosphere 11, 795. https://doi.org/10.3390/atmos11080795

Bockheim, J.G., Prentice, M.L., McLeod, M., 2008. Distribution of glacial deposits, soils, and permafrost in Taylor Valley, Antarctica. Arct. Antarct. Alp. Res. 40, 279–286. https://doi.org/10.1657/1523-0430(06-057)[BOCKHEIM]2.0.CO;2

Büdel, B., Colesie, C., 2014. Biological Soil Crusts, in: Cowan, D.A. (Ed.), Antarctic Terrestrial Microbiology: Physical and Biological Properties of Antarctic Soils. Springer Berlin Heidelberg, Berlin, Heidelberg, pp. 131–161. https://doi.org/10.1007/978-3-642-45213-0_8

Burkins, M.B., Virginia, R.A., Wall, D.H., 2001. Organic carbon cycling in Taylor Valley,

Antarctica: quantifying soil reservoirs and soil respiration. Glob. Chang. Biol. 7, 113–125. https://doi.org/10.1046/j.1365-2486.2001.00393.x

Cannone, N., Guglielmin, M., 2010. Relationships between periglacial features and vegetation development in Victoria Land, continental Antarctica. Antarct. Sci. 22, 703–713. https://doi.org/10.1017/S0954102010000751

Cannone, N., Guglielmin, M., Malfasi, F., Hubberten, H.W., Wagner, D., 2021. Rapid soil and vegetation changes at regional scale in continental Antarctica. Geoderma 394, 115017. https://doi.org/10.1016/j.geoderma.2021.115017

Cerrejón, C., Valeria, O., Mansuy, N., Barbé, M., Fenton, N.J., 2020. Predictive mapping of bryophyte richness patterns in boreal forests using species distribution models and remote sensing data. Ecol. Indic. 119, 106826. https://doi.org/10.1016/j.ecolind.2020.106826

Chen, N., Yu, K., Jia, R., Teng, J., Zhao, C., 2020. Biocrust as one of multiple stable states in global drylands. Sci Adv 6. https://doi.org/10.1126/sciadv.aay3763

Colesie, C., Walshaw, C.V., Sancho, L.G., Davey, M.P., Gray, A., 2023. Antarctica's vegetation in a changing climate. Wiley Interdiscip. Rev. Clim. Change 14. https://doi.org/10.1002/wcc.810

Colesie, C., Gommeaux, M., Allan Green, T.G., Büdel, B., 2014. Biological soil crusts in continental Antarctica: Garwood Valley, southern Victoria Land, and Diamond Hill, Darwin Mountains region. Antarct. Sci. 26, 115–123. https://doi.org/10.1017/S0954102013000291

Convey, P., Peck, L.S., 2019. Antarctic environmental change and biological responses. Sci Adv 5, eaaz0888. https://doi.org/10.1126/sciadv.aaz0888

Cowan, D.A., Khan, N., Pointing, S.B., Craig Cary, S., 2010. Diverse hypolithic refuge communities in the McMurdo Dry Valleys. Antarct. Sci. 22, 714–720. https://doi.org/10.1017/S0954102010000507

Dana, G.L., Wharton, R.A., Jr, Dubayah, R.A., 1998. Solar radiation in the McMurdo dry valleys, Antarctica, in: Priscu, J.C. (Ed.), Ecosystem Dynamics in a Polar Desert: The Mcmurdo Dry Valleys, Antarctica, Antarctic Research Series. American Geophysical Union, Washington, D. C., pp. 39–64. https://doi.org/10.1029/ar072p0039

Doran, P.T., McKay, C.P., Clow, G.D., Dana, G.L., Fountain, A.G., Nylen, T., Lyons, W.B., 2002. Valley floor climate observations from the McMurdo dry valleys, Antarctica,

1986–2000. J. Geophys. Res. 107, 4772. https://doi.org/10.1029/2001JD002045

Elbert, W., Weber, B., Burrows, S., Steinkamp, J., Büdel, B., Andreae, M.O., Pöschl, U., 2012. Contribution of cryptogamic covers to the global cycles of carbon and nitrogen. Nat. Geosci. 5, 459–462. https://doi.org/10.1038/ngeo1486

Elith, J., H. Graham, C., P. Anderson, R., Dudík, M., Ferrier, S., Guisan, A., J. Hijmans, R., Huettmann, F., R. Leathwick, J., Lehmann, A., Li, J., G. Lohmann, L., A. Loiselle, B., Manion, G., Moritz, C., Nakamura, M., Nakazawa, Y., McC. M. Overton, J., Townsend Peterson, A., J. Phillips, S., Richardson, K., Scachetti-Pereira, R., E. Schapire, R., Soberón, J., Williams, S., S. Wisz, M., E. Zimmermann, N., 2006. Novel methods improve prediction of species' distributions from occurrence data. Ecography 29, 129–151. https://doi.org/10.1111/j.2006.0906-7590.04596.x

Evans, J.S., Murphy, M.A., Holden, Z.A., Cushman, S.A., 2011. Modeling Species Distribution and Change Using Random Forest, in: Drew, C.A., Wiersma, Y.F., Huettmann, F. (Eds.), Predictive Species and Habitat Modeling in Landscape Ecology: Concepts and Applications. Springer New York, New York, NY, pp. 139–159. https://doi.org/10.1007/978-1-4419-7390-0_8

Eveland, J., Gooseff, M.N., Lampkin, D.J., Barrett, J.E., Takacs-Vesbach, C., 2012. Spatial and temporal patterns of snow accumulation and aerial ablation across the McMurdo Dry Valleys, Antarctica. Hydrol. Process. 27. https://doi.org/10.1002/hyp.9407

Farman, J.C., Gardiner, B.G., Shanklin, J.D., 1985. Large losses of total ozone in Antarctica reveal seasonal ClOx/NOx interaction. Nature 315, 207–210. https://doi.org/10.1038/315207a0

Feng, H., & Zhang, M., 2015. Global land moisture trends: drier in dry and wetter in wet over land. Scientific Reports, 5, 18018. https://doi.org/10.1038/srep18018

Finger-Higgens, R., Duniway, M.C., Fick, S., Geiger, E.L., Hoover, D.L., Pfennigwerth, A.A., Van Scoyoc, M.W., Belnap, J., 2022. Decline in biological soil crust N-fixing lichens linked to increasing summertime temperatures. Proc. Natl. Acad. Sci. U. S. A. 119, e2120975119. https://doi.org/10.1073/pnas.2120975119

Fountain, A.G., Fernandez-Diaz, J.C., Obryk, M., Levy, J., Gooseff, M., Van Horn, D.J., Morin, P., Shrestha, R., 2017. High-resolution elevation mapping of the McMurdo Dry Valleys, Antarctica, and surrounding regions. Earth System Science Data 9, 435–443.

https://doi.org/10.5194/essd-9-435-2017

Fountain, A.G., Levy, J.S., Gooseff, M.N., Van Horn, D., 2014. The McMurdo Dry Valleys: A landscape on the threshold of change. Geomorphology 225, 25–35. https://doi.org/10.1016/j.geomorph.2014.03.044

Fountain, A.G., Nylen, T.H., Monaghan, A., Basagic, H.J., Bromwich, D., 2010. Snow in the McMurdo Dry Valleys, Antarctica. Int. J. Climatol. 30, 633–642. https://doi.org/10.1002/joc.1933

Freeman, E. and Frescino, T., 2009. ModelMap: Modeling and Map production using Random Forest and Stochastic Gradient Boosting. USDA Forest Service, Rocky Mountain Research Station, 4919 S 1500 W, Suite 200, Riverdale, UT 84405, USA. http://CRAN.R-project.org/

Freeman, E. and Moisen, G., 2008. PresenceAbsence: An R Package for Presence-Absence Model Analysis. Journal of Statistical Software, 23(11):1-31. https://www.jstatsoft.org/v23/i11

Garcia-Pichel, F., Castenholz, R.W., 1991. Characterization and Biological Implications of Scytonemin, a Cyanobacterial Sheath Pigment. J. Phycol. 27, 395–409. https://doi.org/10.1111/j.0022-3646.1991.00395.x

Gooseff, M.N., Barrett, J.E., Adams, B.J., Doran, P.T., Fountain, A.G., Lyons, W.B., McKnight, D.M., Priscu, J.C., Sokol, E.R., Takacs-Vesbach, C., Vandegehuchte, M.L., Virginia, R.A., Wall, D.H., 2017. Decadal ecosystem response to an anomalous melt season in a polar desert in Antarctica. Nature Ecology & Evolution 1, 1334–1338. https://doi.org/10.1038/s41559-017-0253-0

Gooseff, M.N., Barrett, J.E., Doran, P.T., Fountain, A.G., Lyons, W.B., Parsons, A.N., Porazinska, D.L., Virginia, R.A., Wall, D.H., 2003. Snow-Patch Influence on Soil Biogeochemical Processes and Invertebrate Distribution in the McMurdo Dry Valleys, Antarctica. Arct. Antarct. Alp. Res. 35, 91–99.

Green, T.G.A., Broady, P.A., 2001. Biological Soil Crusts of Antarctica, in: Belnap, J., Lange, O.L. (Eds.), Biological Soil Crusts: Structure, Function, and Management. Springer Berlin Heidelberg, Berlin, Heidelberg, pp. 133–139. https://doi.org/10.1007/978-3-642-56475-8_11

Green, T.G.A., Sancho, L.G., Pintado, A., Schroeter, B., 2011. Functional and spatial pressures

on terrestrial vegetation in Antarctica forced by global warming. Polar Biol. 34, 1643–1656. https://doi.org/10.1007/s00300-011-1058-2

Gutterman, W.S., Doran, P.T., Virginia, R.A., Barrett, J.E., Myers, K.F., Tulaczyk, S.M., Foley, N.T., Mikucki, J.A., Dugan, H.A., Grombacher, D.J., Bording, T.S., Auken, E., 2023. Causes and characteristics of electrical resistivity variability in shallow (<4 m) soils in Taylor Valley, east Antarctica. J. Geophys. Res. Earth Surf. 128. https://doi.org/10.1029/2022jf006696

Hao, C., Chen, T.-W., Wu, Y., Chang, L., Wu, D., 2020. Snow microhabitats provide food resources for winter-active Collembola. Soil Biol. Biochem. 143, 107731. https://doi.org/10.1016/j.soilbio.2020.107731

Hijmans, R.J., 2023. raster: Geographic Data Analysis and Modeling. R package version 3.6-20. https://CRAN.R-project.org/package=raster

Hosmer, D.W. and Lemeshow, S., 2000. Applied Logistic Regression. 2nd Ed, Chapter 5. John Wiley and Sons, New York, NY, pp. 160-164. https://doi.org/10.1002/0471722146

Hui, R., Zhao, R., Liu, L., Li, X., 2022. Effect of snow cover on water content, carbon and nutrient availability, and microbial biomass in complexes of biological soil crusts and subcrust soil in the desert. Geoderma 406, 115505. https://doi.org/10.1016/j.geoderma.2021.115505

Kappen, L., 1985. Vegetation and ecology of ice-free areas of Northern Victoria Land, Antarctica. Polar Biol. 4, 227–236. https://doi.org/10.1007/BF00999767

Kappen, L., Breuer, M., 1991. Ecological and physiological investigations in continental Antarctic cryptogams II. Moisture relations and photosynthesis of lichens near Casey Station, Wilkes Land. Antarct. Sci. 3, 273–278. https://doi.org/10.1017/S0954102091000330

Kappen, L., Meyer, M., Bölter, M., 1990. Ecological and Physiological Investigations in Continental Antarctic Cryptogams: I. Vegetation Pattern and its Relation to Snow Cover on a Hill Near Casey Station, Wilkes Land. Flora 184, 209–220. https://doi.org/10.1016/S0367-2530(17)31612-2

Kennedy, A.D., 1993. Water as a Limiting Factor in the Antarctic Terrestrial Environment: A Biogeographical Synthesis. Arct. Alp. Res. 25, 308–315. https://doi.org/10.2307/1551914

Knepel, K., 2003. Determination of Nitrate in 2M KCl soil extracts by Flow Injection Analysis.

QuikChem Method 12-107-04-1-B. Lachat Instruments, Loveland, CO.

Kohler, T.J., Stanish, L.F., Crisp, S.W., Koch, J.C., Liptzin, D., Baeseman, J.L., McKnight, D.M., 2015. Life in the Main Channel: Long-Term Hydrologic Control of Microbial Mat Abundance in McMurdo Dry Valley Streams, Antarctica. Ecosystems 18, 310–327. https://doi.org/10.1007/s10021-014-9829-6

Kohler, T.J., Stanish, L.F., Liptzin, D., Barrett, J.E., McKnight, D.M., 2018. Catch and release: Hyporheic retention and mineralization of N-fixing Nostoc sustains downstream microbial mat biomass in two polar desert streams. Limnology and Oceanography Letters 3, 357–364. https://doi.org/10.1002/lol2.10087

Kuentz, L., Levy, J., Salvatore, M., 2022. Timing and duration of ephemeral Antarctic water tracks and wetlands using high temporal–resolution satellite imagery, high spatial–resolution satellite imagery, and ground-based sensors in the McMurdo Dry Valleys. Arct. Antarct. Alp. Res. 54, 538–561. https://doi.org/10.1080/15230430.2022.2123858

Ladrón de Guevara, M., Maestre, F.T., 2022. Ecology and responses to climate change of biocrust-forming mosses in drylands. J. Exp. Bot. 73, 4380–4395. https://doi.org/10.1093/jxb/erac183

Levy, J.S., 2013. How big are the McMurdo Dry Valleys? Estimating ice-free area using Landsat image data. Antarct. Sci. 25, 119–120. https://doi.org/10.1017/S0954102012000727

Levy, J.S., Fountain, A.G., Gooseff, M.N., Barrett, J.E., Vantreese, R., Welch, K.A., Berry Lyons, W., Nielsen, U.N., Wall, D.H., 2014. Water track modification of soil ecosystems in the Lake Hoare basin, Taylor Valley, Antarctica. Antarct. Sci. 26, 153–162. https://doi.org/10.1017/S095410201300045X

Levy, J.S., Fountain, A.G., Gooseff, M.N., Welch, K.A., Lyons, W.B., 2011. Water tracks and permafrost in Taylor Valley, Antarctica: Extensive and shallow groundwater connectivity in a cold desert ecosystem. Bulletin of the Geological Society of America 123, 2295–2311. https://doi.org/10.1130/B30436.1

Levy, J.S., Schmidt, L.M., 2016. Thermal properties of Antarctic soils: wetting controls subsurface thermal state. Antarct. Sci. 28, 361–370. https://doi.org/10.1017/S0954102016000201

Levy, J.S., Fountain, A.G., Obryk, M.K., Telling, J., Glennie, C., Pettersson, R., Gooseff, M.,

Van Horn, D.J., 2018. Decadal topographic change in the McMurdo Dry Valleys of Antarctica: Thermokarst subsidence, glacier thinning, and transfer of water storage from the cryosphere to the hydrosphere. Geomorphology 323, 80–97. https://doi.org/10.1016/j.geomorph.2018.09.012

Liaw A. and Wiener M., 2002. Classification and Regression by randomForest. R News 2(3), 18--22. http://CRAN.R-project.org/doc/Rnews/

McKnight, D.M., Niyogi, D.K., Alger, A.S., Bomblies, A., Conovitz, P.A., Tate, C.M., 1999. Dry Valley Streams in Antarctica: Ecosystems Waiting for Water. Bioscience 49, 985–995. https://doi.org/10.1525/bisi.1999.49.12.985

Myers, M.E., Doran, P.T., Myers, K.F., 2022. Valley-floor snowfall in Taylor Valley, Antarctica, from 1995 to 2017: spring, summer and autumn. Antarct. Sci. 34, 325–335. https://doi.org/10.1017/S0954102022000256

Nielsen, E.B., Katurji, M., Zawar-Reza, P., Meyer, H., 2023. Extreme temperature events for the past 19 years in the McMurdo Dry Valleys, Antarctica linked to mesoscale meteorological variability. EGU General Assembly 2023, Vienna, Austria, 24-28 Apr 2023, EGU23-8805. https://doi.org/10.5194/egusphere-egu23-8805

Nylen, T.H., Fountain, A.G., Doran, P.T., 2004. Climatology of katabatic winds in the McMurdo dry valleys, southern Victoria Land, Antarctica. J. Geophys. Res. 109, D03114. https://doi.org/10.1029/2003JD003937

Obryk, M.K., Doran, P.T., Fountain, A.G., Myers, M., McKay, C.P., 2020. Climate From the McMurdo Dry Valleys, Antarctica, 1986–2017: Surface Air Temperature Trends and Redefined Summer Season. J. Geophys. Res. D: Atmos. 125, e2019JD032180. https://doi.org/10.1029/2019JD032180

Pannewitz, S., Green, T.G.A., Scheidegger, C., Schlensog, M., Schroeter, B., 2003. Activity pattern of the moss Hennediella heimii (Hedw.) Zand. in the Dry Valleys, Southern Victoria Land, Antarctica during the mid-austral summer. Polar Biol. 26, 545–551. https://doi.org/10.1007/s00300-003-0518-8

Plaza, C., Zaccone, C., Sawicka, K., Méndez, A. M., Tarquis, A., Gascó, G., Heuvelink, G. B. M., Schuur, E. A. G., & Maestre, F. T., 2018. Soil resources and element stocks in drylands to face global issues. Scientific Reports, 8(1), 13788. https://doi.org/10.1038/s41598- 018- 32229- 0

Power, S.N., Salvatore, M.R., Sokol, E.R., Stanish, L.F., Borges, S.R., Adams, B.A., Barrett, J.E., 2024. Remotely characterizing photosynthetic biocrust in snowpack-fed microhabitats of Taylor Valley, Antarctica. Science of Remote Sensing. 9, 100120. https://doi.org/10.1016/j.srs.2024.100120

Power, S.N., Salvatore, M.R., Adams, B.J., Barrett, J.E., 2024. Biophysicochemical properties and hyperspectral reflectance values of biocrust and soil samples, Fryxell Basin, McMurdo Dry Valleys, Antarctica (2022). [Dataset] Environmental Data Initiative. https://doi.org/10.6073/pasta/c6d439ab28cea276054771c748e14d67

Power, S.N., Salvatore, M.R., Sokol, E.R., Stanish, L.F., Barrett, J.E., 2020. Estimating microbial mat biomass in the McMurdo Dry Valleys, Antarctica using satellite imagery and ground surveys. Polar Biol. 43, 1753–1767. https://doi.org/10.1007/s00300-020-02742-y

Prokopy, W.R., 1995. Phosphorus in 0.5 M sodium bicarbonate soil extracts. QuikChem Method 12-115-01-1-B. Lachat Instruments, Milwaukee, WI.

Prăvălie, R., 2016. Drylands extent and environmental issues. A global approach. Earth-Science Reviews, 161, 259–278. https://doi.org/10.1016/j.earsc irev.2016.08.003

Qiu, D., Bowker, M.A., Xiao, B., Zhao, Y., Zhou, X., Li, X., 2023. Mapping biocrust distribution in China's drylands under changing climate. Sci. Total Environ. 905, 167211. https://doi.org/10.1016/j.scitotenv.2023.167211

R Core Team, 2021. R: A language and environment for statistical computing. R Foundation for Statistical Computing, Vienna, Austria. https://www.R-project.org

Reed, S.C., Maestre, F.T., Ochoa-Hueso, R., Kuske, C.R., Darrouzet-Nardi, A., Oliver, M., Darby, B., Sancho, L.G., Sinsabaugh, R.L., Belnap, J., 2016. Biocrusts in the Context of Global Change, in: Weber, B., Büdel, B., Belnap, J. (Eds.), Biological Soil Crusts: An Organizing Principle in Drylands. Springer International Publishing, Cham, pp. 451–476. https://doi.org/10.1007/978-3-319-30214-0_22

Robinson, S.A., Wasley, J., Tobin, A.K., 2003. Living on the edge – plants and global change in continental and maritime Antarctica. Glob. Chang. Biol. 9, 1681–1717. https://doi.org/10.1046/j.1365-2486.2003.00693.x

Robinson, S.A., King, D.H., Bramley-Alves, J., Waterman, M.J., Ashcroft, M.B., Wasley, J., Turnbull, J.D., Miller, R.E., Ryan-Colton, E., Benny, T., Mullany, K., Clarke, L.J., Barry,

L.A., Hua, Q., 2018. Rapid change in East Antarctic terrestrial vegetation in response to regional drying. Nat. Clim. Chang. 8, 879–884. https://doi.org/10.1038/s41558-018-0280-0

Rodriguez-Caballero, E., Belnap, J., Büdel, B., Crutzen, P.J., Andreae, M.O., Pöschl, U., Weber, B., 2018. Dryland photoautotrophic soil surface communities endangered by global change. Nat. Geosci. 11, 185–189. https://doi.org/10.1038/s41561-018-0072-1

Salvatore, M.R., Barrett, J.E., Fackrell, L.E., Sokol, E.R., Levy, J.S., Kuentz, L.C., Gooseff, M.N., Adams, B.J., Power, S.N., Knightly, J.P., Matul, H.M., Szutu, B., Doran, P.T., 2023. The Distribution of Surface Soil Moisture over Space and Time in Eastern Taylor Valley, Antarctica. Remote Sensing 15, 3170. https://doi.org/10.3390/rs15123170

Salvatore, M.R., Barrett, J.E., Borges, S.R., Power, S.N., Stanish, L.F., Sokol, E.R., Gooseff, M.N., 2021. Counting Carbon: Quantifying Biomass in the McMurdo Dry Valleys through Orbital & Field Observations. Int. J. Remote Sens. 42, 8597–8623. https://doi.org/10.1080/01431161.2021.1981559

Salvatore, M.R., Borges, S.R., Barrett, J.E., Sokol, E.R., Stanish, L.F., Power, S.N., Morin, P., 2020. Remote characterization of photosynthetic communities in the Fryxell basin of Taylor Valley, Antarctica. Antarct. Sci. 1–16. https://doi.org/10.1017/S0954102020000176

Salvatore, M.R., 2015. High-resolution compositional remote sensing of the Transantarctic Mountains: application to the WorldView-2 dataset. Antarct. Sci. 27, 473–491. https://doi.org/10.1017/S095410201500019X

Sancho, L. G., Pintado, A., Navarro, F., Ramos, M., De Pablo, M. A., Blanquer, J. M., Raggio, J., Valladares, F., & Green, T. G. A., 2017. Recent warming and cooling in the Antarctic Peninsula region has rapid and large effects on lichen vegetation. Scientific Reports, 7(1), 5689. https://doi. org/10.1038/s41598-017-05989-4

Schimel, D.S., 2010. Climate. Drylands in the Earth system. Science. https://doi.org/10.1126/science.1184946

Schimel, J.P., Bilbrough, C., Welker, J.M., 2004. Increased snow depth affects microbial activity and nitrogen mineralization in two Arctic tundra communities. Soil Biol. Biochem. 36, 217–227. https://doi.org/10.1016/j.soilbio.2003.09.008

Schlaepfer, D.R., Bradford, J.B., Lauenroth, W.K., Munson, S.M., Tietjen, B., Hall, S.A.,

Wilson, S.D., Duniway, M.C., Jia, G., Pyke, D.A., Lkhagva, A., Jamiyansharav, K., 2017. Climate change reduces extent of temperate drylands and intensifies drought in deep soils. Nat. Commun. 8, 14196. https://doi.org/10.1038/ncomms14196

Schwarz, A.M.J., Green, T.G.A., Seppelt, R.D., 1992. Terrestrial vegetation at Canada Glacier, Southern Victoria Land, Antarctica. Polar Biol. 12, 397–404. https://doi.org/10.1007/BF00243110

Siegert, M., Atkinson, A., Banwell, A., Brandon, M., Convey, P., Davies, B., Downie, R., Edwards, T., Hubbard, B., Marshall, G., Rogelj, J., Rumble, J., Stroeve, J., Vaughan, D., 2019. The Antarctic Peninsula Under a 1.5°C Global Warming Scenario. Front. Environ. Sci. Eng. China 7. https://doi.org/10.3389/fenvs.2019.00102

Stone, M.S., Devlin, S.P., Hawes, I., Welch, K.A., Gooseff, M.N., Takacs-Vesbach, C.D., Morgan-Kiss, R.M., Adams, B.J., Barrett, J.E., Priscu, J.C., Doran, P.T., 2024. McMurdo Dry Valley lake edge 'moats': the ecological intersection between terrestrial and aquatic polar desert habitats. Antarct. Sci. 1–17. https://doi.org/10.1017/S0954102024000087

Tarca, G., Guglielmin, M., Convey, P., Worland, M.R., Cannone, N., 2022. Small-scale spatial–temporal variability in snow cover and relationships with vegetation and climate in maritime Antarctica. Catena 208, 105739. https://doi.org/10.1016/j.catena.2021.105739

Thapa-Magar, K.B., Sokol, E.R., Gooseff, M.N., Salvatore, M.R., Barrett, J.E., Levy, J.S., Knightly, P., Power, S.N., *In review*. Remote sensing for species distribution models: An illustration from a sentinel taxon of the world's driest ecosystem.

Turner, J., Phillips, T., Thamban, M., Rahaman, W., Marshall, G.J., Wille, J.D., Favier, V., Winton, V.H.L., Thomas, E., Wang, Z., Broeke, M., Hosking, J.S., Lachlan-Cope, T., 2019. The dominant role of extreme precipitation events in antarctic snowfall variability. Geophys. Res. Lett. 46, 3502–3511. https://doi.org/10.1029/2018gl081517

Vignon, É., Roussel, M.-L., Gorodetskaya, I.V., Genthon, C., Berne, A., 2021. Present and future of rainfall in Antarctica. Geophys. Res. Lett. 48. https://doi.org/10.1029/2020gl092281

Wall, D.H., 2007. Global change tipping points: above- and below-ground biotic interactions in a low diversity ecosystem. Philos. Trans. R. Soc. Lond. B Biol. Sci. 362, 2291–2306. https://doi.org/10.1098/rstb.2006.1950

Walthert, L., Graf, U., Kammer, A., Luster, J., Pezzotta, D., Zimmermann, S., Hagedorn, F.,

2010. Determination of organic and inorganic carbon, δ 13 C, and nitrogen in soils containing carbonates after acid fumigation with HCl. J. Plant Nutr. Soil Sci. 173, 207–216. https://doi.org/10.1002/jpln.200900158

Weber, B., Belnap, J., Büdel, B., Antoninka, A.J., Barger, N.N., Chaudhary, V.B., Darrouzet-Nardi, A., Eldridge, D.J., Faist, A.M., Ferrenberg, S., Havrilla, C.A., Huber-Sannwald, E., Malam Issa, O., Maestre, F.T., Reed, S.C., Rodriguez-Caballero, E., Tucker, C., Young, K.E., Zhang, Y., Zhao, Y., Zhou, X., Bowker, M.A., 2022. What is a biocrust? A refined, contemporary definition for a broadening research community. Biol. Rev. Camb. Philos. Soc. 97, 1768–1785. https://doi.org/10.1111/brv.12862

Wetzel, R.G., 1983. Limnology, 2nd ed. Saunders College Publishing, Philadelphia, Pennsylvania, USA.

Wright, A., Gooseff, M., Bergstrom, A., & Welch, K. (2024). The hydrologic and geochemical contributions from snow to streamflow in the McMurdo Dry Valleys of Antarctica. Hydrological Processes, 38(6), e15195. https://doi.org/10.1002/ hyp.15195

Yang, Y., Liu, W., Adams, J.M., Song, B., 2023. Snow-cover loss attenuates the effects of N addition on desert nutrient cycling and microbial community. Front. Plant Sci. 14, 1166897. https://doi.org/10.3389/fpls.2023.1166897

Zhang, B., Zhang, Y., Zhou, X., Li, X., Zhang, Y., 2021. Snowpack shifts cyanobacterial community in biological soil crusts. J. Arid Land 13, 239–256. https://doi.org/10.1007/s40333-021-0061-x

Figures

Figure 4.1

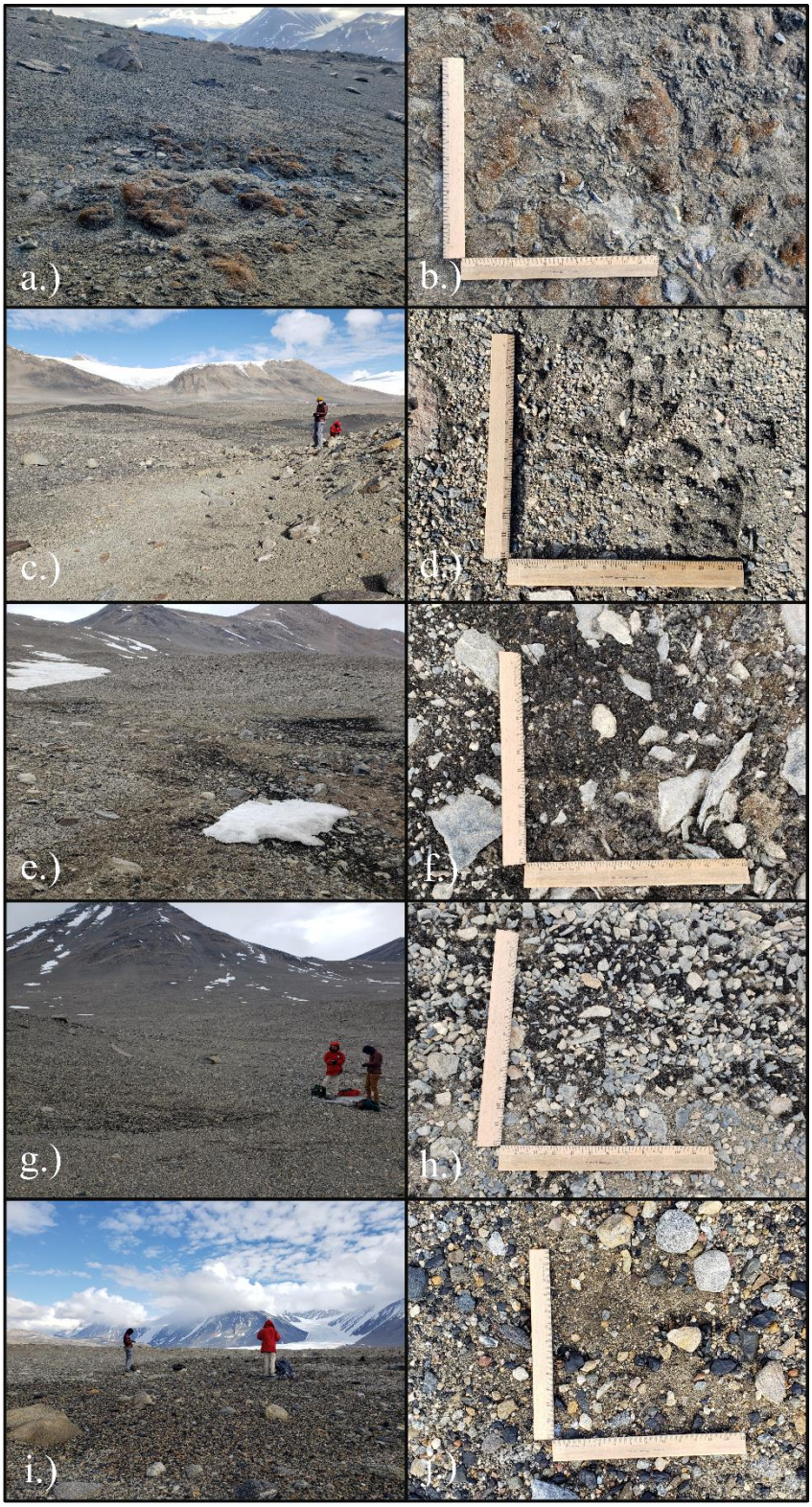

Figure 4.1. Photographs illustrating the composition and density of biocrust communities sampled. Among the represented communities are: a-d.) bryophyte-dominated biocrusts, e-h.) cyanobacteria-dominated biocrusts, and i-j.) incipient biocrusts. Landscape photographs illustrate the patchiness of the communities, and the close-up photographs include 1 ft (~ 30 cm) scales. The following sampling sites are represented: a-b.) site 64, c-d.) site 32, e-f.) site 62, g-h.) site 61, and i-j.) site 36. Photographs taken by S. Power and J. Jorna.

Figure 4.2

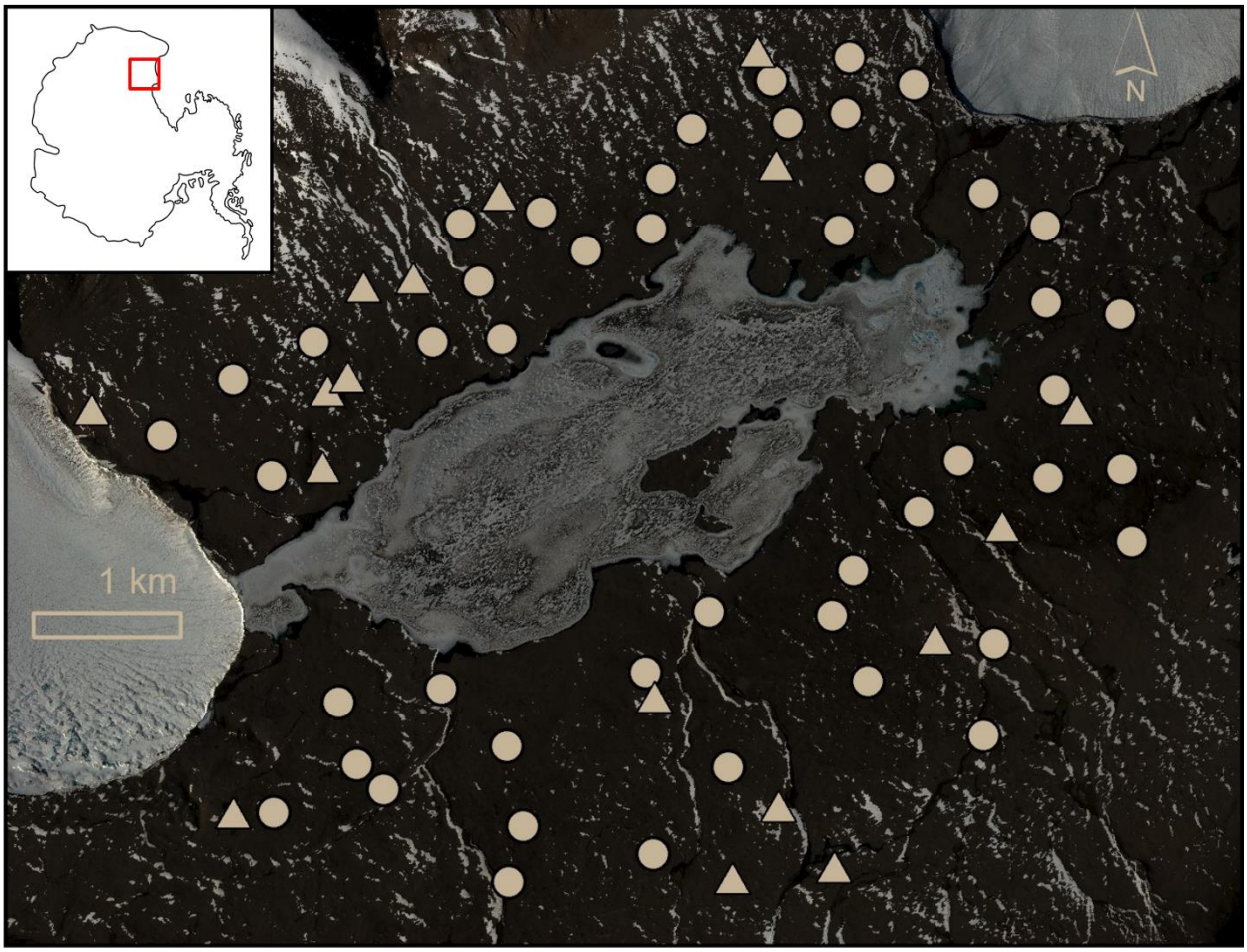

Figure 4.2. Map of Eastern Taylor Valley with 64 field sites labeled with triangles (biocrust present) and circles (biocrust absent). Inset on the top left identifies the McMurdo Dry Valleys, Antarctica with a red square. WorldView-2 imagery (10300100CB9F3900), bands 5 (red), 3 (green), and 2 (blue) © Dec 21 2021 Maxar Technologies, Inc.

Figure 4.3

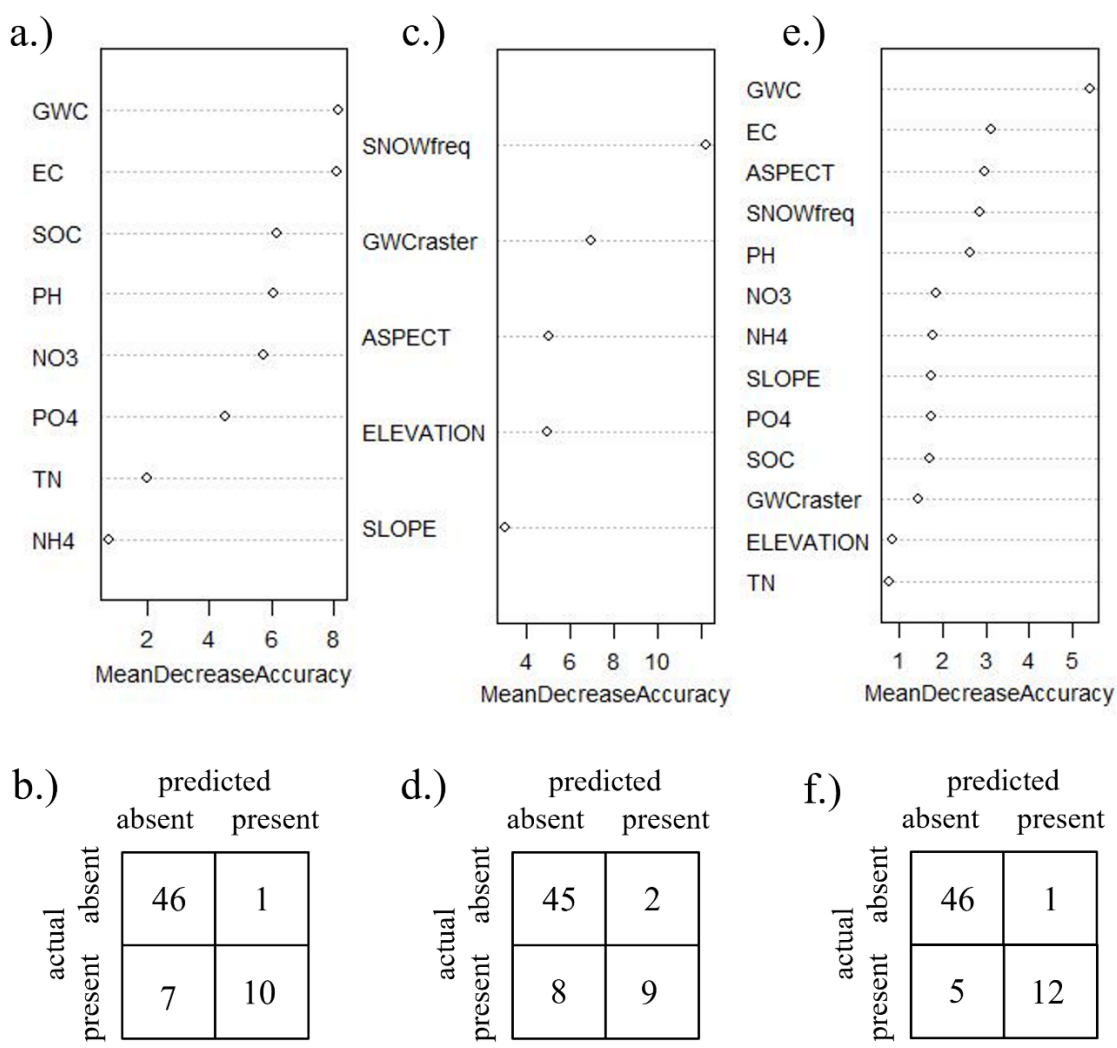

Figure 4.3. Variable importance (illustrated by mean decrease in accuracy) and confusion matrices for random forest models predicting biocrust presence/absence using a, b.) field survey variables, c, d.) geospatial raster variables as predictors, and e, f.) both field survey and geospatial raster variables. The field survey model a, b.) had an overall accuracy of 87.5% and AUC of 0.86. The geospatial model c, d.) had an overall accuracy of 84% and AUC of 0.80. The hybrid model e, f.) had an overall accuracy of 91% and AUC of 0.89. Confusion matrices for the b.) field survey model, d.) geospatial raster model, and f.) hybrid model have class errors for absent and present as follows: 2.1 and 41%, 4.2 and 47%, and 2.1 and 29%.

Figure 4.4

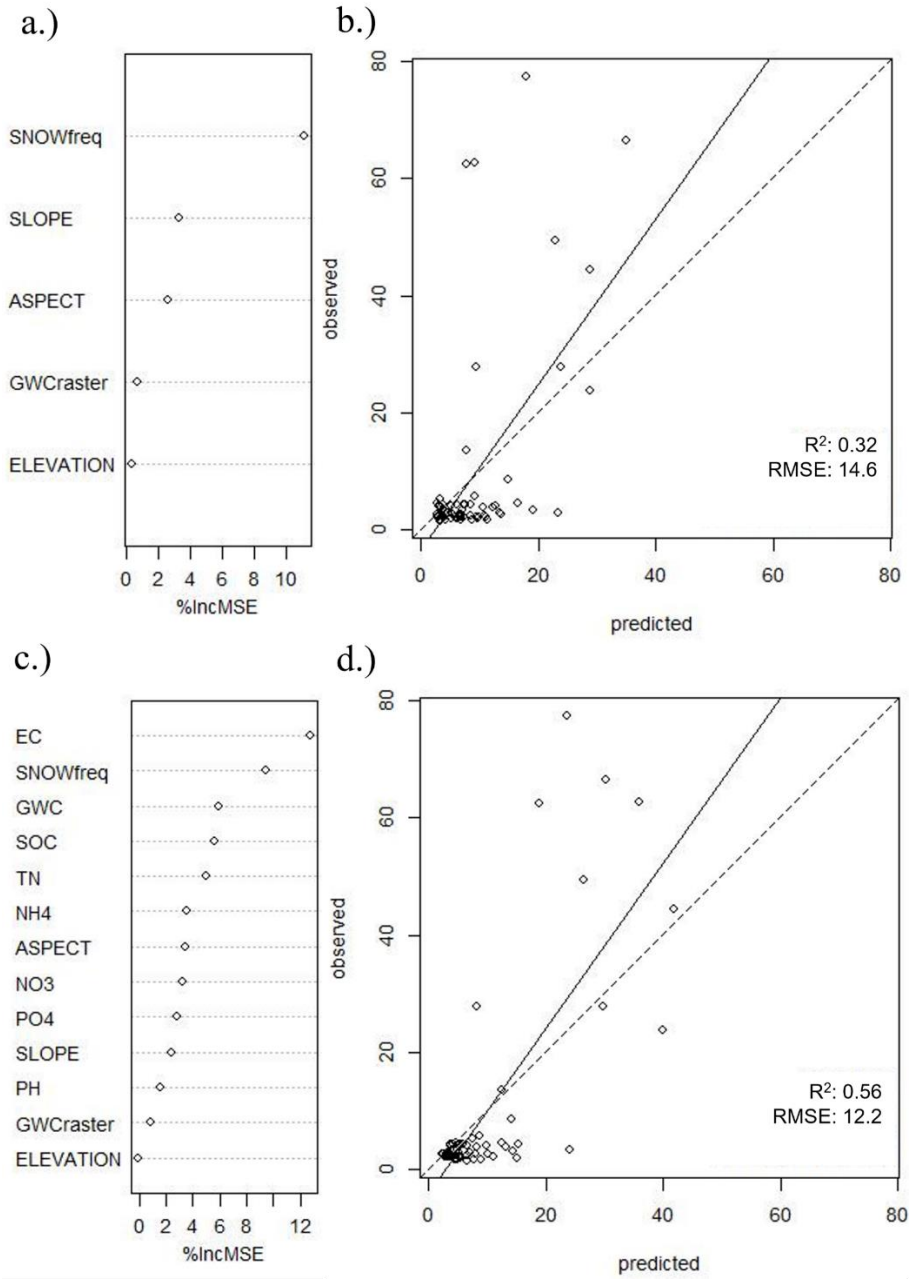

Figure 4.4. Variable importance (illustrated by percent increase in mean square error, MSE) and predicted versus observed plots for random forest models predicting biocrust AFDM using a, b.) geospatial raster variables and c, d.) both field survey and geospatial raster variables as predictors. The geospatial model a, b.) had an R^2 of 0.32 and root mean square error (RMSE) of 14.6. The hybrid model c, d.) had an R^2 of 0.56 and RMSE of 12.2.

Figure 4.5

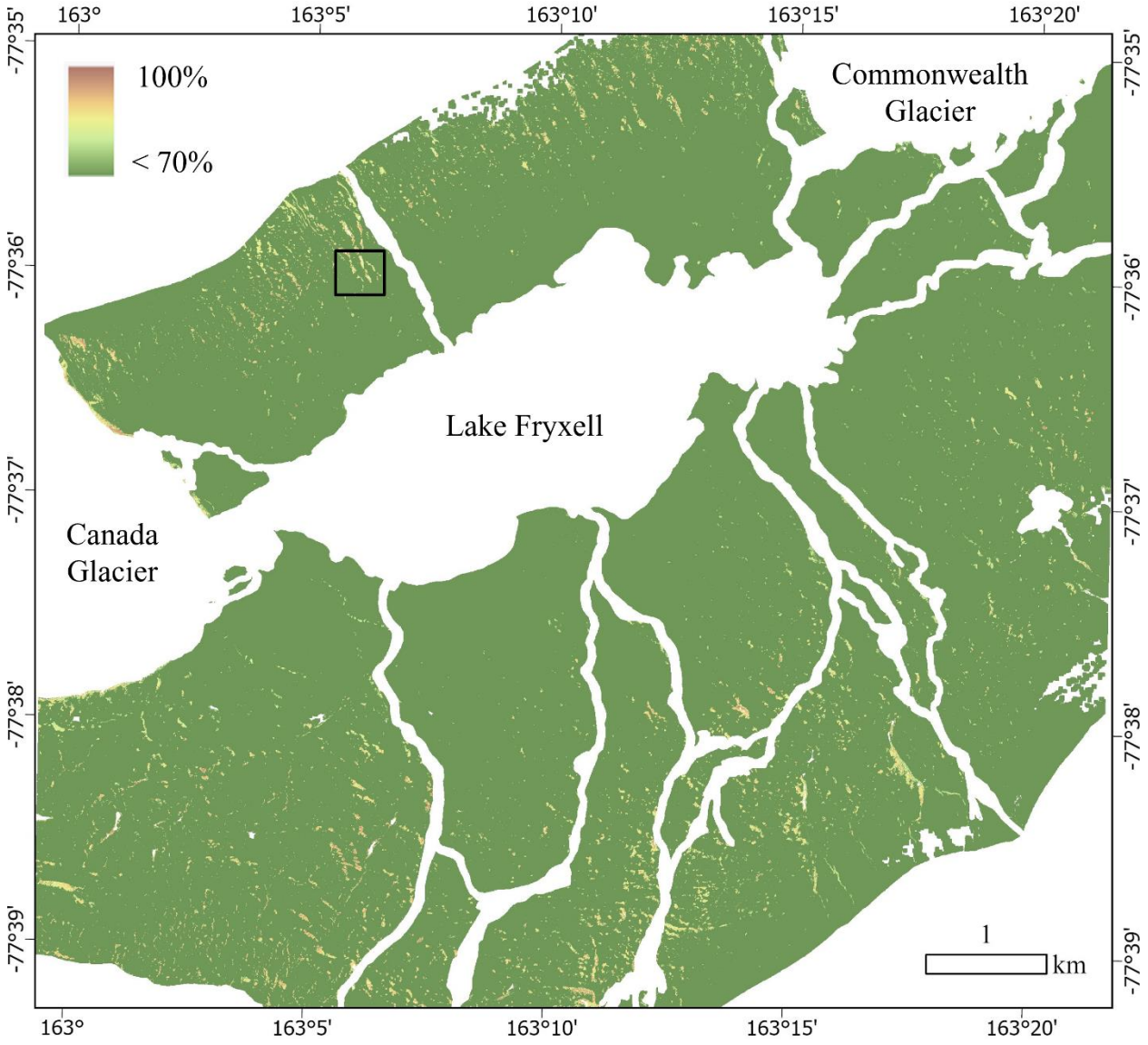

Figure 4.5. Probability surface map for presence of biocrust in the Lake Fryxell basin, Antarctica. The range of probabilities present here illustrates areas of highest (> 70%) probability of biocrust occurrence. Areas shown in white are beyond the spatial limits of the input rasters or are areas masked out (glaciers, lake, streams, and perennial snow) to focus on the terrestrial landscape where biocrusts occur. Black square indicates location of Figure 4.6.

Figure 4.6

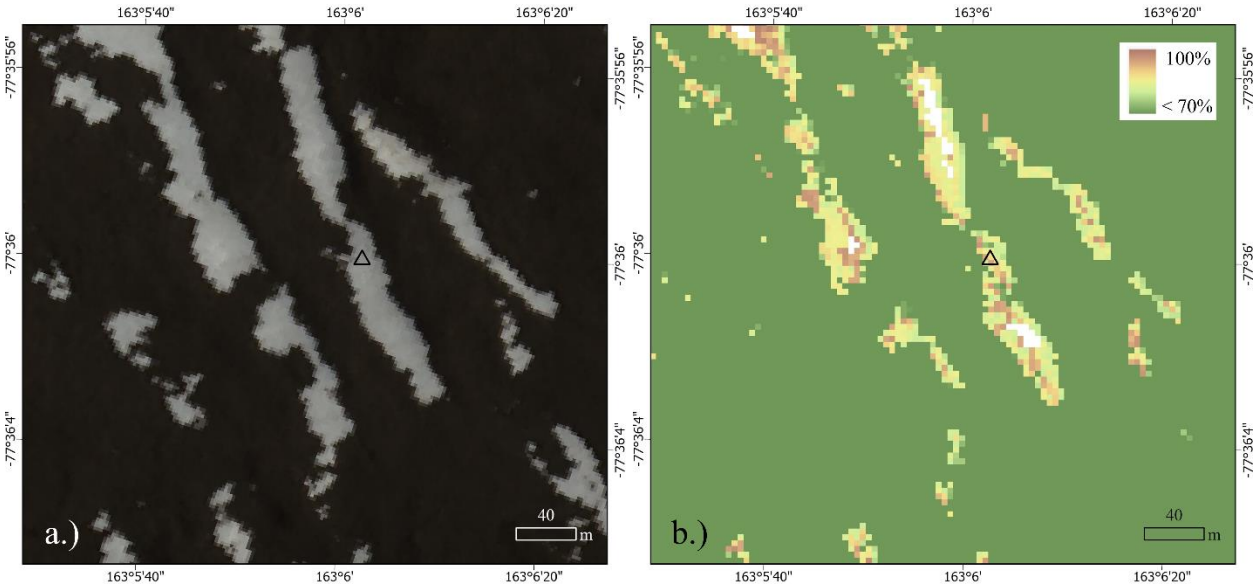

Figure 4.6. Two images of identical location in the Lake Fryxell basin, Antarctica. a.) Close up true-color image showing seasonal snow patches, WorldView-2 imagery (10300100CB9F3900) bands 5 (red), 3 (green), and 2 (blue) © Dec 21 2021 Maxar Technologies, Inc., and b.) Close-up image of the probability surface map for presence of biocrust. The range of probabilities present here illustrates areas of highest (> 70%) probability of biocrust occurrence. Areas shown in white are pixels containing perennial snow cover which required exclusion. Black triangle denotes one of the sampling sites (site 62) containing dense biocrust cover located around snow patch features.

Tables

Table 4.1. Description of the 17 biocrust sites, including their location given by latitude and longitude in decimal degrees, organic matter content as AFDM, and short description of composition based upon field observation and visual assessment.

Site ID	Latitude	Longitude	AFDM (mg cm^{-2})	Dominant Composition	Description
21	-77.60833	163.00967	2.9	cyanobacteria	incipient
23	-77.6116	163.07574	2.6	cyanobacteria	incipient
24	-77.60693	163.07674	23.8	bryophyte	sparse colonies
25	-77.60056	163.08643	4.4	cyanobacteria	incipient
26	-77.59479	163.12459	27.9	bryophyte	dark moss, orange lichen
32	-77.61436	163.26944	66.5	bryophyte	dark moss, nostoc
33	-77.62132	163.25098	13.6	cyanobacteria	light colored
35	-77.63176	163.20731	3.9	cyanobacteria	incipient, hypoliths
36	-77.6362	163.19463	8.6	cyanobacteria	incipient, filaments
37	-77.62522	163.17142	4.4	cyanobacteria	incipient
46	-77.58572	163.19687	49.4	bryophyte	dark moss, yellow/orange lichen
55	-77.63538	163.22357	27.9	cyanobacteria	nostoc
60	-77.6328	163.05199	4.5	cyanobacteria	light colored
61	-77.60608	163.0824	62.7	cyanobacteria	nostoc, dark moss
62	-77.59998	163.1006	44.5	cyanobacteria	nostoc
63	-77.59262	163.20291	62.3	bryophyte	dark moss, orange lichen
64	-77.60715	163.28993	77.3	bryophyte	red moss, nostoc

Table 4.2. Median soil physical and biochemical properties and standard error of the median from each of the 64 sites (n = 17 biocrust present sites, n = 47 biocrust absent sites). GWC as gravimetric water content, EC as electrical conductivity, AFDM as ash-free dry mass, SOC as soil organic carbon, and TN as total nitrogen. Wilcoxon Rank Sum p-values shown based on the medians.

	Median of Biocrust Present Sites	**Median of Biocrust Absent Sites**	**Wilcoxon Rank Sum p-value**
GWC (g/g)	0.08 ± 0.02	0.02 ± 0.01	< 0.0001
pH	8.24 ± 0.20	9.43 ± 0.13	< 0.001
EC ($\mu S\ cm^{-1}$)	167 ± 1127	722 ± 403	< 0.01
AFDM ($g\ m^{-2}$)	238 ± 80	24 ± 2	< 0.0001
Chlorophyll-a ($\mu g\ cm^{-2}$)	0.9 ± 1.0	0.0 ± 0.001	< 0.0001
Carotenoid ($\mu g\ cm^{-2}$)	3.3 ± 1.4	0.03 ± 0.002	< 0.0001
Scytonemin ($\mu g\ cm^{-2}$)	50.7 ± 39.1	0.4 ± 0.1	< 0.0001
NH_4^+ ($\mu g\ N\ g^{-1}$ dry soil)	0.1 ± 0.08	0.1 ± 0.05	0.67
NO_3^- ($\mu g\ N\ g^{-1}$ dry soil)	0.8 ± 38	6.3 ± 8	< 0.05
PO_4^{3-} ($\mu g\ P\ g^{-1}$ dry soil)	1.7 ± 0.6	2.8 ± 0.9	< 0.05
SOC ($g\ C\ m^{-2}$)	147 ± 81	75 ± 7.7	< 0.01
TN ($g\ TN\ m^{-2}$)	22 ± 14	21 ± 2.3	0.33

Supplemental Text

Regression and classification learner performance

Our field survey data and their residuals were not normally distributed and therefore we chose a nonparametric modeling approach rather than a parametric approach. When using MATLAB's classification learner testing 40+ models, all had accuracies > 70%, with several ~ 90%, for both models containing the field survey predictors and the geospatial predictors. The 40+ models tested using MATLAB's regression learner performed adequately well (R^2 of ~ 0.70 for many models using the field survey predictors; R^2 consistently lower for models using geospatial predictors). In both cases, the random forest algorithms performed significantly well, and even though there were some models that performed better than random forest, we focused on the random forest algorithms for this study. We also chose to implement an OOB hold-out which inherently lowers accuracies. Without using an OOB technique, our model accuracies were much higher, though we have chosen to incorporate it as a way to measure prediction error.

Supplemental Figures

Figure S4.1

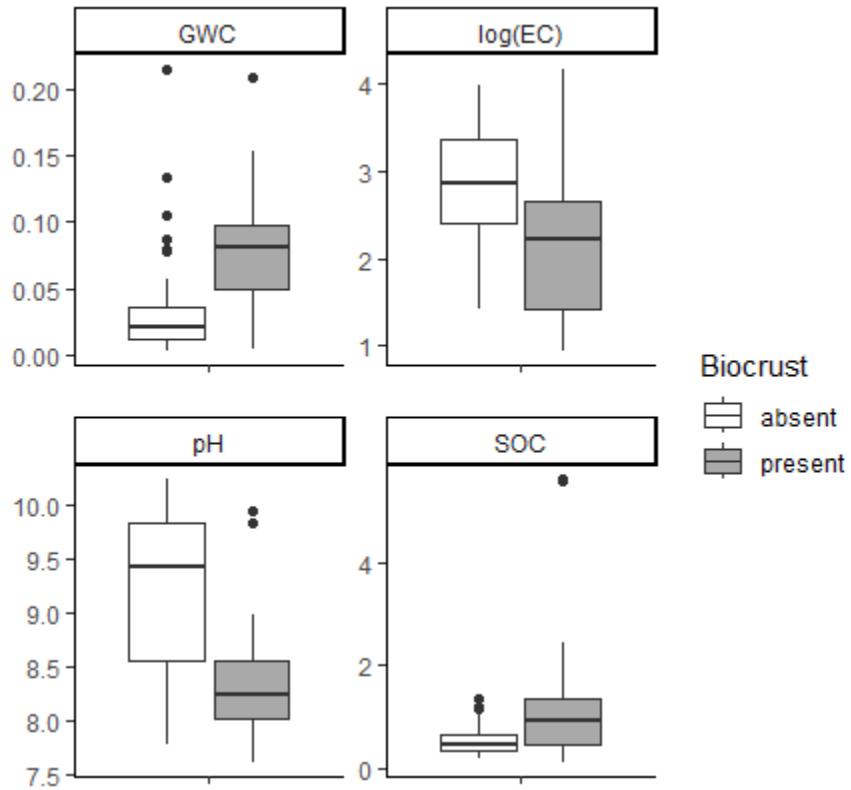

Figure S4.1. Boxplots of key soil characteristics where EC is electrical conductivity in µS cm^{-1}, GWC is gravimetric water content in g/g, and SOC is soil organic carbon in mg C g^{-1} dry soil. Separate box plots are illustrated for plots where biocrust is absent (white) and where biocrust is present (grey). Horizontal lines indicate the median, and the black circles indicate outliers defined by > 1.5 x interquartile range (IQR). The whiskers represent the largest value within 1.5 x IQR above the 75th percentile and the smallest value within 1.5 x IQR below the 25th percentile.

Figure S4.2

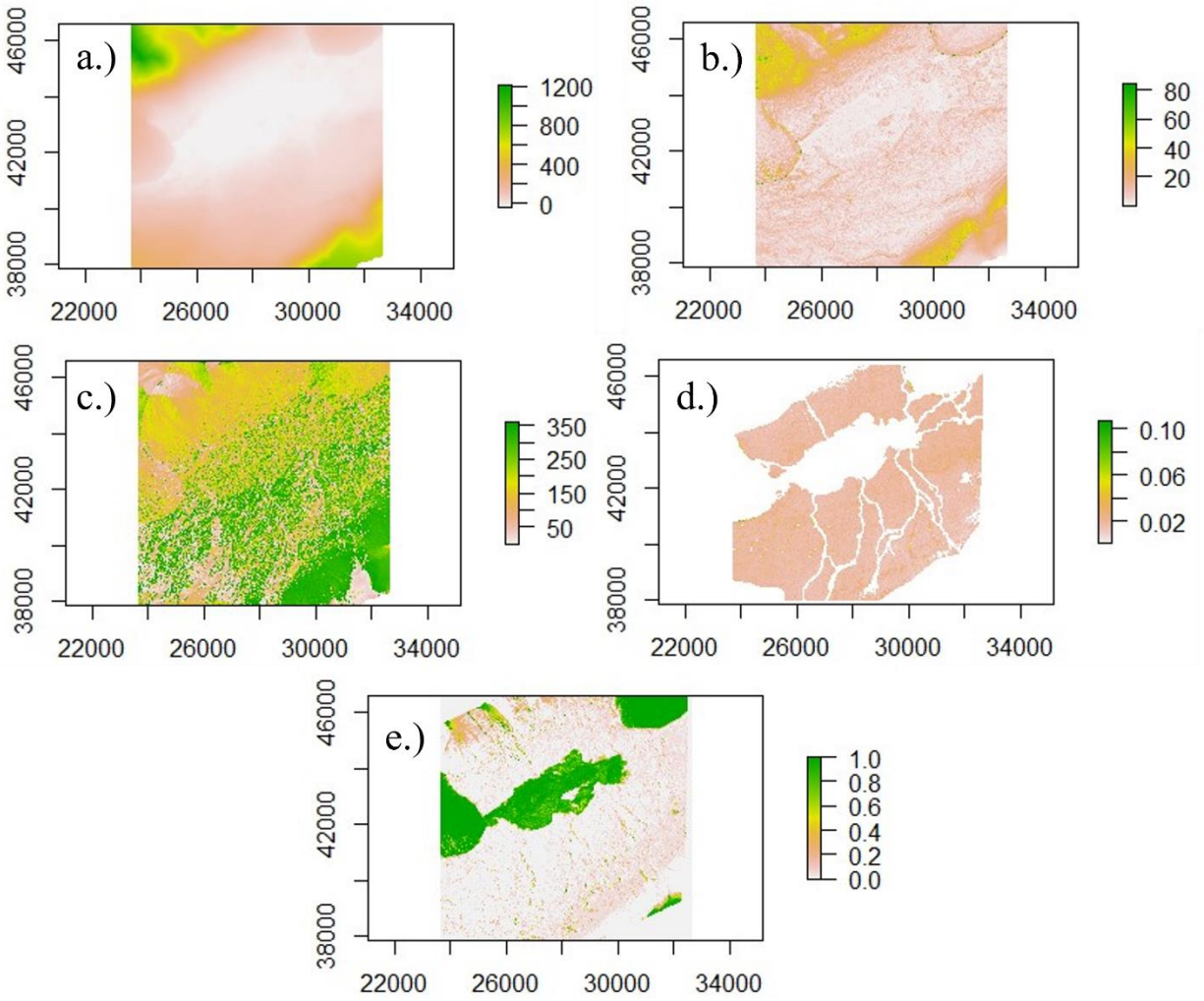

Figure S4.2. Raster images of the geospatial predictors: a.) elevation, b.) slope, c.) aspect, d.) gravimetric water content, e.) snow frequency.

Figure S4.3

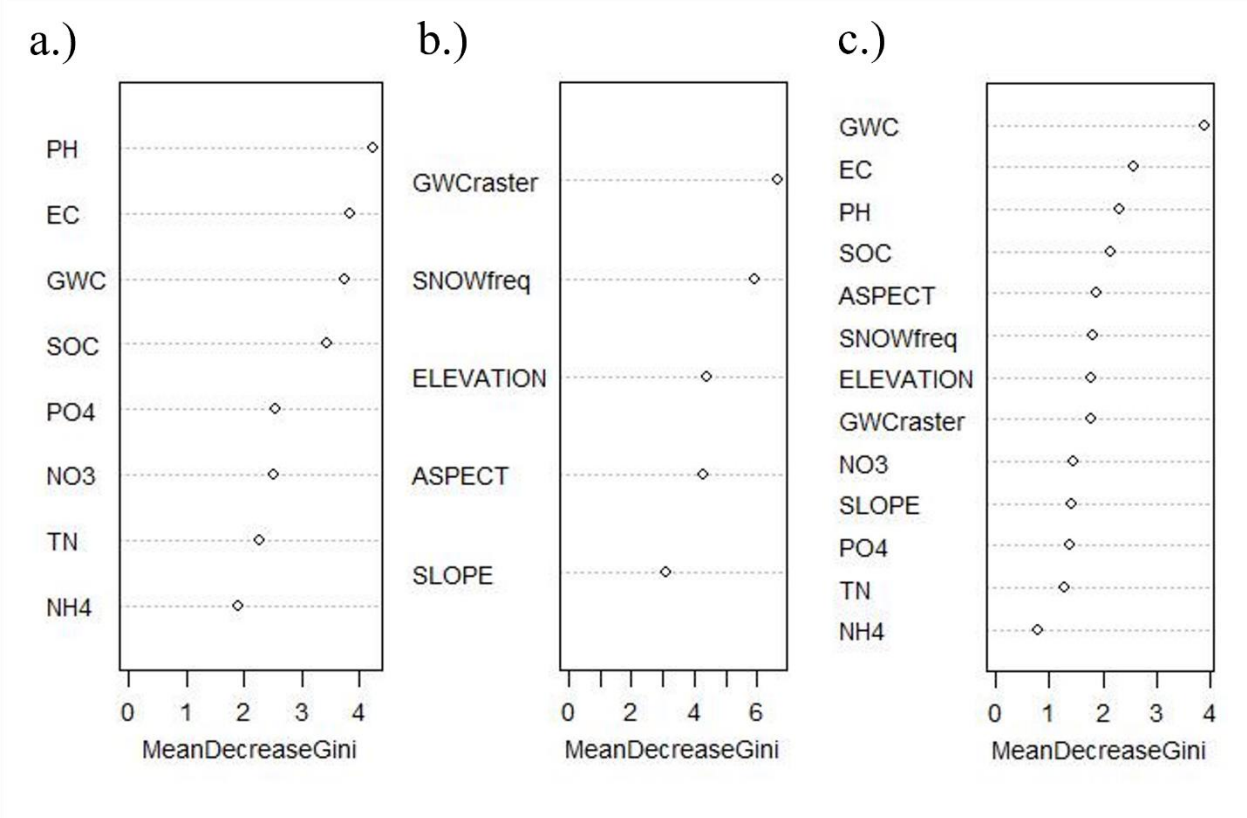

Figure S4.3. Variable importance (illustrated by mean decrease in Gini) for random forest models predicting biocrust presence/absence using a.) field survey variables, b.) geospatial raster variables, and c.) both field survey and geospatial raster variables as predictors.

Figure S4.4

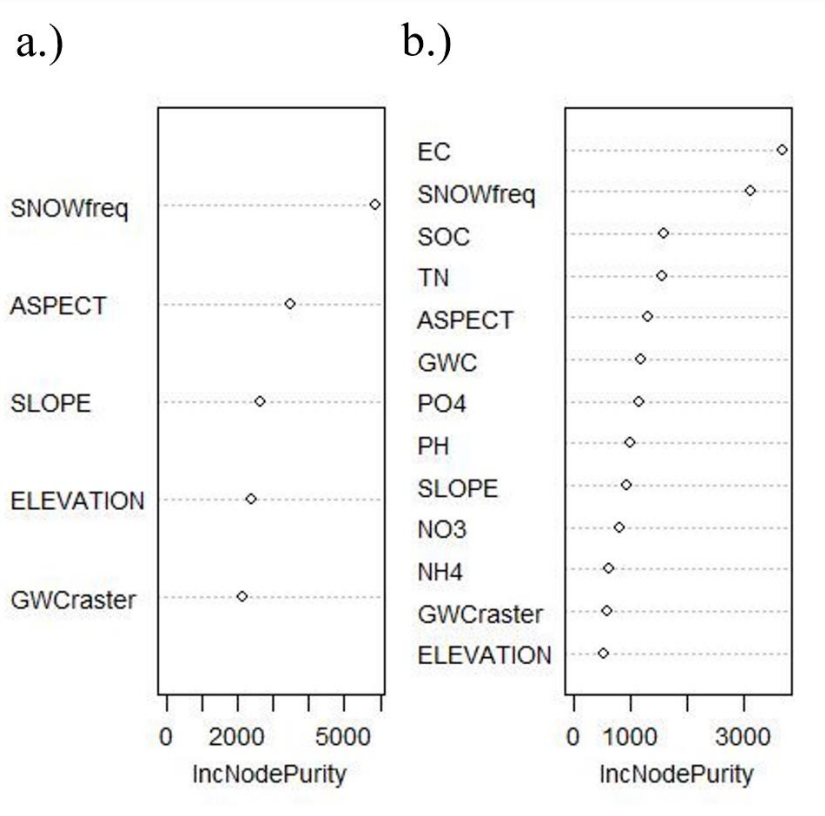

Figure S4.4. Variable importance (illustrated by increase in node purity) for random forest models predicting biocrust AFDM using a.) geospatial raster variables and b.) both field survey and geospatial raster variables as predictors.

Figure S4.5

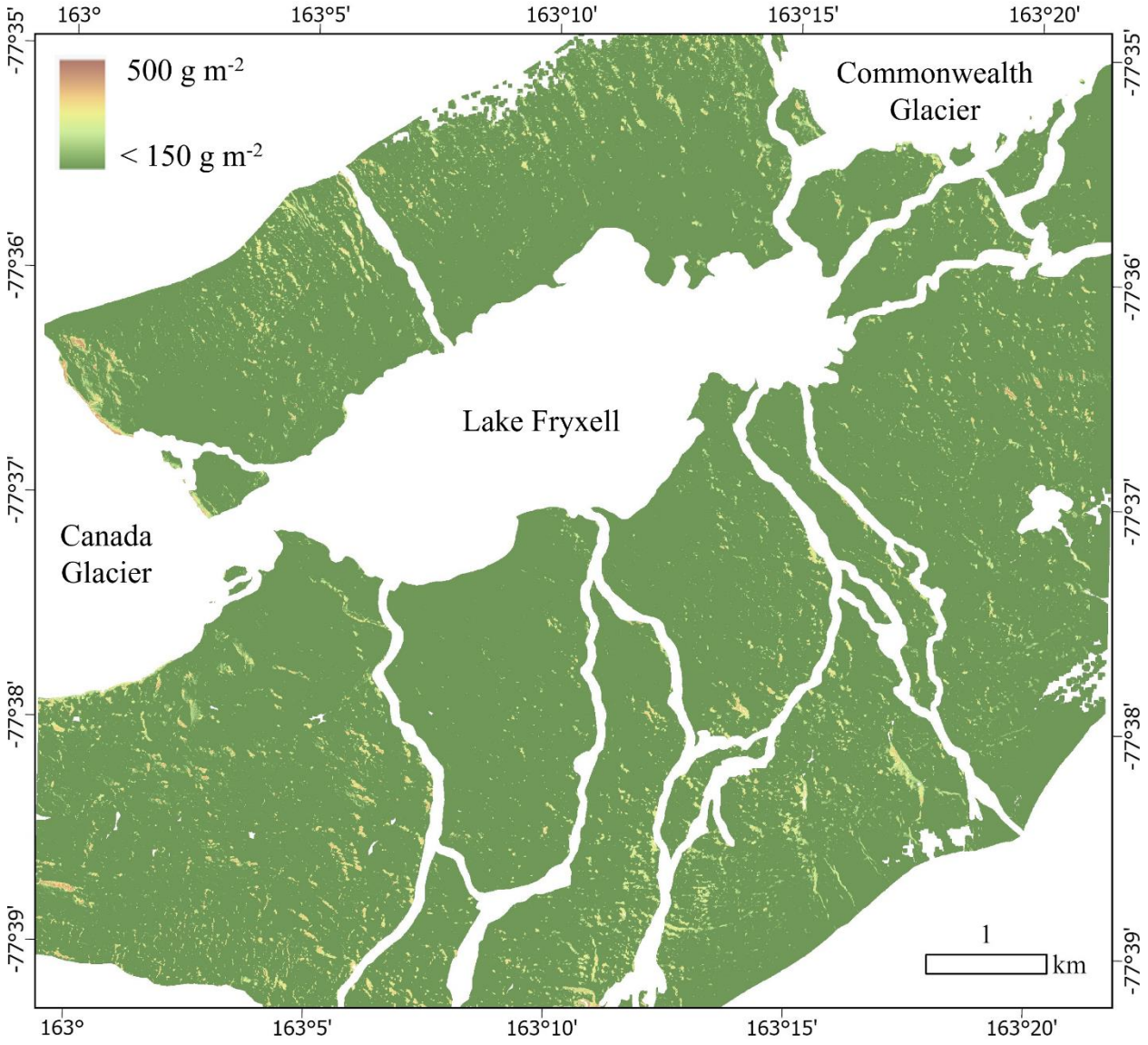

Figure S4.5. Predictive map of biocrust AFDM in the Lake Fryxell basin, Antarctica. The range of AFDM present here illustrates areas of relatively high AFDM (> 150 g m^{-2}) density. Areas shown in white are beyond the spatial limits of the input rasters or are areas masked out (glaciers, lake, streams, and perennial snow) to focus on the terrestrial landscape where biocrusts occur.

Supplemental Tables

Table S4.1. Correlation matrix using Pearson correlation coefficient (r) for all variables collected and tested in this study. All significant r values magnitude > 0.6 are indicated in bold.

	GWC	*pH*	*EC*	*AFDM*	*NH4*	*NO3*	*PO4*	*CHLA*	*CARO*	*SCYTO*	*SOC*	*TN*	*ASPECT*	*SLOPE*	*ELE-VATION*	*GWC raster*	*SNOW freq*
GWC	1																
pH	**-0.62**	1															
EC	0.23	-0.32	1														
AFDM	0.26	-0.39	-0.20	1													
NH4	0.11	-0.08	0.24	0.07	1												
NO3	0.19	-0.28	**0.90**	-0.14	0.34	1											
PO4	-0.02	0.34	0.24	-0.20	-0.11	0.16	1										
CHLA	0.25	-0.38	-0.21	**0.90**	-0.01	-0.14	-0.18	1									
CARO	0.20	-0.36	-0.20	**0.87**	0.03	-0.13	-0.19	**0.96**	1								
SCYTO	0.17	-0.34	-0.19	**0.80**	0.02	-0.12	-0.18	**0.89**	**0.96**	1							
SOC	0.34	-0.39	0.08	0.55	0.15	0.17	-0.08	**0.72**	**0.67**	**0.65**	1						
TN	0.34	-0.41	0.48	0.40	0.30	0.58	0.02	0.52	0.46	0.42	**0.86**	1					
ASPECT	-0.09	0.13	-0.08	-0.17	-0.07	-0.07	-0.14	-0.16	-0.21	-0.27	-0.16	-0.15	1				
SLOPE	-0.31	0.08	-0.14	0.19	-0.03	-0.06	-0.08	0.17	0.17	0.18	0.10	0.07	-0.06	1			
ELEVATION	0.11	-0.14	0.02	0.02	0.16	0.02	-0.31	-0.01	0.04	0.06	0.08	0.08	0.03	0.13	1		
GWCraster	0.39	-0.32	-0.10	0.21	-0.01	-0.12	-0.18	0.19	0.15	0.15	0.00	-0.04	-0.10	-0.04	0.24	1	
SNOWfreq	0.29	-0.30	-0.16	**0.68**	0.02	-0.08	-0.10	**0.69**	0.58	0.42	**0.65**	0.55	-0.11	0.17	0.05	0.09	1

CHAPTER 5 – CONCLUSION

Dissertation Summary

In this dissertation, I described how the landscape history of the McMurdo Dry Valleys has influenced the distribution and composition of microbial mats, how microbial mats have an ecological influence on the underlying soil, and how we can use remote sensing techniques to detect the distribution and abundance of biocrusts, infer their environmental drivers, and quantify their organic matter and carbon (C) content. While previous work has shown that geomorphology and hydrology drive the occurrence and composition of microbial mats in stream channel environments (Kohler et al. 2015; McKnight et al. 1999; Stanish et al. 2011), I found that legacy inorganic phosphorous (P) in the Taylor Valley soils, in part, drives microbial mat distribution and composition outside the flow-paths of perennial channelized streams (Power et al. *In Prep*). This highlights the importance of landscape history, where inorganic P content is of entirely geochemical origin from the weathering of apatite (Bate et al. 2018). In turn, the abundance of microbial mats enriches the underlying soils in nutrients, including organic C. The microbial mats contained an abundance of nitrogen (N) fixing bacteria with high numbers of *nif* and *nifH* genes, which are indicators of N-fixation potential. The microbial mats with the highest potential for N-fixation were located on the high inorganic P soils, suggesting that the abundance of inorganic P selects for active N fixers able to accumulate more biomass and organic C. This demonstrates the critical influence that microbial mats have on the structure and function of the underlying soil ecosystem.

Next, I demonstrated the utility of using remote sensing and satellite imagery to detect lower density biocrusts in the terrestrial environments of eastern Taylor Valley (Power et al. 2024a). When ground truthing my field sites, it was apparent that certain geologic features

(primarily oxidized granite) were impeding the use of commonly used vegetation indices, like the Normalized Difference Vegetation Index (NDVI; Tucker 1979). Using a hyperspectral spectrometer set up for a laboratory environment, I determined that oxidized granite has iron mineral compositions that reflect and absorb light in the same wavelengths specific to vegetation indices. Moving beyond vegetation indices, I discovered that spectral linear unmixing models better predict the distribution and abundance of biocrusts in this environment where the underlying geology is exposed. My work led to the discovery of dense biocrust communities near snow patch features, far away from the streams and lake margins that commonly host dense microbial mat communities. These biocrusts sustain a diverse community of soil organisms below (nematodes, tardigrades, and rotifers) and are enriched in soil organic C.

Finally, I discovered the environmental conditions that drive the presence/absence and abundance of biocrust communities (Power et al. 2024b). Using machine learning algorithms, I found that snow frequency, moisture content, and electrical conductivity (salinity) were the main drivers of biocrust in eastern Taylor Valley. I mapped the distribution and biomass of biocrust in this region using a series of random forest models, which provided an estimate of the surface organic matter and C content of the Lake Fryxell basin biocrust communities. Early studies of the Lake Fryxell basin determined that low elevation soil organic matter was partially derived from ancient lake sediments, representing biologically-fixed C from thousands of years prior (Burkins et al. 2000; Denton et al. 1989; Lawson et al. 2004), and it was unknown if contemporary microbial mat and biocrust communities made significant contributions to these soil ecosystems too. The research I developed in this chapter is a systematic and scalable method that has been needed to address fundamental ecological questions in this region regarding sources of terrestrial organic matter. The major finding of this study was that biocrusts are widely

distributed across the Lake Fryxell basin, contain a significant amount of C in their biomass, and enrich the underlying soils in C.

Dissertation Synthesis

My dissertation illustrates the importance of microbial mats and biocrusts on underlying soils and their overall contributions as soil organic matter, by disentangling the drivers of microbial mat and biocrust presence and the soil responses to their presence (Figure 5.1). I wanted to first assess the ecological importance of microbial mats and biocrusts, and I found that they enrich underlying soils in soil organic matter, primarily total N and soil organic C (Power et al. *In Prep*; Power et al. 2024b). Understanding the ecological importance of these communities led me to study them at an even larger scale. I determined that satellite imagery can be used to detect the presence of patchy biocrusts throughout the Lake Fryxell basin landscape, and that these communities were associated with seasonal snow patches (Power et al. 2024a). The spectral unmixing methods employed were a significant improvement from traditional vegetation indices in terms of accurately detecting biocrusts with less interference from geologic features.

Moving forward, I wanted to develop another remote sensing method for detecting biocrust with even less interference from geologic features, and I wanted to further investigate biocrusts' association with snow patches. I determined that snow frequency, moisture content, and salinity drive biocrust presence and abundance, with areas most suitable for the growth of *dense* biocrusts associated with snow patches and low salinity (Power et al. 2024b). I also estimated that biocrusts contribute between 11,000 and 72,000 kg of C to surface soil in the Lake Fryxell basin, a significant amount in this overall nutrient-limited landscape. My work contributes to an improved, systematic understanding of C budgets of this region, a fundamental

ecological question regarding primary productivity, and contributes to understanding the environmental drivers of biocrusts and microbial mats in the context of a changing climate.

Future Directions

As I was writing my dissertation, Antarctica experienced two massive heatwaves in 2022 and 2024 (Wille et al. 2023; Patel 2024). Dynamic weather events in Antarctica, like heat waves and even rainfall, are occurring more frequently (Barrett et al. 2024; Vignon et al. 2021). My research has demonstrated that snow patches are critical to the distribution of microbial mats and biocrusts and therefore, future snow dynamics and regional weather are extremely important to the survival and distribution of Antarctic vegetation. There is evidence that biocrusts and soil communities are already responding to these changing environmental conditions in other regions of Antarctica and are expected to continue responding in unknown ways due to region-specific climate variability (Colesie et al. 2023). Some regions of Antarctica have shown trends towards a warmer and wetter climate, while other regions have shown a drying trend (*e.g.*, Robinson et al. 2018; Turner et al. 2019).

In the McMurdo Dry Valleys, I predict that microbial mats and biocrusts may respond differently depending on whether the climate trends warmer and wetter or drier. For example, a warmer and wetter climate may increase available habitat for biocrusts and microbial mats. However, biocrusts depend on slow melting snow patches, and if a warmer climate resulted in faster snow melt, this could exhaust the main source of moisture for biocrusts in many habitats. Alternatively, microbial mats along streams and lakes primarily rely on the water from glacial melt and therefore have a more consistent supply of moisture, even if the climate warms considerably. I predict that a drier climate would likely reduce growth and expansion overall for both microbial mats and biocrusts. There are many caveats for predicting how biocrusts and

microbial mats may respond to a changing climate but nonetheless climate change is anticipated to impact vegetation in varying ways across Antarctica (Colesie et al. 2023).

Moving beyond my dissertation, many questions remain unanswered, and I expect many studies will continue researching Antarctic microbial mats and biocrusts. In the coming years, how has the regional climate of the McMurdo Dry Valleys changed? How are microbial mats and biocrusts responding to these changes and are their changes unique depending on their location (stream vs. soil)? Knowing the importance of microbial mats and biocrusts to the organic matter and nutrient content of the underlying soils is also critical in regards to belowground communities. For example, how will the soil fauna (*e.g.*, nematodes, tardigrades) respond to potential changes in mat and biocrust distribution? In the context of a changing climate, I recommend continued research to monitor the distribution and abundance of microbial mats and biocrusts, as well as insights into their structure and function, and their environmental drivers.

Recent studies have found that microbial mats and biocrusts are sensitive to climate change and are already impacted in many ecosystems worldwide (Finger-Higgens et al. 2022; Lingappa et al. 2022; Rodríguez-Caballero et al. 2018). For example, the loss of biocrusts in hot desert ecosystems contributed to eroded soil systems which reduced the soil stabilization necessary for plant diversity (Cantón et al. 2014). Biocrusts covered ~ 12% of Earth's terrestrial surface in 2018 and are expected to decrease by 25 – 40% by 2080. In the coming years, how has the distribution of biocrusts changed globally? How has their distribution altered the ecology of vascular plants, and has desertification and dust storms increased due to biocrust loss? What remediation efforts can be put into practice long term to successfully mitigate biocrust loss and its effects?

I believe that remote sensing is the future of vegetation monitoring globally, but especially in Antarctica and other remote regions that are inaccessible even during summer months. Monitoring vegetation solely through traditional ground sampling methods is destructive, time intensive, and limited to accessible locations. While field sampling cannot be replaced totally by remote sensing, and boots on the ground will always be an essential requirement of validating remote sensing models, advances in remote sensing technology are occurring rapidly and will continue to bring new, powerful tools to bear on old unresolved questions as well as stimulate new questions that will positively impact research in this region.

Recent launches of hyperspectral satellites and other high spatial resolution satellites will be transformative for studies on patchy microbial mats and biocrusts. Additionally, the ability to remotely estimate resistivity of soil (*e.g.*, electrical conductivity of soils) using airborne geophysical techniques (Gutterman et al. 2023) would drastically improve our ability to inform species distribution models for microbial mats, biocrusts, and soil invertebrate communities (Power et al. 2024b). Furthermore, other remote sensing technologies beyond multispectral and hyperspectral sensors, *e.g.*, synthetic aperture radar, could provide higher resolution insights into soil moisture content, which is one of the main drivers of microbial mat and biocrust distribution and activity. There are a multitude of remote sensing technologies and datasets that could be used to further research microbial mats and biocrusts across ecosystems. With greater spatial and spectral resolution and the incorporation of a variety of remote sensing technologies, we will greatly improve our habitat suitability models and hopefully gain a deeper understanding of the spatial extent of these communities and their responses to continuing environmental change.

References

Barrett, J.E., Adams, B.J., Doran, P.T., Dugan, H.A., Myers, K.F., Salvatore, M.R., Power, S.N., Snyder, M.D., Wright, A.T., Gooseff, M.N., 2024. Response of a Terrestrial Polar Ecosystem to the March 2022 Antarctic Weather Anomaly. Earths Future 12, e2023EF004306. https://doi.org/10.1029/2023EF004306

Bate, D.B., Barrett, J.E., Poage, M.A., Virginia, R.A., 2008. Soil phosphorus cycling in an Antarctic polar desert. Geoderma 144, 21–31. https://doi.org/10.1016/J.GEODERMA.2007.10.007

Burkins, M.B., Virginia, R.A., Chamberlain, C.P., Wall, D.H., 2000. Origin and Distribution of Soil Organic Matter in Taylor Valley, Antarctica. Ecology 81, 2377–2391. https://doi.org/10.1890/0012-9658(2000)081[2377:OADOSO]2.0.CO;2

Cantón, Y., Román, J.R., Chamizo, S., Rodríguez-Caballero, E., Moro, M.J., 2014. Dynamics of organic carbon losses by water erosion after biocrust removal. J. Hydrol. Hydromech./Vodohospo. Cas. 62, 258–268. https://doi.org/10.2478/johh-2014-0033

Colesie, C., Walshaw, C.V., Sancho, L.G., Davey, M.P., Gray, A., 2023. Antarctica's vegetation in a changing climate. Wiley Interdiscip. Rev. Clim. Change 14. https://doi.org/10.1002/wcc.810

Denton, G.H., Bockheim, J.G., Wilson, S.C., Stuiver, M., 1989. Late Wisconsin and early Holocene glacial history, inner Ross Embayment, Antarctica. Quat. Res. 31, 151–182. https://doi.org/10.1016/0033-5894(89)90004-5

Finger-Higgens, R., Duniway, M.C., Fick, S., Geiger, E.L., Hoover, D.L., Pfennigwerth, A.A., Van Scoyoc, M.W., Belnap, J., 2022. Decline in biological soil crust N-fixing lichens linked to increasing summertime temperatures. Proc. Natl. Acad. Sci. U. S. A. 119, e2120975119. https://doi.org/10.1073/pnas.2120975119

Gutterman, W.S., Doran, P.T., Virginia, R.A., Barrett, J.E., Myers, K.F., Tulaczyk, S.M., Foley, N.T., Mikucki, J.A., Dugan, H.A., Grombacher, D.J., Bording, T.S., Auken, E., 2023. Causes and characteristics of electrical resistivity variability in shallow (<4 m) soils in Taylor Valley, east Antarctica. J. Geophys. Res. Earth Surf. 128. https://doi.org/10.1029/2022jf006696

Kohler, T.J., Stanish, L.F., Crisp, S.W., Koch, J.C., Liptzin, D., Baeseman, J.L., McKnight, D.M., 2015. Life in the Main Channel: Long-Term Hydrologic Control of Microbial Mat

Abundance in McMurdo Dry Valley Streams, Antarctica. Ecosystems 18, 310–327. https://doi.org/10.1007/s10021-014-9829-6

Lawson, J., Doran, P.T., Kenig, F., Des marais, D.J., Priscu, J.C., 2004. Stable Carbon and Nitrogen Isotopic Composition of Benthic and Pelagic Organic Matter in Lakes of the McMurdo Dry Valleys, Antarctica. Aquat. Geochem. 10, 269–301. https://doi.org/10.1007/s10498-004-2262-2

Lingappa, U.F., Stein, N.T., Metcalfe, K.S., Present, T.M., Orphan, V.J., Grotzinger, J.P., Knoll, A.H., Trower, E.J., Gomes, M.L., Fischer, W.W., 2022. Early impacts of climate change on a coastal marine microbial mat ecosystem. Sci. Adv. 8, eabm7826. https://doi.org/10.1126/sciadv.abm7826

McKnight, D.M., Niyogi, D.K., Alger, A.S., Bomblies, A., Conovitz, P.A., Tate, C.M., 1999. Dry Valley Streams in Antarctica: Ecosystems Waiting for Water. Bioscience 49, 985–995. https://doi.org/10.1525/bisi.1999.49.12.985

Patel, K., 2024. Antarctic temperatures soar 50 degrees above norm in long-lasting heat wave. The Washington Post.

Power, S.N., Salvatore, M.R., Sokol, E.R., Stanish, L.F., Borges, S.R., Adams, B.J., Barrett, J.E., 2024a. Remotely characterizing photosynthetic biocrust in snowpack-fed microhabitats of Taylor Valley, Antarctica. Science of Remote Sensing 9, 100120. https://doi.org/10.1016/j.srs.2024.100120

Power, S.N., Thomas, V.A., Salvatore, M.R., Barrett, J.E., 2024b. Habitat suitability of biocrust communities in a cold desert ecosystem. Ecol. Evol. 14, e11649. https://doi.org/10.1002/ece3.11649

Power, S.N., Osburn, E.D., & Barrett, J.E., *In Prep*, Terrestrial microbial mat composition and activity across a geochemical gradient in Taylor Valley, Antarctica.

Robinson, S.A., King, D.H., Bramley-Alves, J., Waterman, M.J., Ashcroft, M.B., Wasley, J., Turnbull, J.D., Miller, R.E., Ryan-Colton, E., Benny, T., Mullany, K., Clarke, L.J., Barry, L.A., Hua, Q., 2018. Rapid change in East Antarctic terrestrial vegetation in response to regional drying. Nat. Clim. Chang. 8, 879–884. https://doi.org/10.1038/s41558-018-0280-0

Rodríguez-Caballero, E., Belnap, J., Büdel, B., Crutzen, P.J., Andreae, M.O., Pöschl, U., Weber, B., 2018. Dryland photoautotrophic soil surface communities endangered by global

change. Nat. Geosci. 11, 185–189. https://doi.org/10.1038/s41561-018-0072-1

Stanish, L.F., Nemergut, D.R., McKnight, D.M., 2011. Hydrologic processes influence diatom community composition in Dry Valley streams. J. North Am. Benthol. Soc. 30, 1057–1073. https://doi.org/10.1899/11-008.1

Tucker, C.J., 1979. Red and Photographic Infrared Linear Combinations for Monitoring Vegetation. Remote Sens. Environ. 8, 127–150.

Turner, J., Phillips, T., Thamban, M., Rahaman, W., Marshall, G.J., Wille, J.D., Favier, V., Winton, V.H.L., Thomas, E., Wang, Z., Broeke, M., Hosking, J.S., Lachlan-Cope, T., 2019. The dominant role of extreme precipitation events in antarctic snowfall variability. Geophys. Res. Lett. 46, 3502–3511. https://doi.org/10.1029/2018gl081517

Vignon, É., Roussel, M.-L., Gorodetskaya, I.V., Genthon, C., Berne, A., 2021. Present and future of rainfall in Antarctica. Geophys. Res. Lett. 48. https://doi.org/10.1029/2020gl092281

Wille, J.D., Alexander, S.P., Amory, C., Baiman, R., Barthélemy, L., Bergstrom, D.M., Berne, A., Binder, H., Blanchet, J., Bozkurt, D., Bracegirdle, T.J., Casado, M., Choi, T., Clem, K.R., Codron, F., Datta, R., Battista, S.D., Favier, V., Francis, D., Fraser, A.D., Fourré, E., Garreaud, R.D., Genthon, C., Gorodetskaya, I.V., González-Herrero, S., Heinrich, V.J., Hubert, G., Joos, H., Kim, S.-J., King, J.C., Kittel, C., Landais, A., Lazzara, M., Leonard, G.H., Lieser, J.L., Maclennan, M., Mikolajczyk, D., Neff, P., Ollivier, I., Picard, G., Pohl, B., Ralph, M.F., Rowe, P., Schlosser, E., Shields, C.A., Smith, I.J., Sprenger, M., Trusel, L., Udy, D., Vance, T., Vignon, É., Walker, C., Wever, N., Zou, X., 2023. The extraordinary March 2022 East Antarctica “heat” wave. Part II: impacts on the Antarctic ice sheet. J. Clim. 37, 779–799. https://doi.org/10.1175/jcli-d-23-0176.1

Figures

Figure 5.1

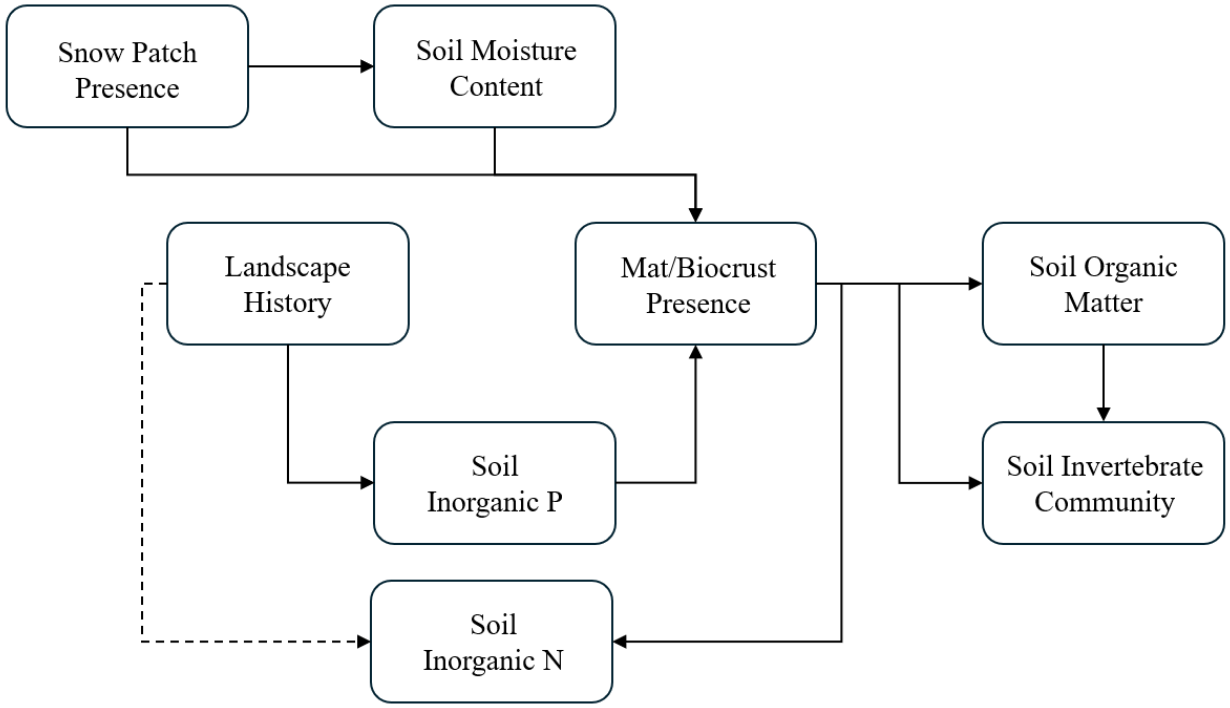

Figure 5.1. Conceptual model illustrating the causal relationships between key soil and environmental conditions that influence microbial mat/biocrust presence, soil organic matter, and soil invertebrate community composition, and vice versa. Arrows indicate variables that are drivers, responses, and both. All relationships are positive. Solid lines indicate strong, positive relationships, while dotted lines indicate weaker, positive relationships.